The genetic, neuronal, and chemical basis for microbial discrimination in *Caenorhabditis elegans*

by

Joshua D. Meisel

M.S. Biology, B.S. Biology, B.A. English
Stanford University, 2007

SUBMITTED TO THE DEPARTMENT OF BIOLOGY
IN PARTIAL FULFILLMENT OF THE REQUIREMENTS FOR THE DEGREE OF

DOCTOR OF PHILOSOPHY
AT THE
MASSACHUSETTS INSTITUTE OF TECHNOLOGY

JUNE 2016

Signature of Author: Signature redacted
Department of Biology
May 20, 2016

Certified by: Signature redacted
Dennis H. Kim
Associate Professor of Biology
Thesis Supervisor

Accepted by: Signature redacted
Amy E. Keating
Professor of Biology
Co-Chair, Biology Graduate Committee

The genetic, neuronal, and chemical basis for microbial discrimination in *Caenorhabditis elegans*

by

Joshua D. Meisel

Submitted to the Department of Biology on May 20, 2016 in Partial Fulfillment of the Requirements for the Degree of Doctor of Philosophy in Biology

ABSTRACT

Discrimination among pathogenic and beneficial microbes is essential for host organism immunity and homeostasis. Increasingly, the nervous system of animals is being recognized as an important site of bacterial recognition, but the molecular mechanisms underlying this process remain unclear. Chapter One discusses how the nematode *Caenorhabditis elegans* can be used to dissect the genetic and neuronal mechanisms that coordinate behavioral responses to bacteria. In Chapter Two, we show that chemosensory detection of two secondary metabolites produced by *Pseudomonas aeruginosa* modulates a neuroendocrine signaling pathway that promotes *C. elegans* avoidance behavior. Specifically, secondary metabolites phenazine-1-carboxamide and pyochelin activate a G protein-signaling pathway in the ASJ chemosensory neuron pair that induces expression of the neuromodulator DAF-7/TGF-β. DAF-7, in turn, activates a canonical TGF-β signaling pathway in adjacent interneurons to modulate aerotaxis behavior and promote avoidance of pathogenic *P. aeruginosa*. This chapter provides a chemical, genetic, and neuronal basis for how the behavior and physiology of a simple animal host can be modified by the microbial environment, and suggests that secondary metabolites produced by microbes may provide environmental cues that contribute to pathogen recognition and host survival.

Genetic dissection of neuronal responses to bacteria in *C. elegans* can also lend insights into neurobiology more generally. In Chapter Three we show that loss of the lithium-sensitive phosphatase bisphosphate 3'-nucleotidase (BPNT-1) results in the selective dysfunction of the ASJ chemosensory neurons. As a result, BPNT-1 mutants are defective in behaviors dependent on the ASJ neurons, such as pathogen avoidance and dauer exit. Acute treatment with lithium also causes reversible dysfunction of the ASJ neurons, and we show that this effect is mediated specifically through inhibition of BPNT-1. Finally, we show that lithium's selective effect on the nervous system is due in part to the limited expression of the cytosolic sulfotransferase SSU-1 in the ASJ neuron pair. Our data suggest that lithium, through inhibition of BPNT-1 in the nervous system, can cause selective toxicity to specific neurons, resulting in corresponding effects on behavior of *C. elegans*. In Chapter Four I discuss the future directions for the genetic dissection of pathogen recognition in *C. elegans*.

Thesis Supervisor: Dennis H. Kim
Title: Associate Professor of Biology

Acknowledgements

I would like to thank my thesis advisor Dennis Kim for his continued support and enthusiasm throughout my graduate career. Dennis has taught me how to transform an exciting observation into a fully developed scientific story and, importantly, how to write about it. Dennis has also taught me how to dance at scientific conferences (never stop), which continues to serve me well.

It is a pleasure to thank the members of my thesis committee. Peter Reddien mentored me when I worked as a technician in his laboratory, and I am fortunate to continue to have his scientific curiosity and logical thinking as a part of my graduate career. I thank Troy Littleton not only for his thoughtful comments on my thesis work, but also for spearheading the Molecular and Cellular Neuroscience program at MIT, from which I have benefited greatly. I am appreciative of Piali Sengupta for reading my thesis and agreeing to be part of my thesis defense committee. I would also like to thank Frank Solomon for his sage advice over the years.

I would like to thank all the members of the Kim Lab from my six years in the lab for their scientific advice and support: Annie, Chi-fong, Claire, Dan, Doug, Erik, Harini, Howard, Jay, Julie, Kirthi, Marissa, Matt, Pete, Spencer, Stephanie, and Zoë (baymates are underlined). Thank you also for agreeing to participate in yearly video projects, and for making the lab environment a place I want to spend my time. The Horvitz Lab across the hall has been a source of intellectual and infrastructural support - special thanks to Na An for providing strains and making things run smoothly, and to my classmate Holly Johnsen for being there from start (7.52) to finish

(graduation). I am grateful for our biochemistry collaborators at Cornell – Oishika Panda, Parag Mahanti, and Frank Schroeder – for their excellent work in identifying bacterial metabolites.

Progressing through graduate school was made easier with the camaraderie of the Biograd and CSBi classes of 2009, which included monthly "Building 68" class lunches. Special thanks to everyone I went running with during graduate school (e.g. Matt, Steve, Doug, Shawn) – it kept me happy and healthy. Thanks to all my friends in Boston, especially the book group with its bureaucratic and byzantine rules.

A huge thank you to my family for supporting me during graduate school, but also for much longer than that. Special thanks to Mom, Dad, Deb, and Zack, for helping me grow into a curious and happy person. I am so fortunate to have attended grad school in Boston, where weekend coffees were always just a phone call away.

Finally, thank you to my wife Jenna, who has literally been helping me with my science projects since we fell in love prying chitons off the beachrock in the intertidal zone. The many weekends spent in lab over the last 11 years have been easy, because most of the time you are here too. Also, thank you for teaching me about the history of science – who knows, maybe one day our love letters will be a valuable primary source.

Table of Contents

Title Page	1
Abstract	2
Acknowledgements	3
Table of Contents	5
List of Figures and Tables	7
Chapter One: Introduction	10
C. elegans Uses Multiple Behavioral Strategies to Find Bacterial Food	13
C. elegans Exhibits Dietary Choice Behavior and Avoids Pathogenic Bacteria	17
Multiple Behaviors Contribute to Pathogen Avoidance in *C. elegans*	22
Conserved Signals and Commonalities with Innate Immunity	28
Genetic Variation in Pathogen Avoidance Behavior	31
Concluding Remarks	33
References	35
Chapter Two: Chemosensation of Bacterial Secondary Metabolites Modulates Neuroendocrine Signaling and Behavior of *C. elegans*	42
Summary	43
Graphical Abstract	44
Introduction	45
Results	47
DAF-7/TGF-β is required for behavioral avoidance of *Pseudomonas aeruginosa*	47
P. aeruginosa induces *daf-7* expression in the ASJ neuron pair and promotes avoidance behavior	50
DAF-7 signals to the RIM/RIC interneurons adjacent to the ASJ neurons to promote pathogen avoidance	56
DAF-7 promotes pathogen avoidance through the modulation of aerotaxis behavior	57

G protein-dependent signaling activates *daf-7* expression in the ASJ neuron pair in response to *P. aeruginosa* 59
Chemosensory recognition of the *P. aeruginosa* secondary metabolites phenazine-1-carboxamide and pyochelin by the ASJ neuron pair of *C. elegans* 63
Microbial discrimination and specificity in the chemosensory response to *P. aeruginosa* 69
Discussion 73
Experimental Procedures 76
Author Contributions 83
Acknowledgements 83
References 84
Supplemental Information 91

Chapter Three: Inhibition of Lithium-Sensitive Phosphatase BPNT-1 Causes Selective Neuronal Dysfunction in *C. elegans* 107
Summary 108
Graphical Abstract 109
Results and Discussion 110
Author Contributions 124
Acknowledgements 124
Experimental Procedures 125
References 132
Supplemental Information 136

Chapter Four: Future Directions 141
Identification of genes coupling microbial detection to neuronal transcription 142
A conserved role for BPNT-1 in mammals? 146
References 147

List of Figures and Tables

Chapter One: Introduction

Figure 1. Multiple behavioral paradigms promote the attraction of *C. elegans* to bacterial food 16

Figure 2. Behavioral assays for studying pathogen avoidance in *C. elegans* 19

Figure 3. Multiple behavioral strategies contribute to avoidance of pathogenic bacteria 27

Chapter Two: Chemosensation of Bacterial Secondary Metabolites Modulates Neuroendocrine Signaling and Behavior of *C. elegans*

Figure 1. DAF-7/TGF-β is required for the protective behavioral avoidance response to *P. aeruginosa* 48

Figure 2. *daf-7* expression is induced in the ASJ neurons upon exposure to *P. aeruginosa* 51

Figure 3. DAF-7 from the ASJ neuron pair signals to the RIM/RIC interneurons to alter aerotaxis behavior and promote avoidance of *P. aeruginosa* 54

Figure 4. GPA-3 and GPA-2 function cell-autonomously in the ASJ neurons to activate *daf-7* expression in response to *P. aeruginosa* 60

Figure 5. Supernatant from *P. aeruginosa* in stationary phase activates *daf-7* expression and contains secondary metabolites 64

Figure 6. The ASJ neurons respond to *P. aeruginosa* secondary metabolites phenazine-1-carboxamide and pyochelin 67

Figure 7. Microbial discrimination of *P. aeruginosa* activates *daf-7* transcription in the ASJ neurons and promotes avoidance behavior 71

Figure S1. Pathogen avoidance behavior reduces the dose of ingested bacteria and is genetically distinct from dauer diapause entry, related to Figure 1 91

Figure S2. The *daf-7* smFISH neuronal expression pattern is specific and includes the OLQ and ADE mechanosensory neurons, related to Figure 2 93

Figure S3. DAF-7 promotes *P. aeruginosa* avoidance through altering aerotaxis behavior and acts in parallel to NPR-1, related to Figure 3 94
Figure S4. GPA-3 and GPA-2 are necessary for *daf-7* expression in ASJ, whereas DAF-11 and TAX-2/TAX-4 are necessary for *daf-7* expression in both ASI and ASJ, related to Figure 4 96
Figure S5. DQF-COSY spectrum of CombiFlash fraction of *P. aeruginosa* metabolome extract reveals presence of phenazine-1-carboxamide and pyochelin, related to Figure 5 98
Figure S6. Dose-dependence of the *daf-7* transcriptional response to pyochelin and phenazine-1-carboxamide, related to Figure 6 100
Table S1. NMR spectroscopic data of Phenazine-1-Carboxamide, related to Figure S5 101
Table S2. NMR spectroscopic data of Pyochelin, related to Figure S5 102
Table S3. Complete list of *C. elegans* strains used in this study 103
Table S4. Complete list of oligos used in this study 105

Chapter Three: Inhibition of Lithium-Sensitive Phosphatase BPNT-1 Causes Selective Neuronal Dysfunction in *C. elegans*

Figure 1. Bisphosphate 3'-nucleotidase (BPNT-1) is required for the function of the ASJ neurons 111
Figure 2. Lithium induces dysfunction of the ASJ neurons through inhibition of BPNT-1 114
Figure 3. Loss of BPNT-1 inhibits the ASJ neurons through accumulation of cytosolic PAP 119
Figure 4. Lithium selectively inhibits the ASJ neurons of *C. elegans* through inhibition of BPNT-1 123
Table. Complete list of *C. elegans* strains used in this study 129
Table. Complete list of DNA oligos used in this study 130
Figure S1. Phylogenetic analysis of the conserved family of lithium-sensitive phosphatases, related to Figure 1 136

Figure S2. The *bpnt-1* expression pattern is broad and not limited to the ASJ neurons, related to Figure 1 138
Figure S3. BPNT-1, but not GPAP-1 or TTX-7, is required for ASJ function partially due to expression of cytosolic sulfotransferase SSU-1, related to Figures 2 and 3 140

Chapter Four: Future Directions

Figure 1. Classification of mutants defective in the induction of *daf-7* in the ASJ neurons 143
Figure 2. Class 3 mutants inhibit inappropriate expression of *daf-7* in the ASJ neurons 145

Chapter One

Introduction

Joshua D. Meisel and Dennis H. Kim

A portion of this chapter was published as: Meisel JD and Kim DH. (2014) Behavioral avoidance of pathogenic bacteria by *Caenorhabditis elegans*. **Trends in Immunology** 35(10): 465-70.

The immune system and the nervous system of animals share the remarkable ability to respond to a diverse range of stimuli. Of paramount importance is the detection of microbes, which is necessary for mounting defenses against invading pathogens. In mammals, innate and adaptive immune systems, using proteins such as Toll-like receptors and immunoglobulins, respectively, are capable of detecting bacteria and initiating protective responses. Ideally such systems would have the ability to discriminate between pathogens, which must be eliminated from the body, and commensals and symbionts (e.g. the gut microbiota) that promote human health. The characterization of neurobehavioral responses to microbial pathogens suggests that the host organism may also bring to bear on the problem of microbial recognition a diverse suite of chemosensory olfactory and gustatory receptors. Increasingly, a role for the nervous system in recognizing microbes has been implicated not only in the induction of host immunity, but in broader effects on host physiology that have been attributed to the microbiota, including metabolism, behavior, and the pathophysiology of disease (Clemente et al. 2012; Tremaroli and Bäckhed 2012; Grenham et al. 2011; Lyte 2013).

The soil-dwelling nematode worm *Caenorhabditis elegans* is an ideal organism for investigating the molecular mechanisms underlying bacterial discrimination by the nervous system. *C. elegans* has been used as a genetically tractable laboratory organism for the past 40 years (Brenner 1974). An adult hermaphrodite is comprised of approximately 1000 cells of invariant developmental linage that give rise to multiple organs including the nervous system, intestine, and reproductive gonad. An adult *C. elegans* hermaphrodite has 302 neurons, each with a defined anatomy and developmental lineage. Moreover, the synaptic connectivity of the *C. elegans* nervous system has been defined by detailed ultrastructural analysis, allowing for the

dissection of neural circuits controlling simple behaviors (White et al. 1986). Chief among these behaviors is the detection of bacteria, which serves as the animal's source of nutrition both in the laboratory and in the environment, but can also represent a lethal pathogenic threat.

For *C. elegans*, the role of the nervous system in microbial recognition is tied to food foraging behaviors, as *C. elegans* is a bacterivore that feeds on microbes in decaying organic matter (Félix and Duveau 2012). The presence of bacterial food has been demonstrated to have wide-ranging effects on *C. elegans* development, including the decision to enter dauer diapause, reproductive egg laying, and feeding rate (Cassada and Russell 1975; Avery and Horvitz 1990; Trent 1982). As such, *C. elegans* uses multiple behavioral strategies to promote attraction to bacterial food, and these behaviors are discussed in the first part of this chapter. However the attraction to bacteria is not absolute – *C. elegans* in the environment and the laboratory can be infected with fungal and bacterial pathogens, and are capable of mounting a protective immune response that includes behavioral avoidance. The genetic analysis of *C. elegans* has begun to reveal the molecular and neuronal basis of host behavioral responses to pathogenic bacteria, and these are discussed in the second part of this chapter. However major questions remain: how does the nervous system of *C. elegans* discriminate between beneficial and pathogenic microbes? Once animals have identified a particular microbe as pathogenic, how is this detection translated into a long-term behavioral response? One might anticipate that, just as mammalian innate immune signaling has ancient evolutionary origins evident in the immune response pathways of invertebrates, features of the chemosensory recognition and response to microbial stimuli may also be conserved in evolutionarily diverse species.

C. elegans Uses Multiple Behavioral Strategies to Find Bacterial Food

A variety of innate behaviors drive *C. elegans* towards bacterial food and promote its occupancy inside of bacterial lawns. Perhaps the most well studied sensory modality is the chemosensation of bacterial-derived volatile and water-soluble cues. The *C. elegans* nervous system is equipped with 12 pairs of bilaterally symmetric ciliated chemosensory neurons in its head known as amphid neurons (AWA, AWB, AWC, AFD, ASE, ADF, ASG, ASH, ASI, ASJ, ASK, and ADL) (White et al. 1986). These amphid neurons are bipolar, with one ciliated dendrite-like process extending to the nose (and in some cases exposed to the environment), and the other axon-like process extending into the nerve ring where it makes synapses *en passent* with other neurons. *C. elegans* contains over 1,000 G protein-coupled receptors in its genome, many of which are expressed in these amphid neurons, and likely act as chemoreceptors for distinct odors and tastes (Troemel et al. 1995; Thomas and Robertson 2008).

Chemotaxis experiments demonstrated that *C. elegans* are attracted to many volatile and water-soluble cues associated with bacterial metabolism, such as diacetyl, alcohols, and esters (Bargmann and Horvitz 1991; Bargmann, Hartwieg, and Horvitz 1993). Ablation of amphid neurons showed that the attractive chemotaxis behavior is dependent on a distributed set of these neurons (AWA and AWC for volatile cues; ASE, ADF, ASG, ASI, and ASK for water-soluble ones), and that individual neurons are capable of responding to many attractive cues. Forward genetics revealed that the attractive chemotaxis to diacetyl is mediated by the G protein-coupled receptor ODR-10 in the AWA neuron (Sengupta, Chou, and Bargmann 1996). Further studies showed that ectopic expression of ODR-10 in the AWB neurons, which normally detect repulsive cues, resulted in avoidance of diacetyl (Troemel, Kimmel, and Bargmann 1997). Using

genetically encoded calcium indicators expressed in subsets of neurons, bacteria-conditioned media and odors such as isoamyl alcohol were shown to activate the AWC neurons (Chalasani et al. 2007). These studies suggest that *C. elegans* have evolved to detect many compounds produced by bacteria, and have encoded them as innately attractive through expression of specific receptors in neurons like AWA and AWC.

C. elegans can also sense physical attributes of their environmental using mechanosensory neurons that respond to force. In the context of bacterial food, this sensory modality can be used to decrease the animal's locomotion once it has entered a lawn of bacteria. Specifically, *C. elegans* removed from bacteria and then transferred to plates that either contained or lacked bacteria moved more slowly upon reentering the bacterial lawn (the "basal slowing response") (Sawin, Ranganathan, and Horvitz 2000). This effect was enhanced if the animals had been starved prior to the behavioral assay (the "enhanced slowing response"). Through mutant analysis and ablation studies, Sawin *et al.* show that the basal slowing response is mediated by mechanosensory dopaminergic neurons (CEP, ADE, and PDE), and that the same slowing effect can be observed when animals enter a lawn of sterile beads. These results suggest that mechanosensation, or the "feel" of a bacterial lawn, can innately promote occupancy inside bacterial food.

The innate aerotaxis behavior of *C. elegans* can also promote attraction to bacterial food. Wild isolates of *C. elegans* aggregate and exhibit clumping around the edge of bacterial lawns due to a preference for oxygen concentrations between 8-12% (Gray et al. 2004; A. J. Chang et al. 2006). As a result, animals actively avoid atmospheric oxygen levels of 20%, and are instead attracted to respiring bacterial lawns that are hypoxic relative to the air. This behavior is

dependent on oxygen sensing neurons (URX, AQR, and PQR) and guanylate cyclases GCY-35 and GCY-36 that bind molecular oxygen (Gray et al. 2004; Cheung et al. 2004). Thus, oxygen concentration preference actively drives *C. elegans* towards bacteria, and once inside a bacterial lawn innate hyperoxia avoidance prevents the animals from leaving.

In addition to the aforementioned innate behaviors, *C. elegans* can undergo associative learning, in which neutral or aversive stimuli become attractive when paired with bacterial food. For example, *C. elegans* will associate the temperature it was raised at (between 15-25°C) in the presence of bacterial food with nutrition, and use thermotaxis behavior to seek out its cultivation temperature later in life (Hedgecock and Russell 1975). In contrast, animals will avoid temperatures associated with starvation. Similarly, when presented with a choice between concentrations of Na^+ and Cl^- ions that naïve worms find equally attractive, *C. elegans* will prefer the ion that had previously been paired with bacterial food (Wen et al. 1997). Conversely, chemotaxis behavior towards NaCl is dramatically reduced when NaCl has been paired with starvation (Saeki, Yamamoto, and Iino 2001). Thus, sensory modalities that are independent of bacteria can be brought to bear on the problem of finding nutrition, and combined with innate chemosensory, mechanosensory, and aerotaxis behaviors, *C. elegans* is robustly attracted to bacterial lawns (Figure 1).

Figure 1

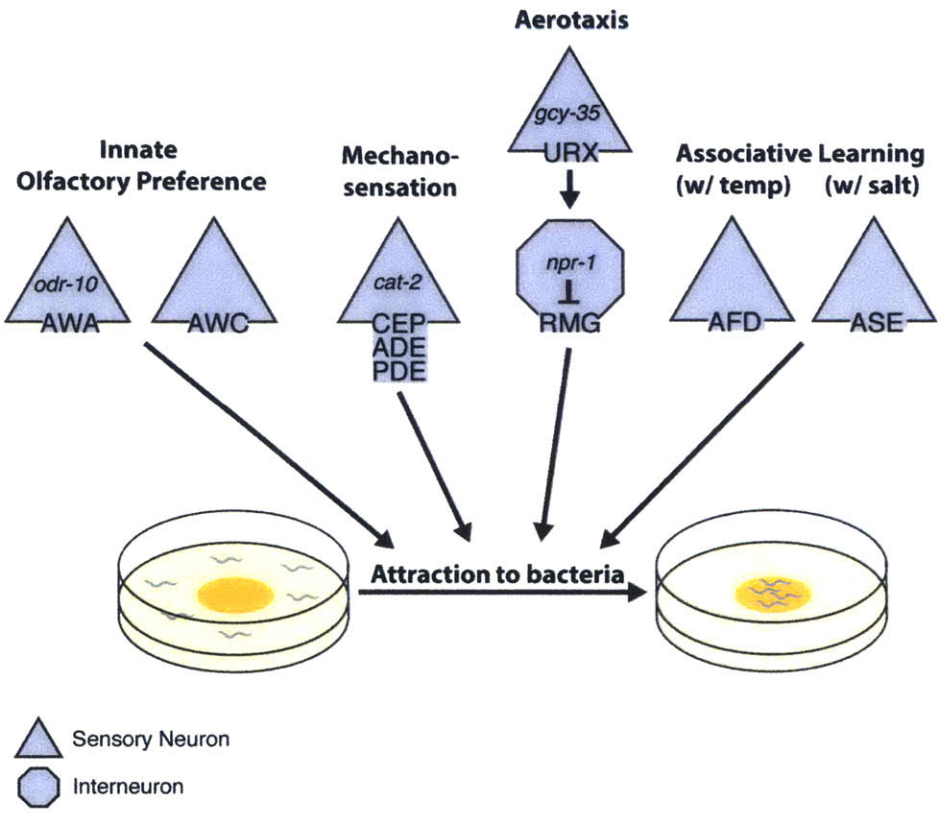

Figure 1. Multiple behavioral paradigms promote the attraction of *C. elegans* to bacterial food. Innate olfactory and gustatory preferences for bacterial-derived cues, sensed by ciliated chemosensory neurons that detect attractive odors and tastes, promote chemotaxis towards bacteria. Once they have entered a bacterial environment, additional cues associated with bacteria, such as oxygen concentrations and the texture of the bacterial lawn, prevent animals from leaving through aerotaxis and mechanosensory behaviors. Finally, associative learning, in which *C. elegans* pair neutral cues such as temperature and salt concentrations with food, can also promote attraction to bacteria.

C. elegans Exhibits Dietary Choice Behavior and Avoids Pathogenic Bacteria

The previous experiments and indeed most work in *C. elegans* have utilized the human gut bacterium *E. coli* (strain OP50) as the animal's food source. Not only is *C. elegans* unlikely to encounter *E. coli* in its natural environment, it will rarely be presented with a single bacterial species. In choice assays where *C. elegans* are presented with multiple bacteria of varying quality (from best to worst: *Comamonas sp., E. coli* HB101, *E. coli* DA837, *B. simplex, B. megaterium*), animals will exhibit behavioral preference to bacteria based on their nutritional value (Shtonda and Avery 2006). In most of the choice assays performed, *C. elegans* did not display an innate preference for the bacteria of high quality, ruling out innate attraction to specific volatile cues as the driving force behind the choice. Instead, animals sampled both food sources and determined over the course of hours which bacteria they preferred. Thus not only are *C. elegans* able to utilize innate and learned behaviors to find bacterial food, they can also evaluate food quality and leave less desirable bacteria if necessary (Shtonda and Avery 2006). The ability to discriminate between bacterial species proves to be especially important when confronted with pathogens, as there is an evolutionary balance between attraction to nutrition and the potential ingestion of a last meal of lethal pathogenic bacteria.

An evolutionary diverse group of environmental pathogens can infect *C. elegans.* Gram-negative bacterial pathogens *Pseudomonas aeruginosa* and *Serratia marcescens* are ingested by *C. elegans* and colonize the animal's intestine resulting in death in a matter of days (Tan, Mahajan-Miklos, and Ausubel 1999; Pujol et al. 2001). Gram-positive bacteria *Enterococcus faecalis, Streptococcus pneumoniae,* and *Staphlococcus aureus* can all kill *C. elegans,* and *E. faecalis* proliferates in intestine resulting in a persistent infection (Garsin et al. 2001).

Microbacterium nematophilum, another gram-positive bacteria which naturally contaminated *C. elegans* cultures, causes deformation of the anal region by adhering to the rectal cuticle (Hodgkin, Kuwabara, and Corneliussen 2000). Numerous parasitic fungi can kill *C. elegans,* including *Drechmeria coniospora,* whose conidia adhere to the cuticle, and *Drechslerella doedycoides* which forms constricting hyphal rings that trap young larvae (Jansson 1994; Maguire et al. 2011). Finally, a eukaryotic intracellular parasite, microsporidium *Nematocidia parisii*, which was isolated from wild *C. elegans,* can infect the animal's intestinal cells (Troemel et al. 2008). Given the multitude of environmental microbes that can kill *C. elegans,* behavioral strategies that indiscriminately drive *C. elegans* towards bacteria must be used with caution.

Indeed one of the primary strategies utilized by *C. elegans* to defend themselves from infection is behavioral avoidance. Upon exposure to pathogenic *Pseudomonas aeruginosa* PA14 and the standard laboratory bacterial food *E. coli* OP50, *C. elegans* exhibits an initial preference for *P. aeruginosa*. But after hours of exposure and presumed intestinal infection, *C. elegans* exhibits an altered preference for *E. coli*, suggestive of an aversive learning response (Y. Zhang, Lu, and Bargmann 2005) (Figure 2A). In the absence of a choice between bacteria, when propagated monoaxenically on pathogens *P. aeruginosa* or *Serratia marcescens*, after an initial attractive phase, *C. elegans* exhibits a gradual evacuation of the bacterial lawn with kinetics comparable to the observed aversive learning response in the choice assay (Pradel et al. 2007; Pujol et al. 2001; Reddy et al. 2009; H. C. Chang, Paek, and Kim 2011) (Figure 2B). This lawn-leaving behavior likely reflects not only olfactory aversive learning, but also the integration of multiple sensory cues from the bacterial lawn.

Figure 2

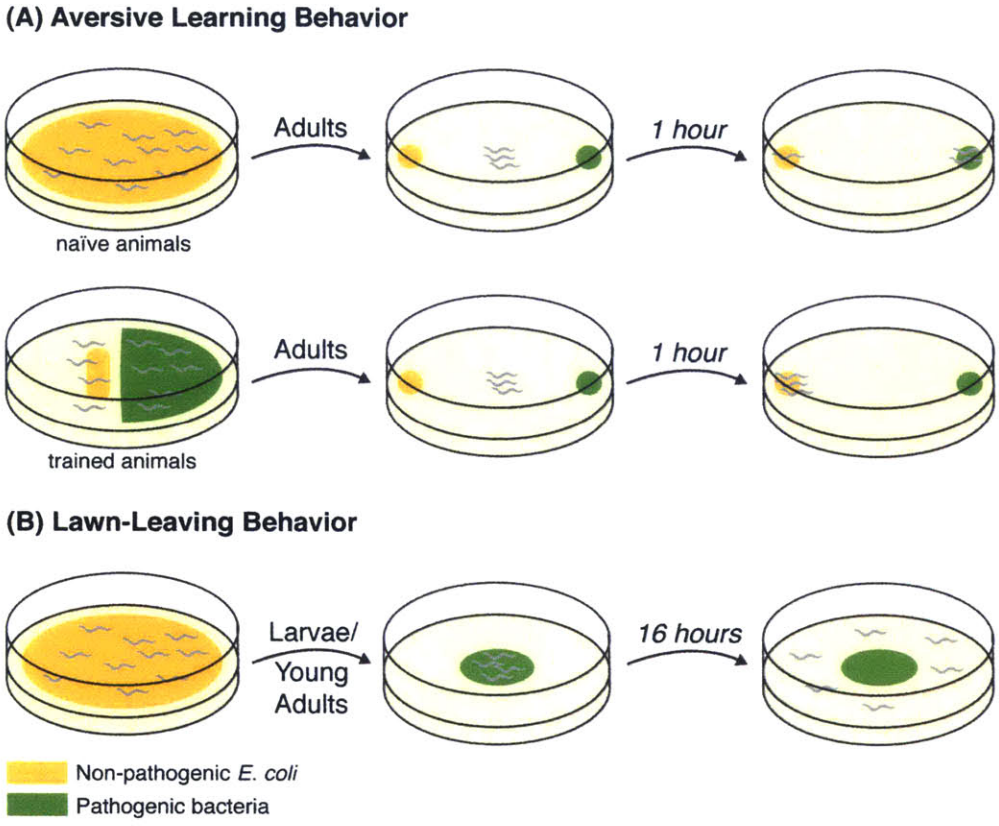
(A) Aversive Learning Behavior
Adults
1 hour
naïve animals
Adults
1 hour
trained animals
(B) Lawn-Leaving Behavior
Larvae/
Young
Adults
16 hours
Non-pathogenic E. coli
Pathogenic bacteria

Figure 2. Behavioral assays for studying pathogen avoidance in *C. elegans*. **(A)** In the Olfactory Aversive Learning Assay animals are exposed to either non-pathogenic *E. coli* ("naïve animals") or pathogenic bacteria, typically *P. aeruginosa* or *S. marcescens* ("trained animals"). Adult *C. elegans* are then transferred to traditional chemotaxis assay plates, in which they are given a choice between spots of two bacterial strains. Occupancy in each bacterial spot is scored after one hour. **(B)** In the lawn-leaving avoidance assay, naïve animals are transferred as larvae or young adults onto agar plates containing a lawn of pathogenic bacteria, typically *P. aeruginosa* or *S. marcescens*. Animals begin inside the bacterial lawn, as both pathogens are initially attractive to *C. elegans,* but through the course of infection animals will slowly evacuate the bacterial lawn. Lawn occupancy is typically scored between 12 and 24 hours.

A key feature of lawn avoidance appears to be the ingestion of bacteria that cause damage to the host. This is suggested by the lack of lawn avoidance of non-pathogenic bacteria or avirulent mutants of *P. aeruginosa*, as well as the kinetics of the aversive learning process that requires time for infection to take hold. Commonly, lawn avoidance is observed in the context of pathogenic species of bacteria, but avoidance behavior can also be observed by feeding *C. elegans* relatively non-pathogenic bacteria that are engineered to harbor plasmids that may be toxic to the host through feeding RNAi of essential genes (Melo and Ruvkun 2012), suggesting the sensing of cellular damage. The involvement of serotonin signaling in this process has been noted to be reminiscent of mammalian gastrointestinal responses to enteric pathogens, in which serotonin signaling may be involved in the activation of nausea responses (Y. Zhang, Lu, and Bargmann 2005; Rubio-Godoy, Aunger, and Curtis 2007).

The choice assay between pathogenic and non-pathogenic bacteria, and the lawn occupancy assay on pathogenic bacteria have provided experimental methods to follow behavioral responses to infection. Such behavioral avoidance has a strong effect on survival, owing to the increased ingestion of pathogenic bacteria when *C. elegans* remains on the bacterial lawn (Reddy et al. 2009). Accordingly, mutant animals with reduced pathogen avoidance have decreased survival relative to their wild-type counterparts when challenged with infection (Reddy et al. 2009; Shivers et al. 2009). Experimental agar plate conditions in which *C. elegans* cannot avoid the bacterial lawn (enforced by covering the agar surface with pathogenic bacteria) can be utilized to infer the contribution of behavioral avoidance mechanisms to susceptibility to infection.

Multiple Behaviors Contribute to Pathogen Avoidance in *C. elegans*

Just as certain bacteria-associated odors may be "hard wired" as attractive to *C. elegans*, microbial cues associated with pathogens may promote avoidance behavior through being innately repulsive. We need look no further than our own personal experiences of disgust to appreciate human chemosensory responses to microbial cues (Curtis 2014). Studies in genetically tractable invertebrate hosts have defined such interactions at the molecular level and their roles in promoting avoidance behavior. In *Drosophila melanogaster* a neuronal circuit for promoting avoidance of pathogenic *Penicillum* mold and *Streptomyces* soil bacteria has been defined (Stensmyr et al. 2012). This behavior was shown to rely on detection of the microbial compound geosmin by the Or56a olfactory receptor. In Chapter Two we take a biochemical approach and identify two secondary metabolites produced by *P. aeruginosa*, pyochelin and phenazine-1-carboxamide, which are detected by chemosensory neurons of *C. elegans.*

In *C. elegans*, the behavioral lawn-leaving response to *S. marcescens* may be mediated by an innate aversion to the bacterial surfactant serrowettin W2. Bacterial mutants defective in serrowettin production were poorly avoided by *C. elegans* although they remained pathogenic, and adding exogenous serrowettin to lawns of non-pathogenic *E. coli* OP50 was sufficient to induce avoidance, implicating an innate aversion of *C. elegans* to this bacterial cue (Pradel et al. 2007). Additionally the AWB chemosensory neurons, required for sensing repulsive cues, were shown through genetic ablation experiments to be necessary for the avoidance of both *S. marcescens* and serrowettin (Pradel et al. 2007). In contrast, certain odors may become repulsive only after aversive learning over the course of infection. Homoserine lactones produced by *P. aeruginosa* have been observed to be initially attractive to *C. elegans*, but following exposure to

pathogenic *P. aeruginosa* these cues become repulsive, thereby promoting avoidance behavior (Beale et al. 2006). In *C. elegans,* neuronal mechanisms for modulating innate behaviors that attract animals to bacteria, such as chemosensation, are critical following infection.

In the case of olfactory aversive learning to *P. aeruginosa*, Ha et al. have established a neural network composed of one circuit that mediates innate olfactory preference to bacterial odors and a second modulatory circuit that is required for the learned olfactory preference (Ha et al. 2010). Through ablation experiments the authors show that the AWB and AWC chemosensory neurons, which are responsible for mediating repulsive and attractive responses to volatile odors, respectively, are necessary for the innate preference of *C. elegans* for *P. aeruginosa*. The authors show that these neurons are activated by the odors of *E. coli* and *P. aeruginosa*, and furthermore show that naïve animals respond to *P. aeruginosa* as the more desirable odor. The neurotransmitters and neuropeptides used by the AWB and AWC neurons to control this innate odor preference have recently been identified through genetic analysis (Harris et al. 2014).

Interestingly, the calcium responses of these neurons to bacterial odors are not altered after training with pathogenic *P. aeruginosa*. Instead, a second circuit, which includes the serotonin-producing ADF neurons, modulates the downstream motor outputs of these neurons (Ha et al. 2010). This learned olfactory preference is dependent on *tph-1*, the rate-limiting enzyme in serotonin synthesis, and infection with *P. aeruginosa* induces increased transcription of *tph-1* and the biosynthesis of serotonin in the ADF chemosensory neurons which promotes avoidance behavior (Y. Zhang, Lu, and Bargmann 2005; Shivers et al. 2009). Through ablation of downstream interneurons the authors were able to effectively decouple the circuit for innate

olfactory preference from the circuit for aversive learning (Ha et al. 2010). This olfactory learning paradigm may be adaptable to novel microbial pathogens, as *C. elegans* also relies on serotonin-dependent aversive learning for avoiding particular strains of *E. coli* that harbor toxic RNAi plasmids (Melo and Ruvkun 2012). This suggests that integration of internal damage-associated cues with environmental odors may be the underlying basis for learned pathogen avoidance behavior.

In the aforementioned aversive learning studies, adult animals were trained on pathogenic bacteria and then assayed for learning within 24 hours. However if young animals in the first larval stage (L1) are exposed to *P. aeruginosa*, and then cleared of infection using antibiotics, days later as adult animals they exhibit an imprinted aversive learning response (Jin, Pokala, and Bargmann 2016). In contrast animals exposed to *P. aeruginosa* at the L2, L3, or L4 larval stages are unable to develop an aversive response, indicating a critical time period for imprinting in the L1 larval stage. Using genetically encoded silencers of neuronal activity the authors show that, similar to aversive learning in adults, imprinted aversive learning requires the AWB and AWC sensory neurons. Interestingly, silencing the AIB or RIM interneurons during the L1 stage blocked imprinting, but silencing these neurons during adulthood did not block the learned olfactory preference. Conversely, silencing the AIY or RIA neurons during L1 did not affect imprinting, but these neurons were required in adulthood for memory retrieval in adulthood (Jin, Pokala, and Bargmann 2016). Thus, early experiences with pathogens can exert long-term affects on how *C. elegans* responds to bacteria in its environment.

Increasingly, neuropeptides are being recognized as critical modulators of preexisting circuits and behaviors, often acting in response to environmental cues (Bargmann 2012; Flavell

et al. 2013; Cheong et al. 2015; Chalasani et al. 2010). In the context of pathogen avoidance, the learned olfactory preference for *E. coli* over pathogenic *P. aeruginosa* depends on expression of an insulin-like peptide, INS-6, from the bacterial food sensing neuron ASI (Chen et al. 2013). INS-6 secreted from ASI antagonizes expression of another insulin-like peptide, INS-7, in a second set of neurons, and the authors hypothesize that secreted INS-7, in turn, negatively affects aversive learning by antagonizing the insulin receptor DAF-2 (Chen et al. 2013). In a second study, the secreted TGF-b ligand DBL-1 was also shown to be necessary for the aversive learning response on *P. aeruginosa* (X. Zhang and Zhang 2012). Thus, at least three neuropeptides promote aversive learning on *P. aeruginosa,* two of which – INS-6 and INS-7 – act through the aforementioned ADF modulatory circuit. Furthermore, the involvement of the food-sensing ASI neuron suggests that nutritional cues and satiety may be integrated with signaling circuitry that regulates pathogen avoidance behavior.

Behavioral strategies that enable *C. elegans* to navigate its microbial environment are not limited to the chemosensation of compounds produced by bacteria. As discussed earlier, wild isolates of *C. elegans* are attracted to oxygen concentrations of 8-10%, such that aerotaxis behavior may drive them towards their food sources (A. J. Chang et al. 2006). The laboratory-adapted N2 strain has, through a gain of function mutation in the *npr-1* gene that encodes a neuropeptide receptor, suppressed this oxygen preference behavior while on bacterial food. In the context of avoidance of pathogenic bacteria, animals with intact hyperoxia avoidance behavior, such as *npr-1* mutants or *C. elegans* wild isolates, fail to avoid lawns of *P. aeruginosa* relative to the laboratory strain N2 (Reddy et al. 2009). Interestingly, in the N2 strain the suppression of aerotaxis behavior by bacterial food is blocked on mucoid bacteria (Reddy et al.

2011). As a result, the N2 wild-type strain fails to avoid a lawn of mucoid *Pseudomonas* as if it were an *npr-1* mutant. Is there a mechanism analogous to the olfactory aversive learning response whereby *C. elegans* can alter their aerotaxis behavior when exposed to pathogenic bacteria? Indeed, we find that activation of the DAF-7/TGF-β neuroendocrine pathway on *P. aeruginosa* modulates aerotaxis behavior to promote avoidance (discussed in Chapter Two).

Mechanosensory responses, which as previously discussed promote slowing once *C. elegans* have entered a bacterial lawn (Sawin, Ranganathan, and Horvitz 2000), are also critical for pathogen avoidance. A naturally occurring polymorphism in the *C. elegans* E3 ubiquitin ligase HECW-1 affects lawn-leaving behavior by altering the mechanosensation of bacteria (H. C. Chang, Paek, and Kim 2011). Reduction of function mutations in *hecw-1* result in enhanced avoidance of *P. aeruginosa. hecw-1* was shown to act in the OLL mechanosensory neurons to inhibit lawn avoidance, and genetic ablation of the OLL neurons in wild-type animals similarly resulted in an increased lawn avoidance. Mutants lacking *hecw-1* and OLL ablated animals were observed to be defective in mechanosensation, implicating mechanosensory processes in the lawn-leaving behavior of *P. aeruginosa.* Finally, the enhanced avoidance and survival phenotypes of the *hecw-1* mutant were suppressed by loss-of-function mutations in *npr-1,* suggesting that HECW-1 inhibits lawn leaving by repressing activity of this neuropeptide receptor (H. C. Chang, Paek, and Kim 2011). Thus, behaviors normally used to attract *C. elegans* to bacterial food sources, such as olfaction, aerotaxis, and mechanosensation, can be instrumental in the avoidance behavior of pathogenic bacteria (Figure 3).

Figure 3

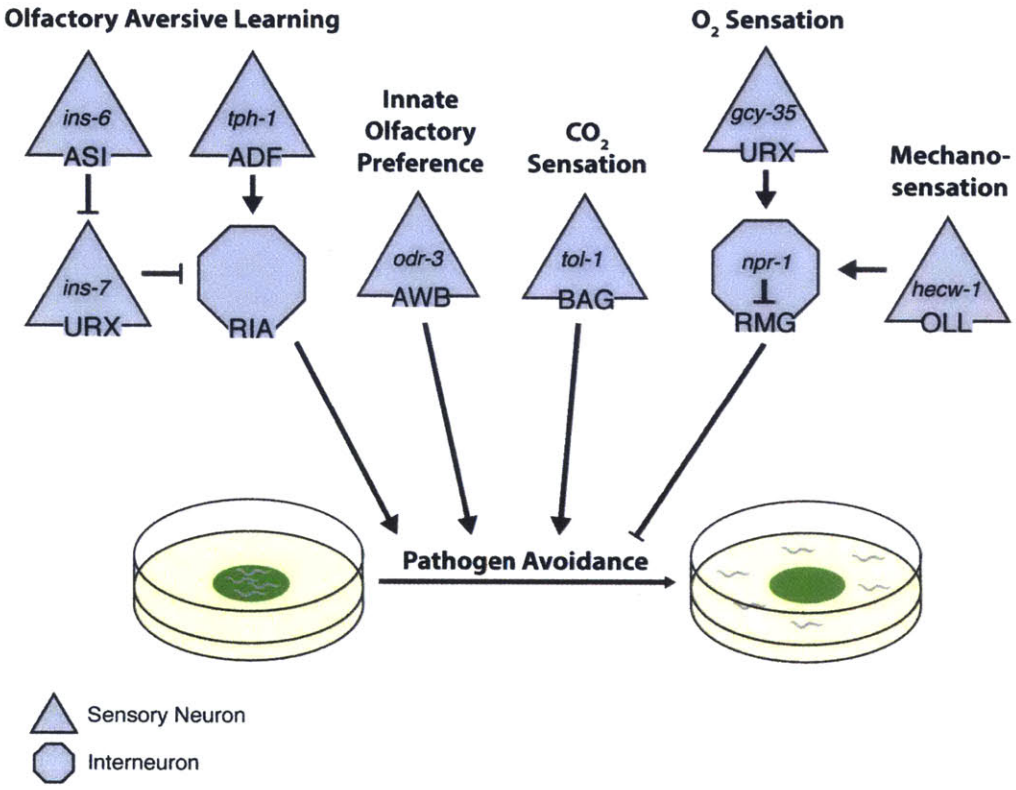

Figure 3. Multiple behavioral strategies contribute to avoidance of pathogenic bacteria. Both innate olfactory preference and learned olfactory preference, mediated by chemosensory neurons that detect attractive and repellent odors, contribute to pathogen avoidance behavior. Additional cues associated with bacteria, such as oxygen tension, carbon dioxide, and the texture of the bacterial lawn, contribute to pathogen avoidance through aerotaxis and mechanosensory behaviors.

Conserved Signals and Commonalities with Innate Immunity

A number of genes with familiar roles in innate immunity also function in behavioral responses of *C. elegans* to pathogenic bacteria. A reverse genetic analysis of Toll signaling components in *C. elegans* identified TOL-1 (Pujol et al. 2001), a homolog of Toll and Toll-like receptors, which in *D. melanogaster* and mammals activate innate immune pathways in response to common microbial features. However no *C. elegans* homolog of NF-kB has been identified, and *tol-1* mutants do not show enhanced susceptibility to infection by *P. aeruginosa* (Pujol et al. 2001), suggesting that TOL-1 may be functioning non-canonically in *C. elegans.* Indeed, *tol-1* mutants were found to be defective in the behavioral avoidance of pathogenic *S. marcescens*, remaining largely inside the lawn after 48 hrs exposure at which time wild-type animals had exited the bacterial lawn (Pradel et al. 2007; Pujol et al. 2001). Expression of *tol-1* was found to be restricted to the nervous system of adult animals, further suggesting that TOL-1 may promote avoidance behavior of pathogenic bacteria. However the mechanism for TOL-1 action remained unclear, for TOL-1 is not required for olfactory aversive learning, and while *tol-1* mutants die faster than wild-type animals on *S. marcescens*, it was unclear whether this is due to an immune deficiency or general sickness of the strain (Y. Zhang, Lu, and Bargmann 2005; Pujol et al. 2001; Tenor and Aballay 2007).

A recent study has identified the mechanism by which TOL-1 promotes behavioral avoidance of *S. marcescens* and in the process uncovered CO_2 detection as a new sensory modality underlying pathogen avoidance. TOL-1 is required for the function of the BAG neurons, ciliated chemosensory neurons that detect increases in CO_2 concentrations (Brandt and Ringstad 2015). The authors confirm that *tol-1* mutants are defective in the avoidance of *S.*

marcescens, and through cell-specific rescue and knock-down experiments show that *tol-1* acts in the BAG neurons to promote pathogen avoidance. GCY-9 mutant animals, which cannot detect CO_2, are also defective in avoidance of *S. marcescens*, confirming a role for CO_2 detection by the BAG neurons in avoidance behavior. Animals dwelling on non-pathogenic *E. coli* lawns also avoided *S. marcescens* odorant (containing 1% CO_2) in a TOL-1- and BAG-dependent manner, but did not avoid 1% CO_2 on its own, indicating that in the presence of pathogen-specific odors CO_2 may provide a necessary contextual cue that promotes lawn-leaving behavior (Brandt and Ringstad 2015).

In *C. elegans,* the NSY-1-SEK-1-PMK-1 mitogen-activated protein kinase (MAPK) cascade, homologous to the mammalian ASK1-MKK3-p38 MAPK pathway, has a conserved role in innate immune defense against pathogenic microbes (Kim et al. 2002). This MAPK pathway regulates expression of predicted antimicrobial factors, which may be secreted into the intestinal lumen to combat infection (Troemel et al. 2006). Tissue-specific rescue experiments of the MAPKK SEK-1 have revealed an additional role for this signaling cascade in the behavioral response to infection. *sek-1* mutants show enhanced susceptibility to killing by *P. aeruginosa*, and this phenotype is partially rescued by expressing *sek-1* either in the intestine or chemosensory neurons (Shivers et al. 2009). However in a killing assay where *P. aeruginosa* has been spread to the edges of the agar plate, making behavioral avoidance impossible for all strains, the *sek-1* intestinal rescue strain was comparable to wild type, whereas the *sek-1* neuronal rescue strain showed no difference relative to the *sek-1* mutant (Shivers et al. 2009). In addition, the induction of *tph-1* on *P. aeruginosa* was shown to be dependent on the NSY-1-SEK-1 MAPK cascade (Shivers et al. 2009). TIR-1 is the *C. elegans* homolog of the mammalian TIR

domain adaptor protein SARM, which in mammals mediates responses to viruses in the central nervous system (Carty et al. 2014), and in *C. elegans* is required for resistance to bacterial and fungal pathogens (Liberati et al. 2004; Couillault et al. 2004). Upregulation of *tph-1* in response to *P. aeruginosa* exposure requires TIR-1 (Shivers et al. 2009), supporting a model in which a TIR-1-NSY-1-SEK-1-MAPK cascade acts in the nervous system to promote behavioral avoidance of pathogens and host survival.

When *C. elegans* are exposed to the bacterial pathogen *Microbacterium nematophilum,* which adheres to the cuticle around the rectal opening, animals mount an innate immune response that involves swelling of the anal region (Hodgkin, Kuwabara, and Corneliussen 2000). After four hours *C. elegans* will also exhibit lawn-leaving of pathogenic *M. nematophilum* and increase their locomotion rate (Yook and Hodgkin 2007; McMullan, Anderson, and Nurrish 2012). Both the behavioral and innate immune responses to *M. nematophilum* require the Gaq protein EGL-30, which acts in a G-protein coupled regulatory cascade presumably downstream of one or more unidentified G-protein coupled receptors (McMullan, Anderson, and Nurrish 2012). Through tissue specific rescue experiments, McMullan et al. show that EGL-30 acts in the cholinergic motor neurons to mediate the behavioral responses to infection and independently in the rectal epithelial cells to promote innate immunity (McMullan, Anderson, and Nurrish 2012). Thus a Gaq-RhoGEF Trio-Rho signaling cascade is another example of a conserved signaling pathway acting in a tissue specific manner to regulate *C. elegans* behavior and innate immunity in response to infection.

Genetic Variation in Pathogen Avoidance Behavior

The study of laboratory-derived mutants from forward genetic screens has provided the foundation for studies of behavior in *C. elegans*. However naturally occurring polymorphisms that have arisen through evolution provide the opportunity for studying the driving forces in animal behavior, although such examples are rare (Bendesky et al. 2011; Osborne et al. 1997). One might expect wild isolates of *C. elegans* that have evolved with geographically distinct microbial ecologies to differ in their behavioral responses to pathogenic bacteria. Such behaviors may be under strong positive selection as pathogen avoidance confers dramatic survival increases. Indeed, the importance of avoidance behavior has been underscored by the characterization of polymorphisms and their mechanisms of action that underlie natural variation in pathogen resistance.

Polymorphisms between the Bristol N2 and Hawaiian strains of *C. elegans* have revealed evolutionary-derived differences in lawn-leaving behavior and survival on *P. aeruginosa* (Reddy et al. 2009; H. C. Chang, Paek, and Kim 2011). In the case of E3 ubiquitin ligase HECW-1, two naturally occurring polymorphisms were identified in a number of *C. elegans* wild isolates. Both polymorphisms resulted in amino acid changes that increased the activity of HECW-1 relative to that seen in the N2 strain, thus inhibiting lawn avoidance of *P. aeruginosa* (H. C. Chang, Paek, and Kim 2011). In the case of the *npr-1* gene, which promotes lawn avoidance of *P. aeruginosa*, the polymorphism between the N2 and Hawaiian strains had previously been identified as the causative mutation in the bordering and aggregation phenotypic differences between these strains (de Bono and Bargmann 1998). Subsequently, polymorphisms between N2 and Hawaiian strains in the globin domain protein *glb-5* and the GABA receptor *exp-1* have also been shown to affect

bordering and aggregation (Bendesky et al. 2012; McGrath et al. 2009; Persson et al. 2009), and may therefore be further examples of polymorphisms that affect pathogen avoidance.

Two additional studies have revealed natural variation in the behavioral responses to pathogens. When naïve *C. elegans* are subjected to a choice assay between *S. marcescens* and *E. coli*, innate olfactory preference drives animals towards *S. marcescens*. However when an array of *C. elegans* wild isolates were assayed, N2 animals were shown to prefer the odors of *S. marcescens* more dramatically than other strains, while the Hawaiian strain preferred *S. marcescens* odors the least (Glater, Rockman, and Bargmann 2014). In addition to innate olfactory preference, aversive learning to pathogenic bacteria may also be subject to natural variation. When a panel of *C. elegans* wild isolates was exposed to a choice assay between pathogenic and non-pathogenic strains of *Bacillus thuringiensis*, after 24 hours animals had largely avoided the pathogenic lawn. However these strains displayed reproducible variation in this response that correlated with their resistance to infection (Schulenburg and Müller 2004). These data suggest considerable natural variation in *C. elegans* behavioral responses to pathogenic bacteria, and genetic interrogation of these phenotypic differences may provide insights into the evolution of animal behavior.

Concluding Remarks

As a soil-dwelling animal that must seek out bacteria for nutrition but can also be infected by environmental pathogens, *C. elegans* is well suited for the study of microbial discrimination. The relatively simple nervous system of *C. elegans* uses chemosensation of water-soluble and volatile cues, mechanosensation, and aerotaxis behavior to navigate its microbial environment, seeking out bacterial food. However many environmental microbes can infect *C. elegans* and trigger a protective behavioral avoidance response that requires modulation of the aforementioned attractive behaviors. What are the cues associated with pathogenic bacteria that *C. elegans* respond to? How does *C. elegans* modulate existing behavioral circuits in the presence of pathogenic bacteria? The study of pathogen avoidance of *C. elegans* has defined neuronal circuits required for olfactory learning, but do similar mechanisms exist for modulating aerotaxis and mechanosensory behaviors?

In this thesis I define a neuroendocrine response to pathogen exposure that is amenable to genetic interrogation. Specifically, I show in Chapter Two that the neuropeptide DAF-7/TGF-β is expressed in the ASJ chemosensory neurons following exposure to *P. aeruginosa.* Expression of DAF-7 modulates the animal's aerotaxis behavior promoting pathogen avoidance. We identify two specific secondary metabolites of *P. aeruginosa*, pyochelin and phenazine-1-carboxamide, which the ASJ neurons detect and use as cues to activate DAF-7 signaling. To identify genes *C. elegans* uses to couple microbial detection to *daf-7* transcription, I screened for mutants defective in *daf-7* expression in the ASJ neurons on *P. aeruginosa.* In Chapter Two I describe genes that act cell-autonomously in the ASJ neurons to activate DAF-7, such as the G protein alpha subunits GPA-2 and GPA-3. In Chapter Three I discuss the lithium-sensitive

phosphatase BPNT-1, which is required not only for *daf-7* transcription in ASJ, but for the global activity of the ASJ neurons. The study of BPNT-1 activity in ASJ leads to a hypothesis for how lithium may be exerting its effects on the nervous system. Finally, in Chapter Four, I discuss the future directions for this project including other genes required for the response to *P. aeruginosa* in the ASJ neurons.

References

Avery, L, and H R Horvitz. 1990. "Effects of Starvation and Neuroactive Drugs on Feeding in Caenorhabditis Elegans.." *The Journal of Experimental Zoology* 253 (3): 263–70. doi:10.1002/jez.1402530305.

Bargmann, C I, and H R Horvitz. 1991. "Chemosensory Neurons with Overlapping Functions Direct Chemotaxis to Multiple Chemicals in C. Elegans.." *Neuron* 7 (5): 729–42.

Bargmann, C I, E Hartwieg, and H R Horvitz. 1993. "Odorant-Selective Genes and Neurons Mediate Olfaction in C. Elegans.." *Cell* 74 (3): 515–27.

Bargmann, Cornelia I. 2012. "Beyond the Connectome: How Neuromodulators Shape Neural Circuits.." *BioEssays : News and Reviews in Molecular, Cellular and Developmental Biology* 34 (6): 458–65. doi:10.1002/bies.201100185.

Beale, E, G Li, M W Tan, and K P Rumbaugh. 2006. "Caenorhabditis Elegans Senses Bacterial Autoinducers." *Applied and Environmental Microbiology* 72 (7): 5135–37. doi:10.1128/AEM.00611-06.

Bendesky, Andres, Jason Pitts, Matthew V Rockman, William C Chen, Man-Wah Tan, Leonid Kruglyak, and Cornelia I Bargmann. 2012. "Long-Range Regulatory Polymorphisms Affecting a GABA Receptor Constitute a Quantitative Trait Locus (QTL) for Social Behavior in Caenorhabditis Elegans." Edited by Marc Hammarlund. *PLoS Genetics* 8 (12): e1003157. doi:10.1371/journal.pgen.1003157.s005.

Bendesky, Andres, Makoto Tsunozaki, Matthew V Rockman, Leonid Kruglyak, and Cornelia I Bargmann. 2011. "Catecholamine Receptor Polymorphisms Affect Decision-Making in C. Elegans." *Nature*, March. Nature Publishing Group, 1–7. doi:10.1038/nature09821.

Brandt, Julia P, and Niels Ringstad. 2015. "Toll-Like Receptor Signaling Promotes Development and Function of Sensory Neurons Required for a C. Elegans Pathogen-Avoidance Behavior.." *Current Biology : CB* 25 (17): 2228–37. doi:10.1016/j.cub.2015.07.037.

Brenner, S. 1974. "The Genetics of Caenorhabditis Elegans.." *Genetics* 77 (1): 71–94.

Carty, Michael, Line Reinert, Søren R Paludan, and Andrew G Bowie. 2014. "Innate Antiviral Signalling in the Central Nervous System." *Trends in Immunology* 35 (2). Elsevier Ltd: 79–87. doi:10.1016/j.it.2013.10.012.

Cassada, R C, and R L Russell. 1975. "The Dauerlarva, a Post-Embryonic Developmental Variant of the Nematode Caenorhabditis Elegans.." *Developmental Biology* 46 (2): 326–42.

Chalasani, Sreekanth H, Nikos Chronis, Makoto Tsunozaki, Jesse M Gray, Daniel Ramot, Miriam B Goodman, and Cornelia I Bargmann. 2007. "Dissecting a Circuit for Olfactory

Behaviour in Caenorhabditis Elegans.." *Nature* 450 (7166): 63–70. doi:10.1038/nature06292.

Chalasani, Sreekanth H, Saul Kato, Dirk R Albrecht, Takao Nakagawa, L F Abbott, and Cornelia I Bargmann. 2010. "Neuropeptide Feedback Modifies Odor-Evoked Dynamics in Caenorhabditis Elegans Olfactory Neurons.." *Nature Publishing Group* 13 (5): 615–21. doi:10.1038/nn.2526.

Chang, Andy J, Nikolas Chronis, David S Karow, Michael A Marletta, and Cornelia I Bargmann. 2006. "A Distributed Chemosensory Circuit for Oxygen Preference in C. Elegans." *PLoS Biology* 4 (9): e274. doi:10.1371/journal.pbio.0040274.st003.

Chang, Howard C, Jennifer Paek, and Dennis H Kim. 2011. "Natural Polymorphisms in C. Elegans HECW-1 E3 Ligase Affect Pathogen Avoidance Behaviour.." *Nature* 480 (7378): 525–29. doi:10.1038/nature10643.

Chen, Zhunan, Michael Hendricks, Astrid Cornils, Wolfgang Maier, Joy Alcedo, and Yun Zhang. 2013. "Two Insulin-Like Peptides Antagonistically Regulate Aversive Olfactory Learning in C. Elegans." *Neuron* 77 (3). Elsevier: 572–85. doi:10.1016/j.neuron.2012.11.025.

Cheong, Mi Cheong, Alexander B Artyukhin, Young-jai You, and Leon Avery. 2015. "An Opioid-Like System Regulating Feeding Behavior in C. Elegans.." *eLife* 4. doi:10.7554/eLife.06683.

Cheung, Benny H H, Fausto Arellano-Carbajal, Irene Rybicki, and Mario de Bono. 2004. "Soluble Guanylate Cyclases Act in Neurons Exposed to the Body Fluid to Promote C. Elegans Aggregation Behavior.." *Current Biology : CB* 14 (12): 1105–11. doi:10.1016/j.cub.2004.06.027.

Clemente, Jose C, Luke K Ursell, Laura Wegener Parfrey, and Rob Knight. 2012. "The Impact of the Gut Microbiota on Human Health: an Integrative View.." *Cell* 148 (6): 1258–70. doi:10.1016/j.cell.2012.01.035.

Couillault, Carole, Nathalie Pujol, Jérôme Reboul, Laurence Sabatier, Jean-François Guichou, Yuji Kohara, and Jonathan J Ewbank. 2004. "TLR-Independent Control of Innate Immunity in Caenorhabditis Elegans by the TIR Domain Adaptor Protein TIR-1, an Ortholog of Human SARM." *Nature Immunology* 5 (5): 488–94. doi:10.1038/ni1060.

Curtis, Valerie A. 2014. "Infection-Avoidance Behaviour in Humans and Other Animals.." *Trends in Immunology* 35 (10): 457–64. doi:10.1016/j.it.2014.08.006.

de Bono, M, and C I Bargmann. 1998. "Natural Variation in a Neuropeptide Y Receptor Homolog Modifies Social Behavior and Food Response in C. Elegans.." *Cell* 94 (5): 679–89.

Félix, Marie-Anne, and Fabien Duveau. 2012. "Population Dynamics and Habitat Sharing Ofnatural Populations of Caenorhabditis Elegans andC. Briggsae." *BMC Biology* 10 (1).

BioMed Central Ltd: 59. doi:10.1186/1741-7007-10-59.

Flavell, Steven W, Navin Pokala, Evan Z Macosko, Dirk R Albrecht, Johannes Larsch, and Cornelia I Bargmann. 2013. "Serotonin and the Neuropeptide PDF Initiate and Extend Opposing Behavioral States in C. Elegans.." *Cell* 154 (5): 1023–35. doi:10.1016/j.cell.2013.08.001.

Garsin, D A, C D Sifri, E Mylonakis, X Qin, K V Singh, B E Murray, S B Calderwood, and F M Ausubel. 2001. "A Simple Model Host for Identifying Gram-Positive Virulence Factors.." *Proceedings of the National Academy of Sciences of the United States of America* 98 (19): 10892–97. doi:10.1073/pnas.191378698.

Glater, Elizabeth E, Matthew V Rockman, and Cornelia I Bargmann. 2014. "Multigenic Natural Variation Underlies Caenorhabditis Elegans Olfactory Preference for the Bacterial Pathogen Serratia Marcescens.." *G3 (Bethesda, Md.)* 4 (2): 265–76. doi:10.1534/g3.113.008649.

Gray, Jesse M, David S Karow, Hang Lu, Andy J Chang, Jennifer S Chang, Ronald E Ellis, Michael A Marletta, and Cornelia I Bargmann. 2004. "Oxygen Sensation and Social Feeding Mediated by a C. Elegans Guanylate Cyclase Homologue.." *Nature* 430 (6997): 317–22. doi:10.1038/nature02714.

Grenham, Sue, Gerard Clarke, John F Cryan, and Timothy G Dinan. 2011. "Brain-Gut-Microbe Communication in Health and Disease.." *Frontiers in Physiology* 2: 94. doi:10.3389/fphys.2011.00094.

Ha, Heon-ick, Michael Hendricks, Yu Shen, Christopher V Gabel, Christopher Fang-Yen, Yuqi Qin, Daniel Colón-Ramos, Kang Shen, Aravinthan D T Samuel, and Yun Zhang. 2010. "Functional Organization of a Neural Network for Aversive Olfactory Learning in Caenorhabditis Elegans." *Neuron* 68 (6). Elsevier Inc.: 1173–86. doi:10.1016/j.neuron.2010.11.025.

Harris, G, Y Shen, H Ha, A Donato, S Wallis, X Zhang, and Y Zhang. 2014. "Dissecting the Signaling Mechanisms Underlying Recognition and Preference of Food Odors." *Journal of Neuroscience* 34 (28): 9389–9403. doi:10.1523/JNEUROSCI.0012-14.2014.

Hedgecock, E M, and R L Russell. 1975. "Normal and Mutant Thermotaxis in the Nematode Caenorhabditis Elegans.." *Proceedings of the National Academy of Sciences of the United States of America* 72 (10): 4061–65.

Hodgkin, J, P E Kuwabara, and B Corneliussen. 2000. "A Novel Bacterial Pathogen, Microbacterium Nematophilum, Induces Morphological Change in the Nematode C. Elegans.." *Current Biology : CB* 10 (24): 1615–18.

Jansson, H B. 1994. "Adhesion of Conidia of Drechmeria Coniospora to Caenorhabditis Elegans Wild Type and Mutants.." *Journal of Nematology* 26 (4): 430–35.

Jin, Xin, Navin Pokala, and Cornelia I Bargmann. 2016. "Distinct Circuits for the Formation and Retrieval of an Imprinted Olfactory Memory.." *Cell* 164 (4): 632–43. doi:10.1016/j.cell.2016.01.007.

Kim, Dennis H, Rhonda Feinbaum, Geneviève Alloing, Fred E Emerson, Danielle A Garsin, Hideki Inoue, Miho Tanaka-Hino, et al. 2002. "A Conserved P38 MAP Kinase Pathway in Caenorhabditis Elegans Innate Immunity.." *Science* 297 (5581): 623–26. doi:10.1126/science.1073759.

Liberati, Nicole T, Katherine A Fitzgerald, Dennis H Kim, Rhonda Feinbaum, Douglas T Golenbock, and Frederick M Ausubel. 2004. "Requirement for a Conserved Toll/Interleukin-1 Resistance Domain Protein in the Caenorhabditis Elegans Immune Response.." *Proceedings of the National Academy of Sciences of the United States of America* 101 (17): 6593–98. doi:10.1073/pnas.0308625101.

Lyte, Mark. 2013. "Microbial Endocrinology in the Microbiome-Gut-Brain Axis: How Bacterial Production and Utilization of Neurochemicals Influence Behavior." Edited by Virginia Miller. *PLoS Pathogens* 9 (11): e1003726. doi:10.1371/journal.ppat.1003726.

Maguire, Sean M, Christopher M Clark, John Nunnari, Jennifer K Pirri, and Mark J Alkema. 2011. "The C. Elegans Touch Response Facilitates Escape From Predacious Fungi.." *Current Biology : CB* 21 (15): 1326–30. doi:10.1016/j.cub.2011.06.063.

McGrath, Patrick T, Matthew V Rockman, Manuel Zimmer, Heeun Jang, Evan Z Macosko, Leonid Kruglyak, and Cornelia I Bargmann. 2009. "Quantitative Mapping of a Digenic Behavioral Trait Implicates Globin Variation in C. Elegans Sensory Behaviors." *Neuron* 61 (5). Elsevier Ltd: 692–99. doi:10.1016/j.neuron.2009.02.012.

McMullan, Rachel, Alexandra Anderson, and Stephen Nurrish. 2012. "Behavioral and Immune Responses to Infection Require Gαq- RhoA Signaling in C. Elegans." Edited by Frederick M Ausubel. *PLoS Pathogens* 8 (2): e1002530. doi:10.1371/journal.ppat.1002530.s003.

Melo, Justine A, and Gary Ruvkun. 2012. "Inactivation of Conserved C. Elegans Genes Engages Pathogen- and Xenobiotic-Associated Defenses.." *Cell* 149 (2): 452–66. doi:10.1016/j.cell.2012.02.050.

Osborne, K A, A Robichon, E Burgess, S Butland, R A Shaw, A Coulthard, H S Pereira, R J Greenspan, and M B Sokolowski. 1997. "Natural Behavior Polymorphism Due to a cGMP-Dependent Protein Kinase of Drosophila.." *Science* 277 (5327): 834–36.

Persson, Annelie, Einav Gross, Patrick Laurent, Karl Emanuel Busch, Hugo Bretes, and Mario de Bono. 2009. "Natural Variation in a Neural Globin Tunes Oxygen Sensing in Wild Caenorhabditis Elegans." *Nature* 458 (7241). Nature Publishing Group: 1030–33. doi:10.1038/nature07820.

Pradel, Elizabeth, Yun Zhang, Nathalie Pujol, Tohey Matsuyama, Cornelia I Bargmann, and Jonathan J Ewbank. 2007. "Detection and Avoidance of a Natural Product From the Pathogenic Bacterium Serratia Marcescens by Caenorhabditis Elegans.." *Proceedings of the National Academy of Sciences of the United States of America* 104 (7): 2295–2300. doi:10.1073/pnas.0610281104.

Pujol, N, E M Link, L X Liu, C L Kurz, G Alloing, M W Tan, K P Ray, R Solari, C D Johnson, and J J Ewbank. 2001. "A Reverse Genetic Analysis of Components of the Toll Signaling Pathway in Caenorhabditis Elegans.." *Current Biology : CB* 11 (11): 809–21.

Reddy, Kirthi C, Erik C Andersen, Leonid Kruglyak, and Dennis H Kim. 2009. "A Polymorphism in Npr-1 Is a Behavioral Determinant of Pathogen Susceptibility in C. Elegans.." *Science* 323 (5912): 382–84. doi:10.1126/science.1166527.

Reddy, Kirthi C, Ryan C Hunter, Nikhil Bhatla, Dianne K Newman, and Dennis H Kim. 2011. "Caenorhabditis Elegans NPR-1-Mediated Behaviors Are Suppressed in the Presence of Mucoid Bacteria.." *Proceedings of the National Academy of Sciences* 108 (31): 12887–92. doi:10.1073/pnas.1108265108.

Rubio-Godoy, M, R Aunger, and V Curtis. 2007. "Serotonin – a Link Between Disgust and Immunity?." *Medical Hypotheses* 68 (1): 61–66. doi:10.1016/j.mehy.2006.06.036.

Saeki, S, M Yamamoto, and Y Iino. 2001. "Plasticity of Chemotaxis Revealed by Paired Presentation of a Chemoattractant and Starvation in the Nematode Caenorhabditis Elegans.." *The Journal of Experimental Biology* 204 (Pt 10): 1757–64.

Sawin, E R, R Ranganathan, and H R Horvitz. 2000. "C. Elegans Locomotory Rate Is Modulated by the Environment Through a Dopaminergic Pathway and by Experience Through a Serotonergic Pathway.." *Neuron* 26 (3): 619–31.

Schulenburg, H, and S Müller. 2004. "Natural Variation in the Response of Caenorhabditis Elegans Towards Bacillus Thuringiensis.." *Parasitology* 128 (Pt 4): 433–43.

Sengupta, P, J H Chou, and C I Bargmann. 1996. "Odr-10 Encodes a Seven Transmembrane Domain Olfactory Receptor Required for Responses to the Odorant Diacetyl.." *Cell* 84 (6): 899–909.

Shivers, Robert P, Tristan Kooistra, Stephanie W Chu, Daniel J Pagano, and Dennis H Kim. 2009. "Tissue-Specific Activities of an Immune Signaling Module Regulate Physiological Responses to Pathogenic and Nutritional Bacteria in C. Elegans." *Cell Host and Microbe* 6 (4). Elsevier Ltd: 321–30. doi:10.1016/j.chom.2009.09.001.

Shtonda, Boris Borisovich, and Leon Avery. 2006. "Dietary Choice Behavior in Caenorhabditis Elegans.." *The Journal of Experimental Biology* 209 (Pt 1): 89–102. doi:10.1242/jeb.01955.

Stensmyr, Marcus C, Hany K M Dweck, Abu Farhan, Irene Ibba, Antonia Strutz, Latha Mukunda, Jeanine Linz, et al. 2012. "A Conserved Dedicated Olfactory Circuit for Detecting Harmful Microbes in Drosophila.." *Cell* 151 (6): 1345–57. doi:10.1016/j.cell.2012.09.046.

Tan, M W, S Mahajan-Miklos, and F M Ausubel. 1999. "Killing of Caenorhabditis Elegans by Pseudomonas Aeruginosa Used to Model Mammalian Bacterial Pathogenesis.." *Proceedings of the National Academy of Sciences of the United States of America* 96 (2): 715–20.

Tenor, Jennifer L, and Alejandro Aballay. 2007. "A Conserved Toll-Like Receptor Is Required for Caenorhabditis Elegans Innate Immunity." *EMBO Reports* 9 (1): 103–9. doi:10.1038/sj.embor.7401104.

Thomas, James H, and Hugh M Robertson. 2008. "The Caenorhabditis Chemoreceptor Gene Families.." *BMC Biology* 6: 42. doi:10.1186/1741-7007-6-42.

Tremaroli, Valentina, and Fredrik Bäckhed. 2012. "Functional Interactions Between the Gut Microbiota and Host Metabolism.." *Nature* 489 (7415): 242–49. doi:10.1038/nature11552.

Trent, C. 1982. "Genetic and Behavioral Studies of the Egg-Laying System in *Caenorhabditis Elegans*." *Thesis (Ph. D.)-Massachusetts Institute of Technology, Dept. of Biology*, June, 1–126.

Troemel, E R, B E Kimmel, and C I Bargmann. 1997. "Reprogramming Chemotaxis Responses: Sensory Neurons Define Olfactory Preferences in C. Elegans.." *Cell* 91 (2): 161–69.

Troemel, E R, J H Chou, N D Dwyer, H A Colbert, and C I Bargmann. 1995. "Divergent Seven Transmembrane Receptors Are Candidate Chemosensory Receptors in C. Elegans.." *Cell* 83 (2): 207–18.

Troemel, Emily R, Marie-Anne Félix, Noah K Whiteman, Antoine Barrière, and Frederick M Ausubel. 2008. "Microsporidia Are Natural Intracellular Parasites of the Nematode Caenorhabditis Elegans." Edited by Gary E Ward. *PLoS Biology* 6 (12): e309. doi:10.1371/journal.pbio.0060309.sg002.

Troemel, Emily R, Stephanie W Chu, Valerie Reinke, Siu Sylvia Lee, Frederick M Ausubel, and Dennis H Kim. 2006. "P38 MAPK Regulates Expression of Immune Response Genes and Contributes to Longevity in C. Elegans." *PLoS Genetics* 2 (11): e183. doi:10.1371/journal.pgen.0020183.st007.

Wen, J Y, N Kumar, G Morrison, G Rambaldini, S Runciman, J Rousseau, and D van der Kooy. 1997. "Mutations That Prevent Associative Learning in C. Elegans.." *Behavioral Neuroscience* 111 (2): 354–68.

White, J G, E Southgate, J N Thomson, and S Brenner. 1986. "The Structure of the Nervous System of the Nematode Caenorhabditis Elegans.." *Philosophical Transactions of the Royal*

Society of London. Series B, Biological Sciences 314 (1165): 1–340.

Yook, K, and J Hodgkin. 2007. "Mos1 Mutagenesis Reveals a Diversity of Mechanisms Affecting Response of Caenorhabditis Elegans to the Bacterial Pathogen Microbacterium Nematophilum." *Genetics* 175 (2): 681–97. doi:10.1534/genetics.106.060087.

Zhang, Xiaodong, and Yun Zhang. 2012. "DBL-1, a TGF-B, Is Essential for Caenorhabditis Elegans Aversive Olfactory Learning.." *Proceedings of the National Academy of Sciences* 109 (42): 17081–86. doi:10.1073/pnas.1205982109.

Zhang, Yun, Hang Lu, and Cornelia I Bargmann. 2005. "Pathogenic Bacteria Induce Aversive Olfactory Learning in Caenorhabditis Elegans." *Nature* 438 (7065): 179–84. doi:10.1038/nature04216.

Chapter Two

Chemosensation of Bacterial Secondary Metabolites Modulates Neuroendocrine Signaling and Behavior of *C. elegans*

Joshua D. Meisel, Oishika Panda, Parag Mahanti,

Frank C. Schroeder, and Dennis H. Kim

This chapter was originally published as: Meisel JD, Panda O, Mahanti P, Schroeder FC, and Kim DH. (2014) Chemosensation of Bacterial Secondary Metabolites Modulates Neuroendocrine Signaling and Behavior of *C. elegans*. **Cell** 159(2): 267-80.

Summary

Discrimination among pathogenic and beneficial microbes is essential for host organism immunity and homeostasis. Here, we show that chemosensory detection of two secondary metabolites produced by *Pseudomonas aeruginosa* modulates a neuroendocrine signaling pathway that promotes avoidance behavior in the simple animal host *Caenorhabditis elegans*. Secondary metabolites phenazine-1-carboxamide and pyochelin activate a G protein-signaling pathway in the ASJ chemosensory neuron pair that induces expression of the neuromodulator DAF-7/TGF-β. DAF-7, in turn, activates a canonical TGF-β signaling pathway in adjacent interneurons to modulate aerotaxis behavior and promote avoidance of pathogenic *P. aeruginosa*. Our data provide a chemical, genetic, and neuronal basis for how the behavior and physiology of a simple animal host can be modified by the microbial environment, and suggest that secondary metabolites produced by microbes may provide environmental cues that contribute to pathogen recognition and host survival.

Graphical Abstract

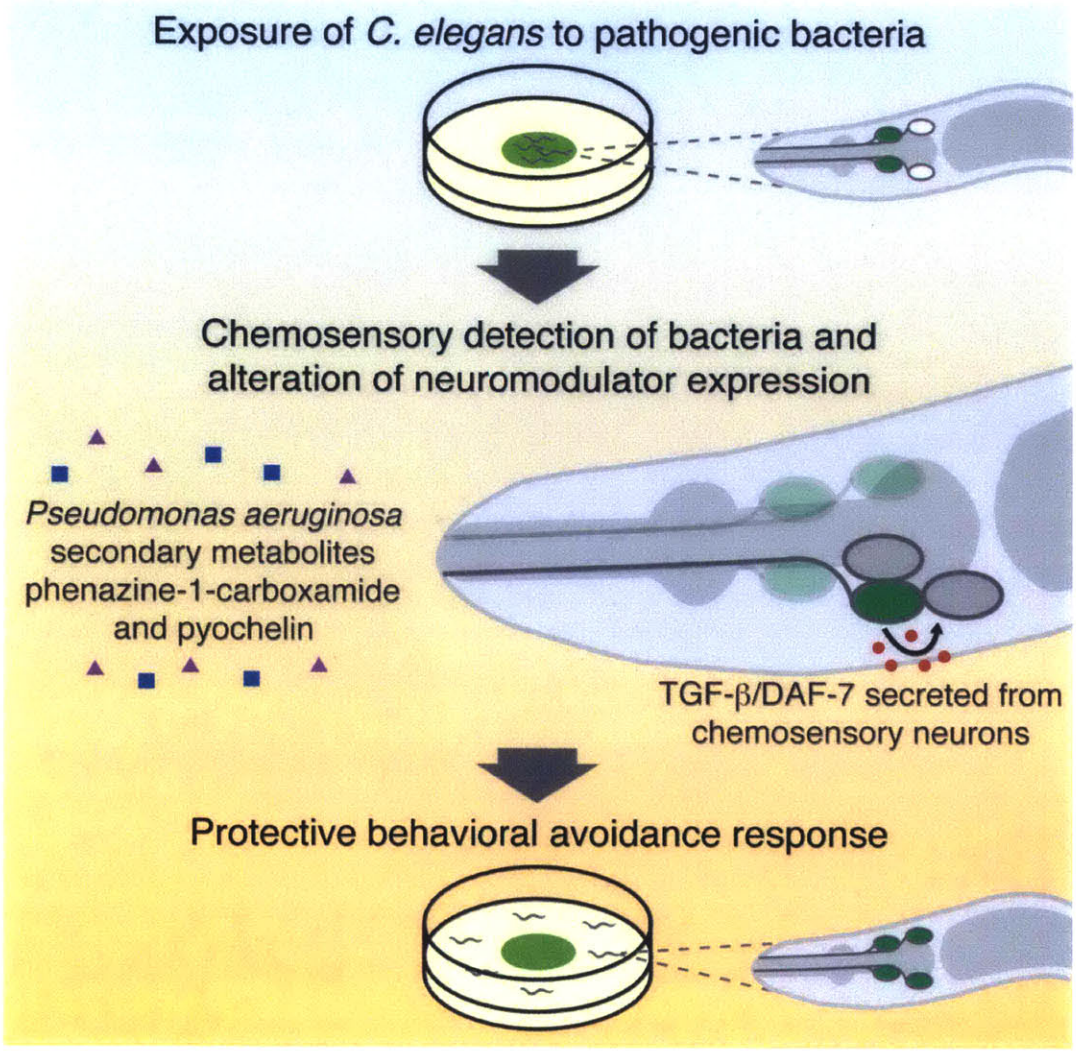

Introduction

The recognition of microbial pathogens and the corresponding danger they represent is essential for the survival of host organisms. Innate immune systems have evolved to respond to foreign structures derived from microbes, which help the host distinguish microbes from self. However, such molecular patterns do not necessarily help the host discriminate a microbe that is pathogenic from one that is commensal. Microbial molecular patterns such as lipopolysaccharide are found on pathogen and commensal alike. In view of the diversity of olfactory receptors present even in relatively simple host organisms, chemosensory responses offer the potential to detect a far greater set of relevant microbial molecules. Candidate receptors and specific bacterial cues that modulate host physiology and avoidance behavior have begun to be explored (Pradel et al. 2007; Rivière et al. 2009; Stensmyr et al. 2012).

The soil dwelling nematode *Caenorhabditis elegans* is a simple host organism that forages on decomposing organic matter for bacterial food (Félix and Duveau 2012). The presence of bacterial food affects diverse behaviors of *C. elegans* such as feeding, locomotion, thermotaxis, and aerotaxis (Avery and Horvitz 1990; A. J. Chang et al. 2006; Hedgecock and Russell 1975; Sawin, Ranganathan, and Horvitz 2000), and differences in the species composition of the food supply can alter aspects of their physiology and behavior (Gusarov et al. 2013; MacNeil et al. 2013; Shtonda and Avery 2006; Watson et al. 2014). Pathogenic bacteria kill *C. elegans* and induce an aversive learning response (Y. Zhang, Lu, and Bargmann 2005) that promotes protective behavioral avoidance (H. C. Chang, Paek, and Kim 2011; Pradel et al. 2007; Pujol et al. 2001; Reddy et al. 2009). Bacterial molecules including *Serratia marcescens* serrawettin and *Pseudomonas aeruginosa* quorum-sensing regulators have been implicated in the

behavioral avoidance of bacterial lawns (Beale et al. 2006; Pradel et al. 2007). As such, *C. elegans* is emerging as a useful model for dissecting the genetic and biochemical mechanisms underlying microbial discrimination in animal hosts.

In this study we focus on how the DAF-7/TGF-β pathway functions in chemosensory neurons of *C. elegans* to regulate behavior in response to changes in the microbial environment. DAF-7 functions in the neuroendocrine regulation of diverse aspects of organismal development and physiology, including the dauer developmental decision, foraging and aggregation behaviors, quiescence, metabolism, and longevity (de Bono et al. 2002; Gallagher et al. 2013; Greer et al. 2008; Milward et al. 2011; Shaw et al. 2007; Swanson and Riddle 1981). In addition, another *C. elegans* TGF-β-family ligand, DBL-1, has been shown to regulate olfactory aversive learning and antifungal defenses (X. Zhang and Zhang 2012; Zugasti and Ewbank 2009). Expression of *daf-7* is limited to the ASI pair of chemosensory neurons and has been shown to respond to the availability of bacterial food (Ren et al. 1996; Schackwitz, Inoue, and Thomas 1996). Here, we show that chemosensory recognition of the pathogenic bacterium *P. aeruginosa* dramatically alters the neuronal expression pattern of DAF-7 to promote avoidance behavior. Through a forward genetic screen we identify conserved components of G protein signaling that act cell-autonomously in the ASJ neurons to activate transcription of *daf-7* in response to *P. aeruginosa*. Finally, we show that the ASJ neurons respond to the secondary metabolites phenazine-1-carboxamide and pyochelin secreted by *P. aeruginosa* during stationary phase. Our findings demonstrate how specific bacteria can exert effects on host behavior and physiology, and point to how secondary metabolites may serve as environmental cues that contribute to pathogen discrimination and avoidance.

Results

DAF-7/TGF-β is required for behavioral avoidance of *Pseudomonas aeruginosa*

We previously observed that mutants defective in the DAF-7/TGF-β pathway display enhanced susceptibility to infection by *P. aeruginosa* (Reddy et al. 2009). In the standard pathogenesis assay, *daf-7* mutants die faster than the wild-type strain N2 and exhibit a failure to avoid the bacterial lawn (Figures 1A and 1C). Initially, animals begin inside the lawn, but by 15 h wild-type N2 animals avoid the lawn of pathogenic bacteria, while *daf-7* mutants remain inside the lawn of *P. aeruginosa* (Figures 1C and 1D). In a modified pathogenesis assay in which *C. elegans* are unable to avoid the lawn of pathogenic bacteria, *daf-7* mutants display the same susceptibility phenotype as wild-type animals, demonstrating that the failure to avoid *P. aeruginosa* is the principal determinant in the susceptibility to infection of *daf-7* animals (Figure 1B). We also confirmed that *daf-7* animals were indeed being exposed to a higher dose of pathogenic bacteria by repeating the experiment with a *P. aeruginosa* lawn containing red fluorescent beads that serve as markers of the bacterial load in the intestine (Figure S1A).

Once secreted, DAF-7 binds to the TGF-β type I receptor DAF-1 and the TGF-β type II receptor DAF-4, which then act to antagonize the co-SMAD DAF-3 (Figure 1E) (Estevez et al. 1993; Georgi, Albert, and Riddle 1990; Patterson et al. 1997). Other mutants in the DAF-7/TGF-β-signaling pathway such as *daf-1* and the R-SMAD *daf-8* also display *P. aeruginosa* avoidance defects (Figure S1B), and we observed complete suppression of the *daf-7(ok3125)* avoidance defect by a mutation in *daf-3* (Figure 1D). These results indicate that the DAF-7 pathway is specifically required for avoidance of *P. aeruginosa*, functioning through the canonical DAF-3 signaling pathway to promote survival by limiting host exposure to pathogenic bacteria.

Figure 1

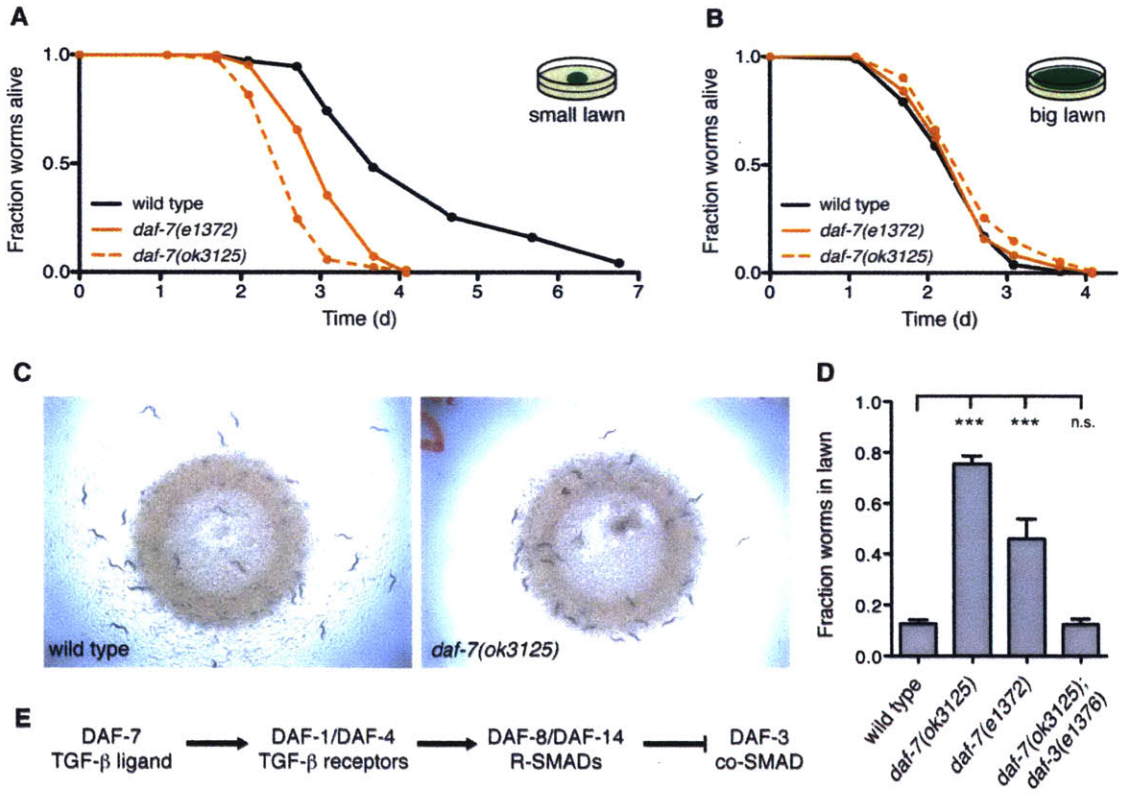
A
Fraction worms alive
1.0
0.5
0.0
0
1
2
3
4
5
6
7
Time (d)
wild type
daf-7(e1372)
daf-7(ok3125)
small lawn
B
Fraction worms alive
1.0
0.5
0.0
0
1
2
3
4
Time (d)
wild type
daf-7(e1372)
daf-7(ok3125)
big lawn
C
wild type
daf-7(ok3125)
D
Fraction worms in lawn
1.0
0.8
0.6
0.4
0.2
0.0
***
***
n.s.
wild type
daf-7(ok3125)
daf-7(e1372)
daf-7(ok3125); daf-3(e1376)
E
DAF-7
TGF-β ligand
DAF-1/DAF-4
TGF-β receptors
DAF-8/DAF-14
R-SMADs
DAF-3
co-SMAD

Figure 1. DAF-7/TGF-β is required for the protective behavioral avoidance response to *P. aeruginosa*

(A) Fraction animals alive after being transferred to plates seeded with *P. aeruginosa* strain PA14. (B) Fraction animals alive after being transferred to a "Big Lawn" of *P. aeruginosa* in which the bacteria has been spread to the edges of the plate. All data points represent the average of at least three independent replicates. (C) Photographs of wild-type and *daf-7* animals after 15 h exposure to *P. aeruginosa.* (D) Lawn occupancy of animals on *P. aeruginosa* after 15 h. *** $P < 0.001$ as determined by one-way ANOVA followed by Dunnett's Multiple Comparison Test. n.s. = not significant. Values represent means of at least three independent experiments. Error bars indicate standard error. See also Figure S1.

P. aeruginosa induces _daf-7_ expression in the ASJ neuron pair and promotes avoidance behavior

The TGF-β ligand *daf-7* was previously shown to be expressed exclusively in the ASI pair of ciliated chemosensory neurons, with expression levels responsive to changes in the availability of standard *E. coli* food and *C. elegans* pheromones (Ren et al. 1996; Schackwitz, Inoue, and Thomas 1996). To monitor *daf-7* expression in the presence of *P. aeruginosa* we used a transgenic strain carrying a *daf-7p::gfp* transcriptional reporter. Unexpectedly, we observed that exposure to *P. aeruginosa* induced fluorescence in four cells—the ASI neuron pair as well as a second bilaterally symmetric pair of ciliated chemosensory neurons (Figures 2A-2B). Through co-localization experiments with the lipophilic dye DiI, we identified the additional cells as the ASJ chemosensory neurons (Figures 2C-2F). We quantified the *daf-7p::gfp* fluorescence increase in the ASJ neurons and found that the reporter was induced at least 1000-fold on *P. aeruginosa* relative to *E. coli* (Figure 2G). We also observed that the *daf-7p::gfp* fluorescence in the ASI neurons increased 2-fold on *P. aeruginosa* (Figure 2G).

We used fluorescent *in situ* hybridization of mRNA molecules to corroborate our observations made with the *daf-7p::gfp* transcriptional reporter. We did not detect fluorescence in the ASJ neuron pair when the laboratory wild-type strain N2 was propagated on *E. coli* OP50 (Figures 2H and 2J). In contrast, upon exposure of *C. elegans* to *P. aeruginosa*, we observed *daf-7* mRNA expression in two additional cells corresponding to the ASJ neuron pair (Figures 2I and 2J). Confirming the specificity of the fluorescence for *daf-7* mRNA, we did not detect *daf-7* mRNA in a *daf-7(ok3125)* mutant strain carrying a 664 bp deletion, using probes designed to hybridize exclusively to the sequence within the deletion (Figure S2A). Of note, we observed

Figure 2

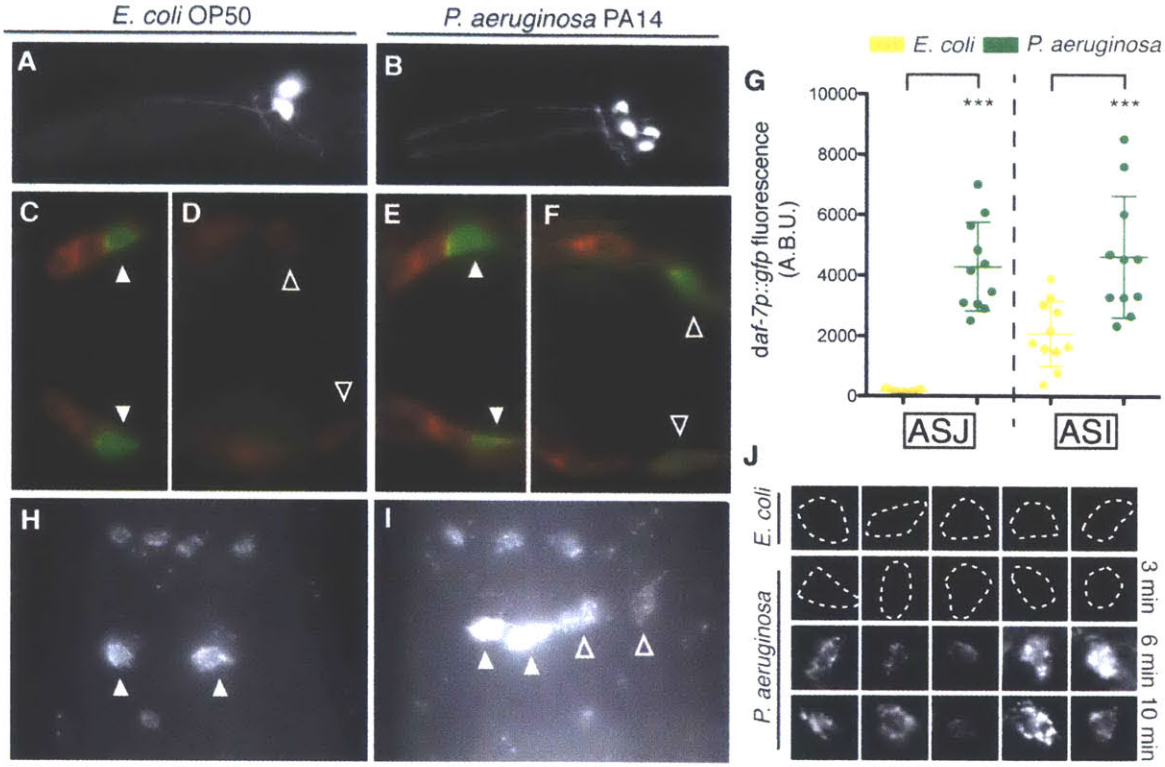
E. coli OP50
P. aeruginosa PA14
A
B
C
D
E
F
H
I
G
E. coli
P. aeruginosa
daf-7p::gfp fluorescence (A.B.U.)
10000
8000
6000
4000
2000
0
***
***
ASJ
ASI
J
E. coli
P. aeruginosa
3 min
6 min
10 min

Figure 2. *daf-7* expression is induced in the ASJ neurons upon exposure to *P. aeruginosa*

(A-B) *daf-7p::gfp* expression pattern in *C. elegans* on *E. coli* (A) and *P. aeruginosa* (B). (C-F) Co-localization of *daf-7p::gfp* expression and DiI staining (red) in animals on *E. coli,* dorsal view (C) and ventral view (D), and in animals on *P. aeruginosa,* dorsal view (E) and ventral view (F). Filled triangles indicate ASI neurons; empty triangles indicate ASJ neurons. (G) Maximum fluorescence values of *daf-7p::gfp* in the ASJ or ASI neurons after 16 h exposure to indicated bacteria. *** $P < 0.001$ as determined by one-way ANOVA followed by Tukey's Multiple Comparison Test. Error bars indicate standard deviation. (H-I) *daf-7* FISH in wild-type N2 animals on *E. coli* (H) and *P. aeruginosa* (I). Filled triangles indicate ASI neurons; empty triangles indicate ASJ neurons. Additional cells expressing *daf-7* mRNA are the OLQ neurons (top) and the ADE neurons (bottom). (J) *daf-7* FISH in the ASJ neurons (co-localized with *trx-1p::gfp*) on *E. coli* and *P. aeruginosa* after various exposure times. Dashed lines indicate cell boundaries. Each image represents an individual animal. See also Figure S2.

that when the wild-type strain was propagated on *E. coli*, in addition to previously described expression in the ASI neuron pair, *daf-7* mRNA was also present in six other sensory neurons, which we identified using reporter co-localization experiments as the ADE neuron pair and the OLQ neurons (Figures 2H-2I and S2B-S2G). ADE and OLQ are mechanosensory neurons that have been implicated in bacterial food sensing (Hart, Sims, and Kaplan 1995; Sawin, Ranganathan, and Horvitz 2000), and likely represent additional previously unknown sites of DAF-7/TGF-β expression.

To follow the kinetics of the endogenous *daf-7* transcriptional response to *P. aeruginosa* in the ASJ neurons, we fixed animals following exposures to *P. aeruginosa* ranging in duration from 3 min to 24 h and probed for *daf-7* mRNA. On *E. coli* or following a 3 min exposure to *P. aeruginosa* we did not detect *daf-7* mRNA in the ASJ neurons (Figure 2J). However after a 6 min exposure to *P. aeruginosa daf-7* mRNA was present in the ASJ neurons and did not appear to increase further over time (Figure 2J). The rapid kinetics of this transcriptional response, far faster than the kinetics of intestinal infection or aversive learning behavior (Tan, Mahajan-Miklos, and Ausubel 1999; Y. Zhang, Lu, and Bargmann 2005), led us to hypothesize that the ASJ chemosensory neurons may be responding directly to specific *P. aeruginosa* cues.

We determined that transgenic overexpression of *daf-7* under the native *daf-7* promoter or the ASJ-specific *trx-1* promoter, as well as under the ASI-specific *str-3* promoter, were each sufficient to restore wild-type pathogen avoidance and susceptibility in the *daf-7(ok3125)* mutant background (Figures 3A and 3C), consistent with the activity of DAF-7 as a secreted ligand. We also observed that the genetic ablation of the ASJ neuron pair conferred a partial deficit in *P. aeruginosa* avoidance and susceptibility (Figures 3B and 3D), demonstrating that the ASJ

Figure 3

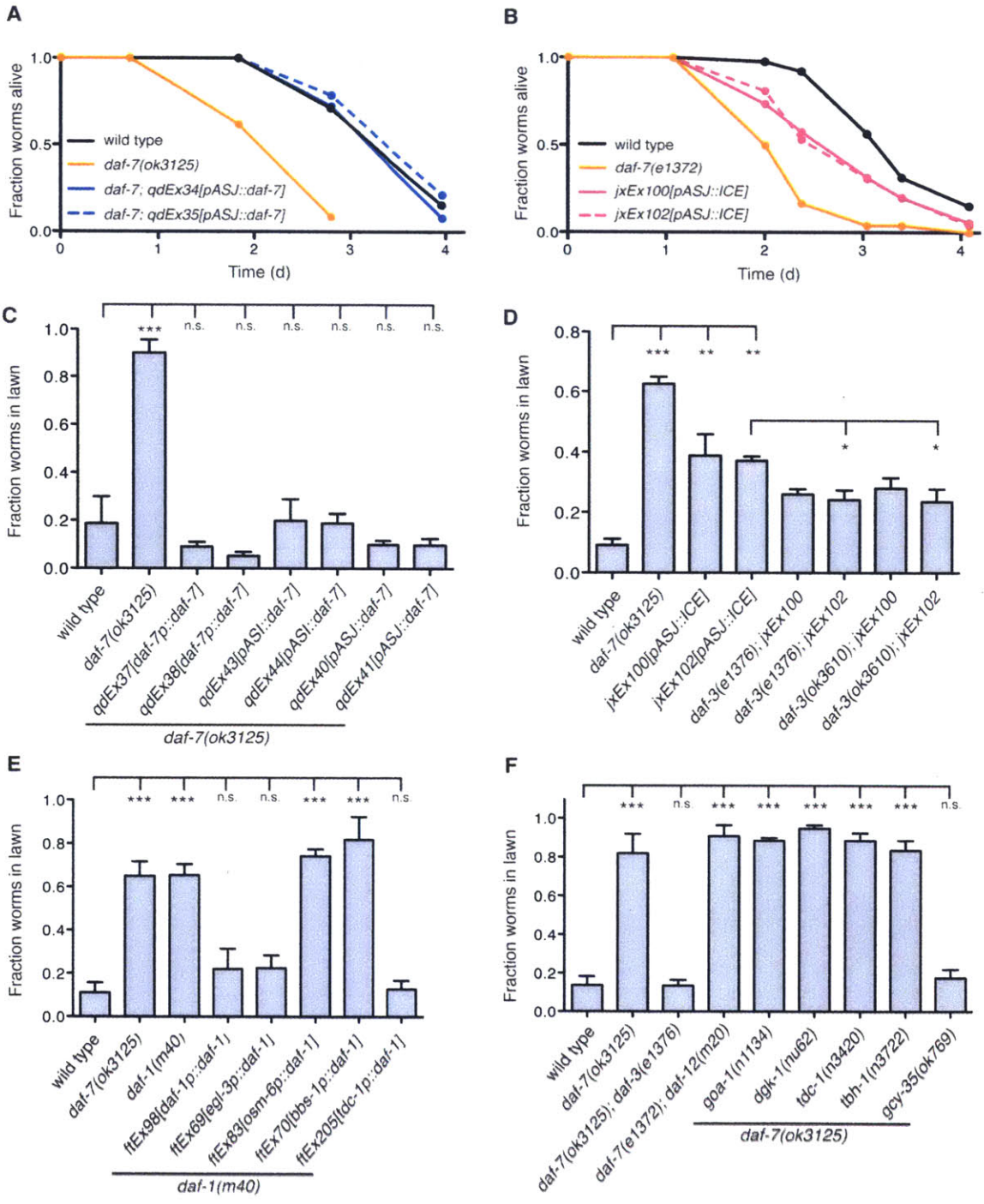
A
Fraction worms alive
Time (d)
wild type
daf-7(ok3125)
daf-7; qdEx34[pASJ::daf-7]
daf-7; qdEx35[pASJ::daf-7]
B
Fraction worms alive
Time (d)
wild type
daf-7(e1372)
jxEx100[pASJ::ICE]
jxEx102[pASJ::ICE]
C
Fraction worms in lawn
wild type
daf-7(ok3125)
qdEx37[daf-7p::daf-7]
qdEx38[daf-7p::daf-7]
qdEx43[pASI::daf-7]
qdEx44[pASI::daf-7]
qdEx40[pASJ::daf-7]
qdEx41[pASJ::daf-7]
daf-7(ok3125)
D
Fraction worms in lawn
wild type
daf-7(ok3125)
jxEx100[pASJ::ICE]
jxEx102[pASJ::ICE]
daf-3(e1376); jxEx100
daf-3(e1376); jxEx102
daf-3(ok3610); jxEx100
daf-3(ok3610); jxEx102
E
Fraction worms in lawn
wild type
daf-7(ok3125)
daf-1(m40)
ftEx98[daf-1p::daf-1]
ftEx69[egl-3p::daf-1]
ftEx83[osm-6p::daf-1]
ftEx70[bbs-1p::daf-1]
ftEx205[tdc-1p::daf-1]
daf-1(m40)
F
Fraction worms in lawn
wild type
daf-7(ok3125)
daf-7(ok3125); daf-3(e1376)
daf-7(e1372); daf-12(m20)
goa-1(n1134)
dgk-1(nu62)
tdc-1(n3420)
tbh-1(n3722)
gcy-35(ok769)
daf-7(ok3125)

Figure 3. DAF-7 from the ASJ neuron pair signals to the RIM/RIC interneurons to alter aerotaxis behavior and promote avoidance of *P. aeruginosa*

(A-B) Fraction animals alive after being transferred to plates seeded with *P. aeruginosa*. All data points represent the average of at least three independent replicates. (C-F) Lawn occupancy of animals on *P. aeruginosa* after 15 h. *** $P < 0.001$, ** $P < 0.01$, * $P < 0.05$ as determined by one-way ANOVA followed by Dunnett's Multiple Comparison Test. n.s. = not significant. Error bars indicate standard deviation. See also Figure S3.

neurons are necessary for the complete protective response to *P. aeruginosa*. To determine if the ASJ-ablation avoidance phenotype was due to a loss of DAF-7 secretion from those neurons, we introduced mutations in the downstream co-SMAD *daf-3* that is epistatic to *daf-7* (Figure 1E). Mutant *daf-3* alleles were able to partially suppress the avoidance defect of both ASJ-ablation lines, consistent with the ASJ-ablation phenotype being due in part to a loss of *P. aeruginosa*-induced DAF-7 secretion (Figure 3D). These data establish a functional role for the induction of *daf-7* in the ASJ neuron pair upon exposure to *P. aeruginosa*.

DAF-7 signals to the RIM/RIC interneurons adjacent to the ASJ neurons to promote pathogen avoidance

To understand how expression of *daf-7* from the ASJ neurons promotes pathogen avoidance, we proceeded to examine the involvement of downstream signaling components of the canonical DAF-7/TGF-β pathway in the behavioral avoidance of *P. aeruginosa*. The *daf-1* gene encodes the TGF-β Type I receptor that binds DAF-7 and is expressed in over 80 neurons including ciliated sensory neurons, pharyngeal neurons, and interneurons (Gunther, Georgi, and Riddle 2000). We found that *daf-1* mutants, like *daf-7* mutants, are deficient in avoidance of *P. aeruginosa* (Figure 3E). Using *daf-1* mutant strains in which transgenic expression of *daf-1* is directed in subsets of neurons, we observed that *daf-1* expression under its native promoter or the pan-neuronal *egl-3* promoter rescued *P. aeruginosa* avoidance to wild-type levels, but no rescue was observed when *daf-1* was expressed in ~60 ciliated sensory neurons (including ASI and ASJ) using either the *osm-6* or *bbs-1* promoters (Figure 3E). Expression of *daf-1* in only the RIM/RIC interneurons under the *tdc-1* promoter was sufficient to restore pathogen avoidance

behavior in the *daf-1* mutant to wild-type levels (Figure 3E). Previous work showed that DAF-1 also acts in the RIM/RIC interneurons to mediate wild-type development, feeding rate, and quiescence (Gallagher et al. 2013; Greer et al. 2008), suggesting that despite the broad expression of *daf-1* the RIM/RIC neurons may be the primary site of DAF-1 activity with regard to regulation of *C. elegans* behavior and physiology. The close proximity of the left and right ASJ neurons to the corresponding RIM/RIC interneurons on the ventral side of the amphid are in striking contrast to the location of the ASI neuron pair on the far dorsal side (White et al. 1986), and suggest an anatomical basis for how *P. aeruginosa* promotes enhanced DAF-7/TGF-β–dependent signaling (Figure 7D).

DAF-7 promotes pathogen avoidance through the modulation of aerotaxis behavior

DAF-7-dependent regulation of dauer entry, feeding rate, and fat storage similarly rely on repression of the co-SMAD DAF-3 in the RIM/RIC interneurons, but downstream regulation of each of these physiological processes diverges genetically and utilizes distinct sets of neurons (Greer et al. 2008). Mutations in the steroid hormone receptor *daf-12*, for example, are able to suppress the constitutive dauer entry phenotype of *daf-7* but not the increased fat storage or decreased feeding rate phenotypes. Similarly, mutations in the tyramine and octopamine synthesizing enzymes *tdc-1* and *tbh-1* suppress only the feeding rate phenotype of *daf-7*, while mutations in the $G_o\alpha$ signaling molecules *goa-1* and *dgk-1* suppress only the fat storage phenotype of *daf-7* (Greer et al. 2008). We determined that mutations in *daf-12, tdc-1, tbh-1, goa-1,* and *dgk-1* were all unable to suppress the avoidance phenotypes of *daf-7* mutants,

indicating the existence of an additional signaling output by the RIM/RIC interneurons (Figure 3F).

In the presence of bacterial food, the laboratory wild-type strain of *C. elegans* N2 does not exhibit a distinct oxygen preference, and in particular does not avoid high atmospheric oxygen concentrations (i.e. 20% O_2). In contrast, *daf-7* mutants have altered aerotaxis behavior preferring oxygen concentrations near 8% and avoiding higher atmospheric oxygen levels (A. J. Chang et al. 2006). We have previously shown that the *P. aeruginosa* lawn is hypoxic, and that altered oxygen preference can affect bacterial lawn avoidance (Reddy et al. 2009; Reddy et al. 2011). To determine whether a similar mechanism underlies the pathogen avoidance behavior promoted by *daf-7*, we introduced a mutation in the soluble guanylate cyclase *gcy-35,* which is responsible for responding to increases in oxygen concentration (Zimmer et al. 2009), and observed full suppression of the *daf-7* avoidance defect on *P. aeruginosa* (Figure 3F). In addition, we performed the pathogen avoidance assay in an oxygen chamber at low oxygen concentrations, such that the surrounding environment would fall within the preferred oxygen concentration range of the animals. In this context *daf-7* mutants show no avoidance defect relative to wild-type animals, supporting our conclusion that *daf-7* mutants fail to avoid *P. aeruginosa* due to aberrant aerotaxis behavior (Figure S3A). We also conducted further experiments to demonstrate that the observed effects of DAF-7 on aerotaxis behavior and pathogen avoidance are not limited to the laboratory-adapted N2 strain (Figure S3B). Our model suggests that by activating *daf-7* expression in the ASJ neurons in response to *P. aeruginosa*, inhibition of DAF-3 activity in the adjacent RIM/RIC interneurons is increased, modifying the response of *C. elegans* to oxygen levels and promoting exit from the lawn of *P. aeruginosa.*

G protein-dependent signaling activates *daf-7* expression in the ASJ neuron pair in response to *P. aeruginosa*

The rapid kinetics and functional consequence of *P. aeruginosa*-induced *daf-7* expression in the ASJ neuron pair motivated use of the *daf-7p::gfp* reporter to identify signaling mechanisms coupling *P. aeruginosa* exposure to this robust transcriptional response. We began by analyzing mutants known to have reduced *daf-7* expression levels in the ASI neuron pair, such as the guanylate cyclase DAF-11 and the cyclic nucleotide-gated channel encoded by *tax-2/tax-4* (A. J. Chang et al. 2006; Murakami, Koga, and Ohshima 2001), which are downstream of G protein signaling in *C. elegans* chemosensory neurons (Bargmann 2006). No *daf-7* expression was observed in either the ASI or ASJ neurons on *P. aeruginosa* in these mutant backgrounds, consistent with *daf-11, tax-2,* and *tax-4* acting upstream of *daf-7* expression in all tissues (Figures 4A-4D and S4A-S4C). These results suggest that the ASJ response to *P. aeruginosa* is downstream of G protein signaling and further motivate the identification of genes that specifically regulate *daf-7* expression in the ASJ neurons.

We performed a forward genetic screen to identify mutants in which the *daf-7p::gfp* reporter failed to be expressed in the ASJ neurons on *P. aeruginosa* but GFP fluorescence remained unchanged in the ASI neurons. One such mutant, *qd262* (Figures S4D-S4E), mapped to a region of chromosome V containing the G protein alpha subunit *gpa-3.* Sequencing revealed that the *qd262* mutant carries a missense mutation in *gpa-3* that converts a glycine residue (conserved from yeast to humans) into aspartic acid. Confirming the identity of the *qd262* mutant as an allele of *gpa-3,* we crossed the *gpa-3* deletion allele *pk35* into the *daf-7p::gfp* reporter and observed reduced fluorescence in the ASJ neurons on *P. aeruginosa* (Figures 4E and 4M).

Figure 4

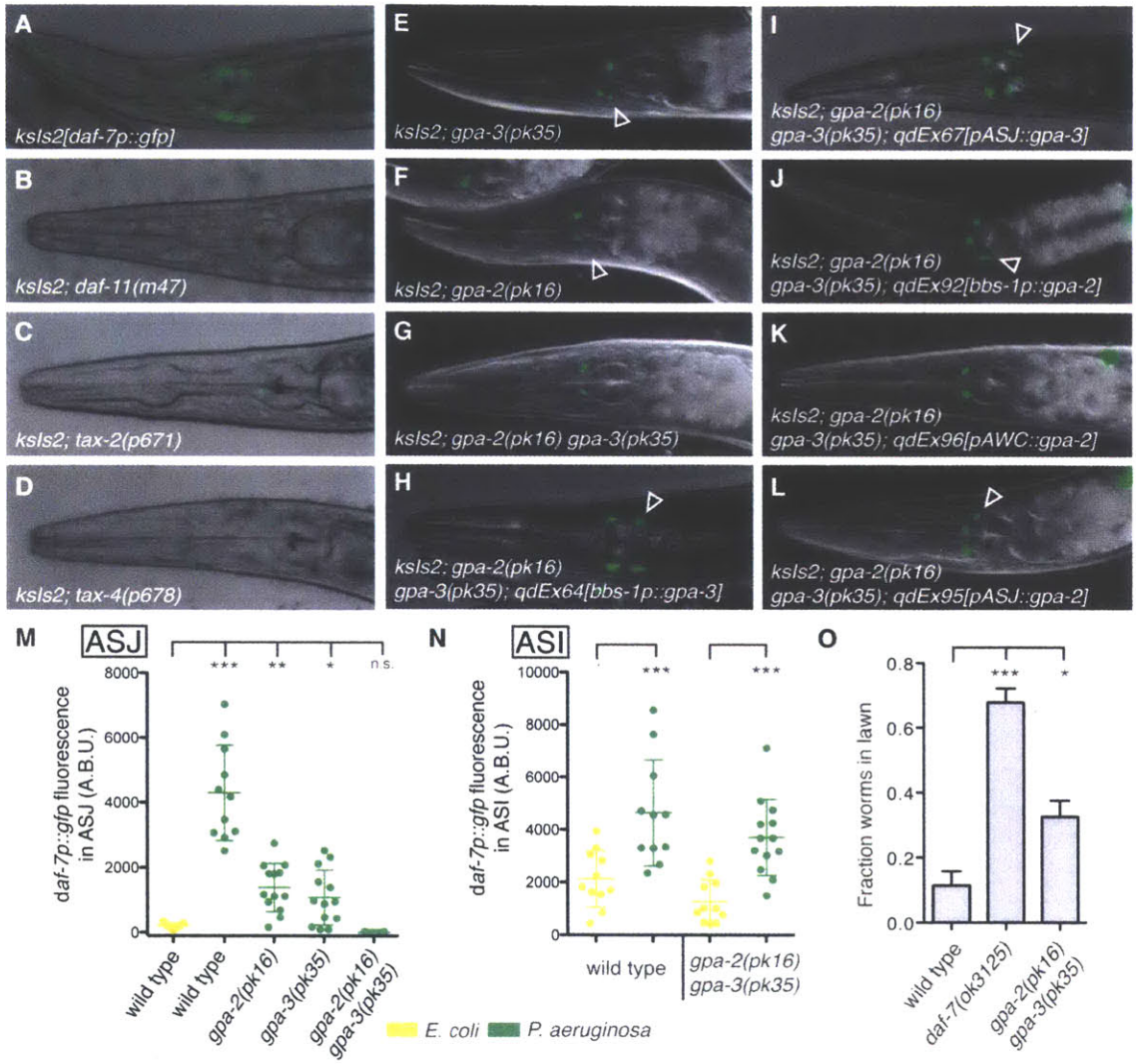
A
ksIs2[daf-7p::gfp]
B
ksIs2; daf-11(m47)
C
ksIs2; tax-2(p671)
D
ksIs2; tax-4(p678)
E
ksIs2; gpa-3(pk35)
F
ksIs2; gpa-2(pk16)
G
ksIs2; gpa-2(pk16) gpa-3(pk35)
H
ksIs2; gpa-2(pk16)
gpa-3(pk35); qdEx64[bbs-1p::gpa-3]
I
ksIs2; gpa-2(pk16)
gpa-3(pk35); qdEx67[pASJ::gpa-3]
J
ksIs2; gpa-2(pk16)
gpa-3(pk35); qdEx92[bbs-1p::gpa-2]
K
ksIs2; gpa-2(pk16)
gpa-3(pk35); qdEx96[pAWC::gpa-2]
L
ksIs2; gpa-2(pk16)
gpa-3(pk35); qdEx95[pASJ::gpa-2]
M
ASJ
daf-7p::gfp fluorescence in ASJ (A.B.U.)
8000
6000
4000
2000
0
***
**
*
n.s.
wild type
wild type
gpa-2(pk16)
gpa-3(pk35)
gpa-2(pk16) gpa-3(pk35)
N
ASI
daf-7p::gfp fluorescence in ASI (A.B.U.)
10000
8000
6000
4000
2000
0
***
***
wild type
gpa-2(pk16) gpa-3(pk35)
E. coli
P. aeruginosa
O
Fraction worms in lawn
0.8
0.6
0.4
0.2
0.0
***
*
wild type
daf-7(ok3125)
gpa-2(pk16) gpa-3(pk35)

Figure 4. GPA-3 and GPA-2 function cell-autonomously in the ASJ neurons to activate *daf-7* expression in response to *P. aeruginosa*

(A-L) *daf-7p::gfp* expression on *P. aeruginosa* in various genetic backgrounds. Empty triangles indicate ASJ neurons. (M-N) Maximum fluorescence values of *daf-7p::gfp* in the ASJ (M) or ASI (N) neurons after 16 h exposure to indicated bacteria. (O) Lawn occupancy of animals on *P. aeruginosa* after 15 h. *** $P < 0.001$, ** $P < 0.01$, * $P < 0.05$ as determined by one-way ANOVA followed by Dunnett's Multiple Comparison Test. Error bars indicate standard deviation. See also Figure S4.

Mutants carrying a deletion in a second highly homologous G protein alpha subunit, *gpa-2*, also displayed reduced *daf-7p::gfp* fluorescence in ASJ (Figures 4F and 4M), and the *gpa-2 gpa-3* double mutant was completely deficient in the ASJ-response to *P. aeruginosa* (Figures 4G and 4M). Interestingly, the *gpa-2(pk16) gpa-3(pk35)* double mutant was still able to upregulate expression of *daf-7p::gfp* in the ASI neuron on *P. aeruginosa*, indicating that the ASJ and ASI responses to *P. aeruginosa* are genetically distinct (Figure 4N). The *C. elegans* nervous system is equipped with approximately 1,300 G protein-coupled receptors that act as chemoreceptors (Thomas and Robertson 2008), and we hypothesize that GPA-3 and GPA-2 may be acting downstream of one or more GPCRs responsible for sensing *P. aeruginosa.*

gpa-3 is expressed in at least ten pairs of amphid sensory neurons (including ASJ), and its known functions include mediating responses to *C. elegans* pheromone in ASK, odorant attraction in AWA and AWC, and odorant avoidance in ASH (Hilliard et al. 2004; Jansen et al. 1999; K. Kim et al. 2009; Lans, Rademakers, and Jansen 2004; Zwaal et al. 1997). To determine if GPA-3 acts cell-autonomously in the ASJ neurons to mediate the response to *P. aeruginosa*, we expressed wild-type copies of *gpa-3* cDNA under heterologous promoters in the *gpa-2(pk16) gpa-3(pk35)* background. Under control of either the pan-ciliated neuronal promoter *bbs-1*, or the ASJ-specific promoter *trx-1*, *gpa-3* cDNA was able to rescue the *daf-7* ASJ expression defect, indicating that GPA-3 acts cell-autonomously in ASJ to mediate the response to *P. aeruginosa* (Figures 4H-4I and S4F-S4I).

gpa-2 is reported to be expressed in only one pair of chemosensory neurons (AWC) and functions in the processes of olfaction and dauer induction (Lans, Rademakers, and Jansen 2004; Zwaal et al. 1997). To determine the site of action for *gpa-2* in the response to *P. aeruginosa*, we

expressed wild-type copies of *gpa-2* cDNA under heterologous promoters in the *gpa-2(pk16) gpa-3(pk35)* background. To our surprise, expression of *gpa-2* driven by either the pan-ciliated neuronal promoter *bbs-1* or the ASJ-specific promoter *trx-1* was able to rescue the *daf-7p::gfp* phenotype, but expression of *gpa-2* in the AWC neurons under the *ceh-36* promoter was not able to rescue the *gpa-2 gpa-3* mutant phenotype (Figures 4J-4L and S4J-S4K). This indicates that GPA-2, like GPA-3, also acts cell-autonomously in ASJ to induce *daf-7* expression in response to *P. aeruginosa.* To confirm that *gpa-2* was indeed expressed in the ASJ neurons we used single molecule FISH to probe for *gpa-2* mRNA. Using probes specific for *gpa-2,* we observed 5-10 mRNA molecules in each ASJ neuron (data not shown). This novel expression supports our neuron-specific rescue data and indicates that GPA-2 and GPA-3 act together in the ASJ neurons to activate *daf-7* expression in response to *P. aeruginosa.* Finally, we tested the *gpa-2 gpa-3* double mutant for a *P. aeruginosa* avoidance defect, and observed a partial deficit in lawn avoidance that we hypothesize is due to a loss of DAF-7 secretion from the ASJ neurons (Figure 4O). These experiments identify a conserved G protein signaling pathway that acts cell-autonomously in the ASJ neurons to induce *daf-7* expression in response to *P. aeruginosa.*

Chemosensory recognition of the *P. aeruginosa* secondary metabolites phenazine-1-carboxamide and pyochelin by the ASJ neuron pair of *C. elegans*

We next sought to identify the specific bacterial cues inducing expression of *daf-7* in the ASJ neuron pair of *C. elegans*. We observed that exposure of *C. elegans* to filtered *P. aeruginosa* supernatant was sufficient to induce *daf-7* expression (Figures 5A and 6A-6B). Furthermore, by testing supernatants from liquid cultures at various growth stages we determined that *P.*

Figure 5

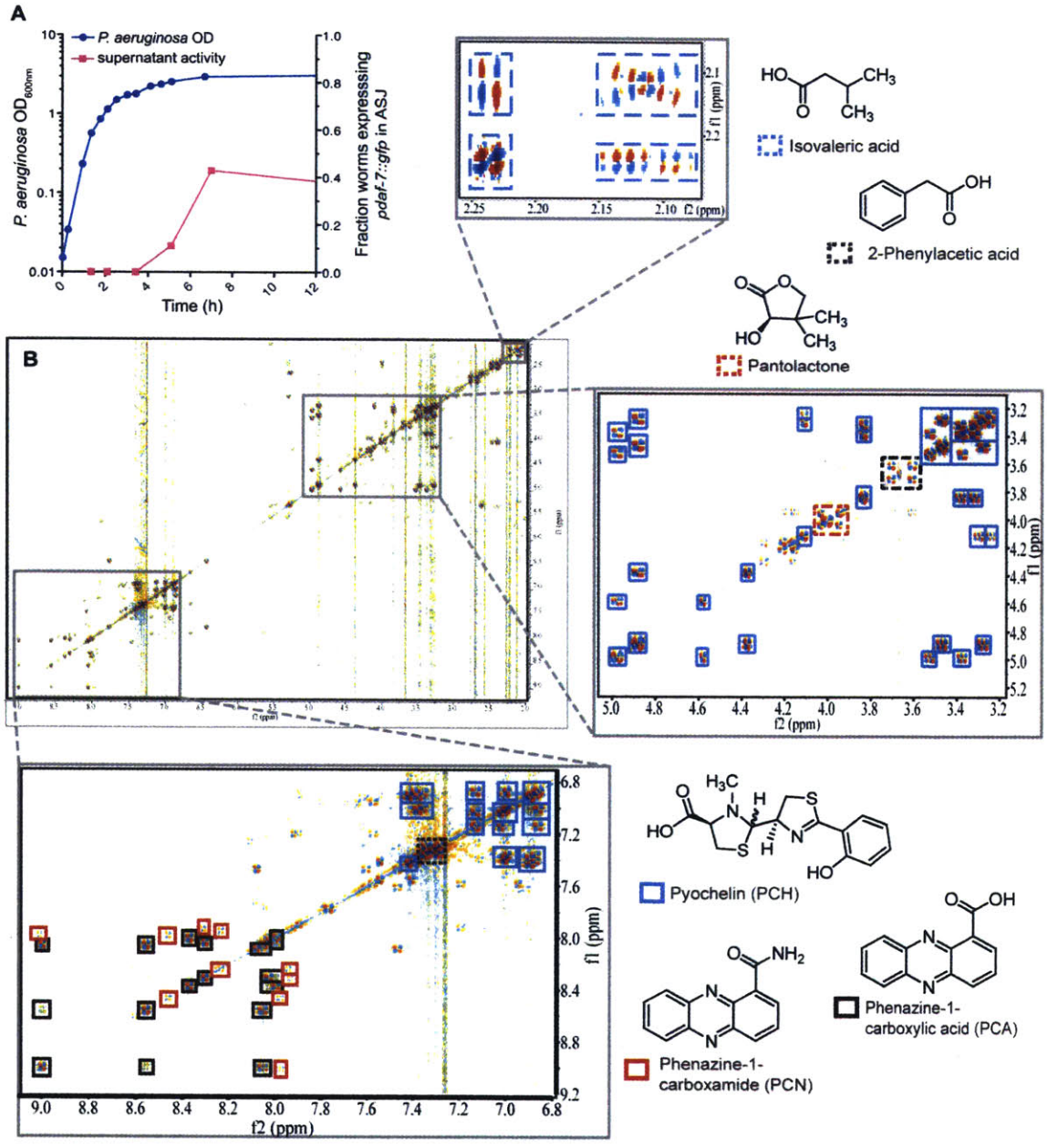
A
P. aeruginosa OD
supernatant activity
P. aeruginosa OD600nm
Fraction worms expressing pdef-7::gfp in ASJ
Time (h)
Isovaleric acid
2-Phenylacetic acid
Pantolactone
B
f2 (ppm)
f1 (ppm)
Pyochelin (PCH)
Phenazine-1-carboxamide (PCN)
Phenazine-1-carboxylic acid (PCA)

Figure 5. Supernatant from *P. aeruginosa* in stationary phase activates *daf-7* expression and contains secondary metabolites

(A) Growth curve of *P. aeruginosa* as measured by OD_{600nm} (blue circles) and activity of bacterial supernatant in inducing *daf-7p::gfp* expression in the ASJ neurons (magenta squares). (B) DQF-COSY spectrum of active metabolome fraction of *P. aeruginosa* media extract. Enlarged sections show cross-peaks of the most abundant metabolites present in this fraction. See also Figure S5.

aeruginosa in stationary phase induced *daf-7* expression in ASJ neurons most dramatically (Figure 5A), leading us to hypothesize that specific secondary metabolites produced under high cell density were being sensed by *C. elegans*. Metabolite identification was accomplished via activity-guided fractionation followed by 2D NMR spectroscopic profiling. Supernatant from large volumes of stationary phase *P. aeruginosa* was fractionated using an automated chromatography system, and individual fractions were tested for activity in the *daf-7p::gfp* assay. 1D and 2D NMR (dqfCOSY, HSQC, HMBC) spectroscopic data of the active fractions were then analyzed. Such NMR spectroscopic analysis of metabolome fractions of lowered complexity shifts focus onto testing individual identified components in bioassays, thereby reducing the need for further time-intensive purification (Taggi, Meinwald, and Schroeder 2004).

2D NMR spectra of the active fractions revealed the presence of pantolactone (Nakata et al. 2013), isovaleric acid (Niu et al. 2008), phenazine-1-carboxylic acid (Mehnaz et al. 2013), phenazine-1-carboxamide (PCN, see Table S1), the siderophore pyochelin (see Table S2) and phenyl acetic acid (Korsager, Taaning, and Skrydstrup 2013) as major components (Figures 5B, S5A, and S5B), in addition to small quantities of monoacyl glycerides and β-hydroxy fatty acids. When synthetic and HPLC-purified samples of these compounds were tested, PCN and pyochelin displayed concentration-dependent activity in the *daf-7p::gfp* assay, regardless of solvent (Figures 6A and S6), whereas the other identified metabolites were not active in this assay. Furthermore, we found that other *P. aeruginosa*-produced phenazines (e.g. pyocyanin and phenazine-1-carboxylic acid) and pyoverdine, another unrelated *P. aeruginosa* siderophore, do not induce *daf-7* expression in the ASJ neurons (Figure 6A), indicating that general properties of these compounds are likely not the cause of their activity. We quantified the *daf-7p::gfp*

Figure 6

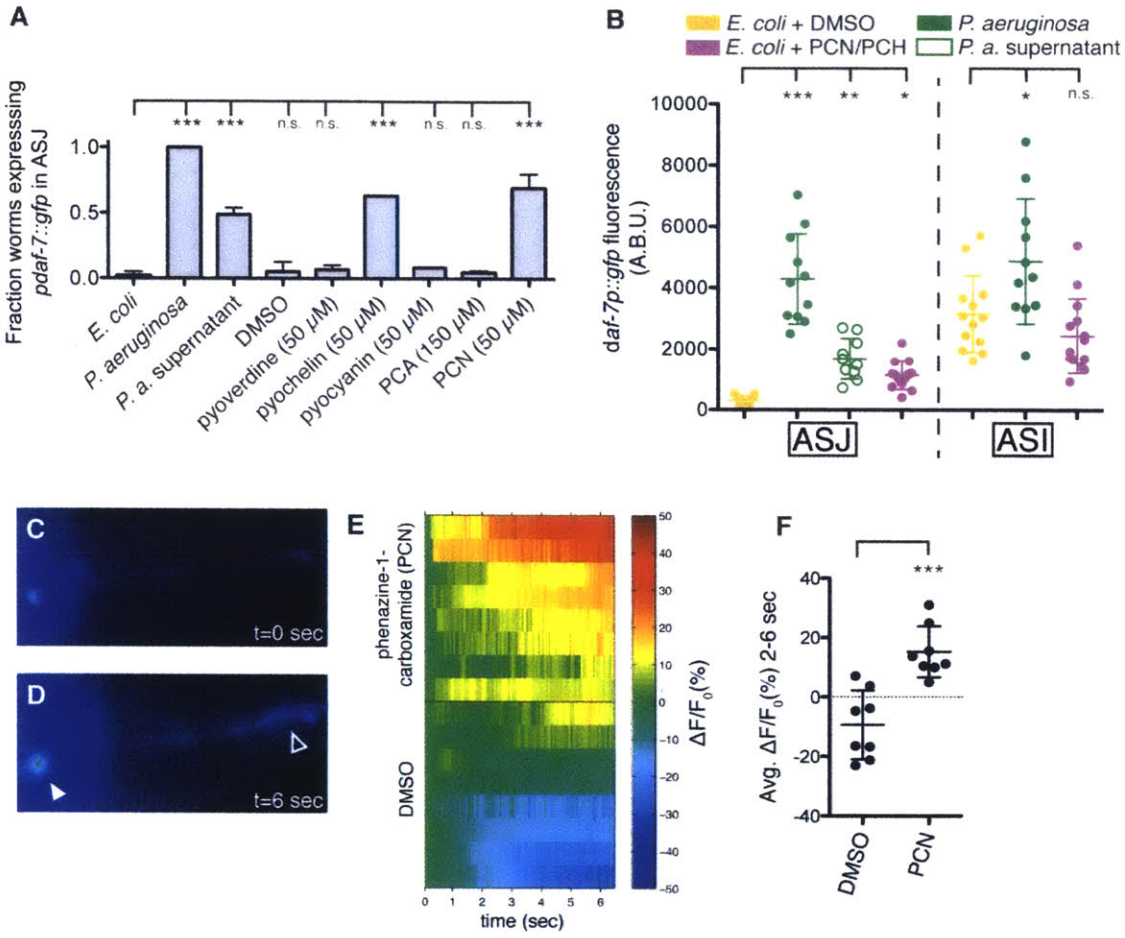
A
Fraction worms expresssing pdaf-7::gfp in ASJ
1.0
0.5
0.0
*** *** n.s. n.s. *** n.s. n.s. ***
E. coli
P. aeruginosa
P. a. supernatant
DMSO
pyoverdine (50 μM)
pyochelin (50 μM)
pyocyanin (50 μM)
PCA (150 μM)
PCN (50 μM)
B
E. coli + DMSO
E. coli + PCN/PCH
P. aeruginosa
P. a. supernatant
daf-7p::gfp fluorescence (A.B.U.)
10000
8000
6000
4000
2000
0
*** ** * * n.s.
ASJ
ASI
C
t=0 sec
D
t=6 sec
E
phenazine-1-carboxamide (PCN)
DMSO
time (sec)
0 1 2 3 4 5 6
ΔF/F0 (%)
50 40 30 20 10 0 -10 -20 -30 -40 -50
F
Avg. ΔF/F0 (%) 2-6 sec
40 20 0 -20 -40
***
DMSO
PCN

Figure 6. The ASJ neurons respond to *P. aeruginosa* secondary metabolites phenazine-1-carboxamide and pyochelin

(A-B) *daf-7p::gfp* expression in the ASJ or ASI neurons after 16 h exposure to *E. coli*, *P. aeruginosa*, or *E. coli* supplemented with indicated material. Data represent (A) the fraction of animals expressing *daf-7p::gfp* in ASJ above background or (B) the maximum fluorescence values of *daf-7p::gfp* in ASJ and ASI. All compounds were dissolved in DMSO. *** $P < 0.001$, ** $P < 0.01$, * $P < 0.05$ as determined by one-way ANOVA followed by Dunnett's Multiple Comparison Test. n.s. = not significant. Error bars indicate standard deviation. (C-D) GCaMP5 expression in the ASJ neurons immediately prior to (C) or following (D) addition of PCN. Filled triangle indicates the ASJ cell body and open triangle indicates the ASJ sensory projection. (E) GCaMP5 fluorescence changes in individual animals following the addition of PCN or DMSO at t = 0 seconds. (F) Average changes in GCaMP fluorescence in the 2-6 s following addition of either PCN or DMSO. *** $P < 0.001$ as determined by unpaired t-Test. Error bars indicate standard deviation. See also Figure S6.

fluorescence increase in the ASJ neurons following addition of pyochelin and PCN and found the response was similar to that induced by *P. aeruginosa* supernatant (Figure 6B). Interestingly we found that these compounds had no effect on *daf-7p::gfp* fluorescence in the ASI neurons, further decoupling the responses of the ASJ and ASI neurons to *P. aeruginosa* (Figure 6B).

Given the rapid transcriptional response of the ASJ neurons to the presence of *P. aeruginosa* secondary metabolites, we tested the ability of phenazine-1-carboxamide (PCN) to activate the ASJ neurons. We constructed a transgenic strain in which the genetically encoded calcium indicator GCaMP5 (Akerboom et al. 2012) is expressed exclusively in the ASJ neuron pair. Upon administration of PCN, but not the carrier control DMSO, we observed increased GCaMP5 fluorescence in both the ASJ cell body and ASJ ciliated projection that is exposed to the environment (Figures 6C-6D). We quantified the change in fluorescence in the ASJ cell body and observed a significant difference between PCN and the carrier control (Figures 6E-6F). These data suggest that ASJ may be sensing the *P. aeruginosa* metabolite PCN directly and, in turn, activating *daf-7* transcription.

Microbial discrimination and specificity in the chemosensory response to *P. aeruginosa*

In the natural environment *C. elegans* are unlikely to be presented with homogeneous bacterial lawns consisting of a single bacterial species, and so we wondered how sensitive the *daf-7p::gfp* response is to the concentration of *P. aeruginosa*. We created heterogeneous bacterial lawns consisting of *E. coli* and *P. aeruginosa* and assayed *daf-7p::gfp* fluorescence. We observed that the induction of *daf-7* expression does not function as a binary switch but rather can respond in a more subtle manner that is proportional to the fraction of *P. aeruginosa* present

in the mixed *E. coli/P. aeruginosa* lawn (Figures 7A-7B). Interestingly, the *P. aeruginosa* concentration range over which *daf-7* is activated corresponds to the range sufficient to induce the *C. elegans* behavioral avoidance response (Figures 7A-7B).

Finally, we investigated how specific the induction of *daf-7* transcription in the ASJ neuron pair was to *P. aeruginosa* as compared to other environmental microbes. We exposed *daf-7p::gfp* animals to a wide array of bacterial species and strains, covering pathogenic and non-pathogenic alpha-, beta-, and gammaproteobacteria as well as gram-positive bacterial species. We observed that a number of non-*E. coli* species can induce *daf-7* expression in the ASJ neuron pair on the order of 10-fold, but that the response is 1-2 orders of magnitude greater upon exposure to *P. aeruginosa* PA14 (Figure 7C). This result indicates that the identity of the microbial species is the principal determinant in inducing *daf-7* expression in the ASJ neuron pair, likely due to the relatively species-specific production of *P. aeruginosa* metabolites PCN and pyochelin (see Discussion). The presence of low-level activity in bacterial strains other than *P. aeruginosa* is consistent with the existence of additional, unidentified bacterial determinants that also contribute to the induction of *daf-7* in the ASJ neuron pair.

PCN and pyochelin are secondary metabolites produced by *P. aeruginosa* at high cell density that promote biofilm formation in soil as well as chronic infections in human lungs (Cornelis and Dingemans 2013; Price-Whelan, Dietrich, and Newman 2006). In *P. aeruginosa* production of phenazines and pyochelin are both positively regulated by GacA, a global activator of cell-density-dependent gene expression and virulence (Reimmann et al. 1997; Wei et al. 2013). We observed that the *P. aeruginosa gacA* mutant was deficient in inducing *daf-7p::gfp* expression in the ASJ neurons relative to wild-type bacteria (Figure 7C). As such, these

Figure 7

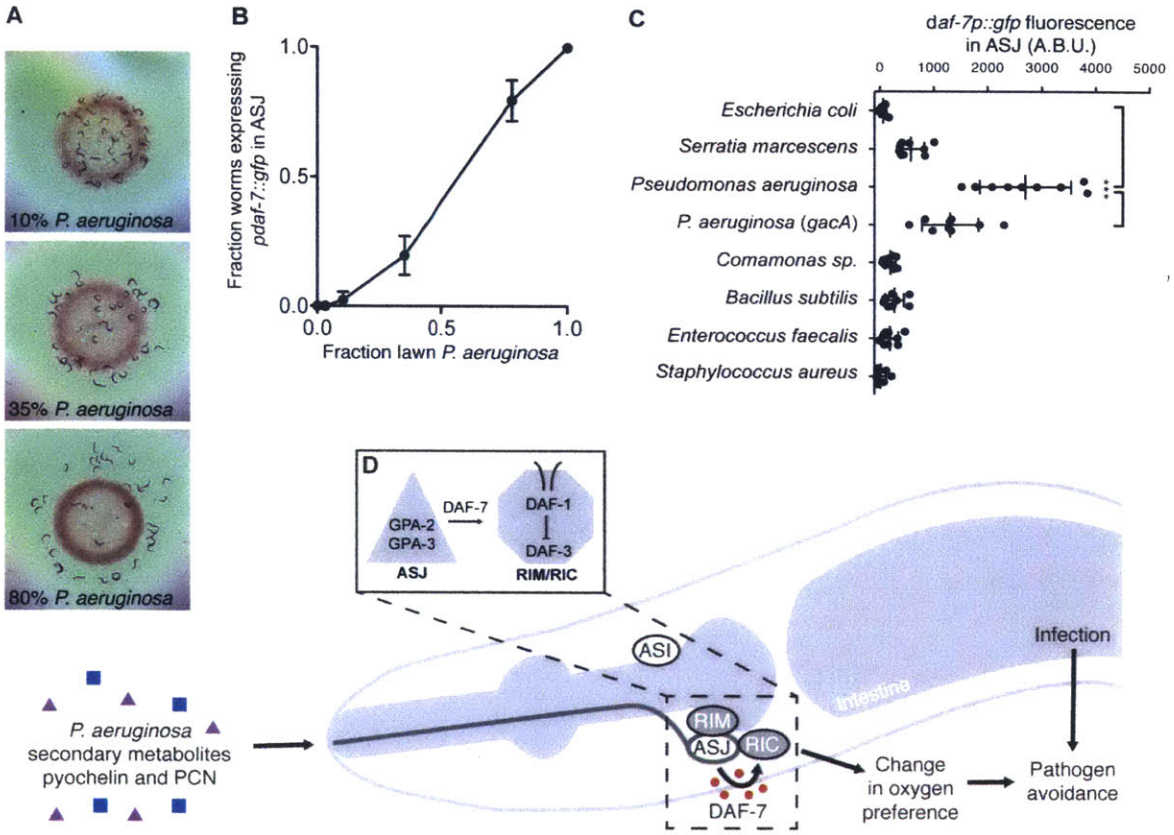
A
10% P. aeruginosa
35% P. aeruginosa
80% P. aeruginosa
B
Fraction worms expressing pdaf-7::gfp in ASJ
1.0
0.5
0.0
0.0
0.5
1.0
Fraction lawn P. aeruginosa
C
daf-7p::gfp fluorescence in ASJ (A.B.U.)
0
1000
2000
3000
4000
5000
Escherichia coli
Serratia marcescens
Pseudomonas aeruginosa
P. aeruginosa (gacA)
Comamonas sp.
Bacillus subtilis
Enterococcus faecalis
Staphylococcus aureus
D
GPA-2
GPA-3
ASJ
DAF-7
DAF-1
DAF-3
RIM/RIC
ASI
RIM
ASJ
RIC
DAF-7
intestine
Infection
P. aeruginosa
secondary metabolites
pyochelin and PCN
Change
in oxygen
preference
Pathogen
avoidance

Figure 7. Microbial discrimination of *P. aeruginosa* activates *daf-7* transcription in the ASJ neurons and promotes avoidance behavior

(A) *C. elegans* after 16 h exposure to bacterial lawns consisting of *E. coli* OP50 and *P. aeruginosa* PA14. Fraction of bacteria that were *P. aeruginosa* when *daf-7p::gfp* was assayed is indicated. (B) Fraction of animals expressing *daf-7p::gfp* in the ASJ neurons after 16 h exposure to *E. coli*, *P. aeruginosa*, or mixtures of *E. coli* and *P. aeruginosa*. Error bars indicate standard deviation. (C) Maximum fluorescence values of *daf-7p::gfp* in ASJ neurons after 16 h exposure to indicated bacteria. *** $P < 0.001$ as determined by one-way ANOVA followed by Tukey's Multiple Comparison Test. Error bars indicate standard deviation. (D) In response to *P. aeruginosa* exposure, or *P. aeruginosa* metabolites phenazine-1-carboxamide (PCN) and pyochelin, *daf-7* expression is activated via G-protein alpha subunits GPA-3 and GPA-2 in the ASJ neurons. Secreted DAF-7 signals to the TGF-β receptor DAF-1 the adjacent RIM/RIC interneurons. DAF-7/TGF-β signaling acts to alter aerotaxis behavior and promote avoidance of pathogenic bacteria.

molecules may serve as bacterial growth-stage-specific cues for *C. elegans*, alerting the host to the presence of bacteria in a "pathogenic state," and inducing a correspondingly beneficial behavioral avoidance response.

Discussion

Our data suggest that *C. elegans* responds to secondary metabolites produced by bacterial pathogens using G protein signaling pathways in their chemosensory neurons. *C. elegans* lack the antigen-specific responses of vertebrate immunity, but the utilization of chemosensory neurons and the repertoire of an estimated 1,300 GPCRs may provide a means by which a simple host organism can detect microbial pathogens. Bacterial secondary metabolism can generate a wide range of molecules that are often largely specific with regard to producer organism and regulated by environmental and growth conditions. Redox-active phenazine-1-carboxamide and the siderophore pyochelin are two such secondary metabolites of *P. aeruginosa,* produced under conditions of high cell density and low oxygen. Interestingly, while a number of other bacterial species produce phenazines, such as *Burkholderia, Brevibacterium,* and *Streptomyces,* the modifying enzyme responsible for producing phenazine-1-carboxamide, *phzH*, is not part of the canonical phenazine operon, but rather found elsewhere in the genome and limited to *P. aeruginosa* and *P. chlororaphis* (Chin-A-Woeng et al. 2001; Mavrodi et al. 2001). Similarly, pyochelin production is restricted to *Pseudomonas* and *Burkholderia* species (Gross and Loper 2009). As such, these two metabolites may act as pathogen-specific cues for *C. elegans* navigation, providing a molecular readout not only of the presence of *P. aeruginosa* itself, but

the presence of *P. aeruginosa* in a "pathogenic state" that is more strongly associated with virulence.

Our data demonstrate that DAF-7 neuroendocrine signaling is necessary for the behavioral avoidance response to *P. aeruginosa*. The decision to occupy or avoid a lawn of *P. aeruginosa* integrates multiple sensory inputs including chemosensation of bacterial compounds, chemosensation of oxygen, and mechanosensation (H. C. Chang, Paek, and Kim 2011; Ha et al. 2010; Pradel et al. 2007; Reddy et al. 2009). Once *C. elegans* have learned to avoid a particular food source, a process that requires the association of bacterial infection with specific odors and occurs many hours after exposure to pathogenic bacteria (Y. Zhang, Lu, and Bargmann 2005), they are confronted with conflicting environmental stimuli: the odor of pathogenic bacteria drives animals out of the lawn, while the relatively low oxygen concentration of the bacterial environment keeps animals inside the lawn. The DAF-7 pathway suppresses this latter tendency, and thus increasing the activity of DAF-7 in response to pathogenic bacteria promotes subsequent avoidance behavior. For *C. elegans*, which must balance attraction to bacterial food with avoidance of microbial pathogens, suppressing behaviors such as aerotaxis that keep the animal inside the bacterial lawn may be just as essential as activating behaviors that drive it away.

Whereas defining the connectivity of the *C. elegans* nervous system has provided the anatomical foundation for functional studies of neuronal circuitry (White et al. 1986), genetic studies of behavior have revealed pivotal roles for neuromodulators, such as neurotransmitters and neuropeptides, which modify the activity of synaptic circuits in response to environmental cues (Bargmann 2012). Prior studies have illustrated how a change in the neuronal expression

pattern of a single component of neuromodulator signaling can have dramatic effects on complex behavior (Lim et al. 2004; Pocock and Hobert 2010). Our study establishes that patterns of neuromodulator expression and activity may be subject to dramatic modification by the microbial environment. There has been an emerging appreciation of the profound influence that the animal microbiota can have on host organisms (Clemente et al. 2012; Lyte 2013), and our study provides a genetic, neuronal, chemical basis for how microbes may influence host neuroendocrine physiology and behavior.

Experimental Procedures

C. elegans Strains

C. elegans was maintained on *E. coli* OP50 as previously described (Brenner 1974). Constitutive dauer strains were grown at the permissive temperature of 16°C until they had passed the dauer developmental decision. For assays in which a synchronized population of animals was required, strains were egg-prepped in bleach and arrested overnight in M9 buffer at the L1 larval stage. For a complete list of strains used in this study see Table S3.

Genetic Screening and Mapping

daf-7p::gfp animals were EMS mutagenized and 500 P0s were egg-laid to produce 32 independent pools each containing 400 F1 animals (approximately 25,000 haploid genomes). The F1 pools were egg-prepped to create synchronized populations of F2s, which were grown on *E. coli* OP50 until the L4 larval stage. Mutagenized F2s were then transferred onto 10 cm NGM plates seeded with *P. aeruginosa* PA14, incubated overnight at 25°C, and screened the following day for a lack of GFP fluorescence in the ASJ neurons. After retesting and backcrossing, mutants were SNP mapped using a Hawaiian strain carrying the *daf-7p::gfp* transgene and sequenced using Illumina technology.

daf-7p::gfp Induction Assays and Bacterial Strains

For testing the dynamics of *daf-7* expression on *P. aeruginosa* PA14, an overnight culture of PA14 was grown in 2-3 mL LB at 37°C, and the following morning 7 µL of culture was seeded onto 3.5 cm SKA plates as previously described (Tan, Mahajan-Miklos, and Ausubel 1999).

PA14 plates were grown overnight at 37°C and then grown for an additional day at room temperature. Animals at the L4 larval stage were then picked onto the center of the bacterial lawn, incubated at 25°C, and scored for changes in GFP expression 15-20 h later. Cell identification was performed using the lipophilic dye DiI from Molecular Probes. Images were acquired with an Axioimager Z1 microscope using animals anaesthetized in 50 mM sodium azide. To quantify GFP fluorescence animals were imaged at 40x magnification and the maximum intensity value within the ASJ neuron was determined using FIJI software. The same procedure (with the indicated modifications) was followed for: *Escherichia coli* OP50, *Serratia marcescens* DB10, *Bacillus subtilis* PY79, *Comamonas sp.* DA1877, *Enterococcus faecalis* OG1RF (grown overnight in Brain Heart Infusion Broth), and *Staphylococcus aureus* NCTC8325 (grown overnight in Tryptic Soy Broth). To test the activity of bacterial supernatant, fractionated supernatant, and purified compounds, 3.5 cm SKA plates were seeded with 5 µL *E. coli* OP50. Prior to adding *C. elegans*, 25 µL of test material was added to the bacterial lawn and allowed to dry. All compounds were dissolved in DMSO. To generate bacterial lawns that contained mixtures of *E. coli* and *P. aeruginosa,* plates were seeded with *E. coli* and allowed to grow for two days as above, at which time 7 µL of liquid *P. aeruginosa* culture (diluted to varying degrees) was added to the *E. coli* lawn and allowed to dry. After the experiment had concluded the fraction of the lawn corresponding to each bacterial species was measured by counting CFUs of *E. coli* and *P. aeruginosa* (distinguished by colony morphology).

P. aeruginosa Avoidance and Killing Assays

Plates for *P. aeruginosa* avoidance assays were prepared as above. 30 animals at the L4 larval

stage were transferred to the center of PA14 lawns, incubated at 25°C, and scored for avoidance 15 h later. For avoidance experiments in hypoxia, plates were placed in a Coy Laboratory Products Inc. Hypoxic In Vitro Cabinet and incubated at 1%-4% O_2 at room temperature. Plates for measuring accumulation of red fluorescent beads were prepared as above with addition of Fluoresbrites 0.2 μm microspheres (Polyscience, Inc.) to the PA14 culture prior to seeding at a ratio of 50:1 (bacteria:beads). Plates for *P. aeruginosa* slow killing assays were prepared as above with the addition of 50 μg/mL 5-fluorodeoxyuridine (FUdR). 30 animals at the L4 larval stage were transferred to the center of PA14 lawns, incubated at 25°C, and scored for killing over the course of 5 days. For "Big Lawn" slow killing assays the following modifications were made: 15 μL of PA14 culture was spread to the edges of the SKA plate and 75 animals were added to each plate. Statistical analysis was performed using GraphPad Prism Software.

Single Molecule Fluorescent *In Situ* Hybridization

smFISH was performed as previously described (Raj et al. 2008). Briefly, *C. elegans* were fixed in 4% formaldehyde for 45 min at room temperature. After washing with PBS, larvae were resuspended in 70% EtOH and incubated overnight at 4°C. The following day fixed larvae were transferred into hybridization solution with the smFISH probe and incubated overnight at 30°C. The *daf-7* and *gpa-2* probes were constructed by pooling 25 unique DNA oligos that tile the coding regions deleted in the *daf-7(ok3125)* and *gpa-2(pk16)* mutants and coupling them to Cy5 dye. For a complete list of oligos see Table S4. Images were acquired with a Nikon Eclipse Ti Inverted Microscope outfitted with a Princeton Instruments PIXIS 1024 camera. Data were

analyzed using FIJI software; images presented in Figures 2H, 2I, and S2A are maximum intensity z-projections of 30 stacked exposures.

Generation of Transgenic Animals

The *daf-7* promoter (3.1 kb), *trx-1* promoter (1.1 kb) (Fierro González et al. 2011), *str-3* promoter (2.8 kb), and *ceh-36* promoter (<1 kb) (K. Kim, Kim, and Sengupta 2010) were amplified by PCR from genomic DNA. The *bbs-1* promoter (1.9 kb) was amplified by PCR from plasmid pKA40 (laboratory of K. Ashrafi). *daf-7* cDNA was amplified by PCR from an ORFeome RNAi clone. *gpa-3* and *gpa-2* cDNAs were amplified by PCR from cDNA generated with an Ambion RETROscript Kit. The GCaMP5G gene was amplified from Plasmid 31788: pCMV-GCaMP5G (Addgene). The *unc-54* 3-prime UTR was amplified by PCR from Fire Vector pPD95.75. DNA constructs (promoter::cDNA::*unc-54* 3'UTR) were synthesized using PCR fusion as previously described (Hobert 2002). PCR fusion products were cloned into pGEM-T Easy plasmids, sequenced to confirm identity, and injected into animals at a concentration of 50 ng/µL along with a plasmid carrying either *ges-1p::gfp* or *ofm-1p::gfp* (50 ng/µL). At least three independent transgenic lines were analyzed for each rescue construct. For a complete list of primers used in this study see Table S4.

Biochemical Identification of *P. aeruginosa* Metabolites

To generate *P. aeruginosa* supernatant, overnight bacterial cultures were grown in 500 mL LB at 37˚C shaking at 200 rpm. Once the cultures had reached OD_{600} = 3.0 they were passed through a 0.22 µm PES filter system. The filtrate was lyophilized and the residue was extracted twice with

50 mL of 4:1 dichloromethane:methanol mixture over 12 h. The resulting suspension was centrifuged at 4,750 rpm at 4°C for 15 min and the supernatant liquid was collected. The solvent was evaporated *in vacuo* at room temperature to produce the *P. aeruginosa* supernatant extract used for chromatographic separations and analysis. For details, see Supplemental Experimental Procedures. NMR spectra were recorded on a Varian Inova 600 MHz NMR spectrometer equipped with an HCN indirect detection probe. Spectra were baseline corrected, phased and calibrated to the solvent peak ($CHCl_3$ singlet at 7.26 ppm) using Varian VNMR and MestreLab's Mnova software packages. Non-gradient phase-cycled double-quantum filtered correlation spectroscopy (DQF-COSY) spectra were acquired using the following parameters: 0.6 s acquisition time, 512 complex increments, 16 scans per increment. DQF-COSY spectra were zero filled to 8,192 x 4,096, and 90°-shifted sine bell window functions were applied in both dimensions before Fourier transformation. Heteronuclear single quantum coherence spectroscopy (HSQC) and heteronuclear multiple bond correlation spectroscopy (HMBC) spectra were acquired using the following parameters: 0.25 s acquisition time, 400-600 complex increments, 16 scans per increment. HSQC and HMBC spectra were zero filled to 2,048 x 2,048, and 90°-shifted sine bell window functions were applied in both dimensions. Unit mass-resolution HPLC-MS was performed using an Agilent 1100 Series HPLC system equipped with a diode array detector and connected to a Quattro II mass spectrometer (Micromass/Waters). MassLynx software was used for MS data acquisition and processing. UV-Vis spectra were recorded on Agilent Technologies 8453 UV-Vis spectrophotometer. For testing the activity of candidate compounds, phenazine-1-carboxamide was purchased from Princeton Biomolecular Research (PBMR030086), phenazine-1-carboxylic acid was purchased from Apollo Scientific

(OR01490), pyochelin was purchased from Cfm Oskar Tropitzsch (164104-31-8/164104-32-9), and pyocyanin (P0046) and pyoverdine (P8374) were purchased from Sigma-Aldrich.

Protocol used for Fractionation of *P. aeruginosa* supernatant extract

P. aeruginosa supernatant extract (1.8 g) in dichloromethane:methanol (4:1, 100 mL) was added to Celite powder (10 g), prewashed with ethyl acetate. After rotary evaporation the Celite was dry-loaded into an empty 25 g RediSepRf loading cartridge. Fractionation was performed using a Teledyne ISCO CombiFlash system over a RediSep*Rf* GOLD 40 g HP Silica Column using a normal phase dichloromethane-methanol solvent system, starting with 100% dichloromethane and a linear increase in methanol content up to 10% at 7 column volumes, followed by another linear increase up to 30% at 11 column volumes, followed by a third linear increase in methanol content up to 100% at 12 column volumes, which was then continued up to 18.2 column volumes. 42 fractions (25 mL each) generated from the CombiFlash run were individually evaporated *in vacuo* and prepared for bio-assays and analyses by NMR spectroscopy (^{1}H NMR, DQF-COSY, HSQC and HMBC) and HPLC-MS.

Protocol for further fractionation via HPLC

Extract fractions of interest were evaporated *in vacuo*, resuspended in 450 µL of methanol and submitted to HPLC analysis, using an Agilent 1100 Series HPLC system equipped with an Agilent Eclipse XDB C-18 column (25 cm x 9.4 cm, 5 µm particle diameter. A 0.1% acetic acid in water ("aqueous") – acetonitrile ("organic") solvent system was used, starting with 5% organic solvent for 2 min, which was increased linearly to 100% over a period of 28 min and

continued at 100% organic solvent for 10 min. Fraction collection times were decided based on the UV trace of the chromatogram. Fractions were collected using a Teledyne ISCO Foxy 200 X-Y fraction collector from 2 to 29 min. Collected fractions were individually evaporated *in vacuo* for further analysis by NMR spectroscopy.

Calcium Imaging

To measure the activity of the ASJ neurons GCaMP5G was expressed exclusively in the ASJ neurons under the *trx-1* promoter. Animals were immobilized on NGM agar pads using Surgi-lock 2oc instant tissue adhesive (Meridian) and imaged at 40X using a Zeiss AxioVert S100 inverted microscope outfitted with an Andor iXon EMCCD camera. Ten seconds after imaging had begun approximately 3 μL of stimulant (either PCN 10 mg/mL or DMSO) was added to the agar pad. In Figures 6C-6F time = 0 refers to the addition of stimulant. Data were analyzed using custom MATLAB software written by Nikhil Bhatla.

Author Contributions

J.D.M. performed *C. elegans* and *P. aeruginosa* experiments. O.P. and P.M. performed fractionation and NMR analysis. J.D.M., O.P., F.C.S., and D.H.K, analyzed the data and interpreted results. J.D.M. and D.H.K. wrote the paper with input from O.P. and F.C.S.

Acknowledgements

We thank J. Alcedo, K. Ashrafi, F. Ausubel, H. R. Horvitz, the *C. elegans* Knockout Consortium, and the *Caenorhabditis* Genetics Center (which is supported by the NIH, Office of the Director) for providing strains and reagents. We thank N. Bhatla, C. Engert, C. Pender, and S. Sando for technical assistance. J.D.M. was supported by a Graduate Research Fellowship from the National Science Foundation. This study was supported by the NIH (GM084477 to D.H.K. and GM088290 to F.C.S.) and an Ellison New Scholar Award (to D.H.K.).

References

Akerboom, J, T W Chen, T J Wardill, L Tian, J S Marvin, S Mutlu, N C Calderon, et al. 2012. "Optimization of a GCaMP Calcium Indicator for Neural Activity Imaging." *Journal of Neuroscience* 32 (40): 13819–40. doi:10.1523/JNEUROSCI.2601-12.2012.

Avery, L, and H R Horvitz. 1990. "Effects of Starvation and Neuroactive Drugs on Feeding in Caenorhabditis Elegans.." *The Journal of Experimental Zoology* 253 (3): 263–70. doi:10.1002/jez.1402530305.

Bargmann, Cornelia I. 2006. "Chemosensation in C. Elegans.." *WormBook*, 1–29. doi:10.1895/wormbook.1.123.1.

Bargmann, Cornelia I. 2012. "Beyond the Connectome: How Neuromodulators Shape Neural Circuits.." *BioEssays : News and Reviews in Molecular, Cellular and Developmental Biology* 34 (6): 458–65. doi:10.1002/bies.201100185.

Beale, E, G Li, M W Tan, and K P Rumbaugh. 2006. "Caenorhabditis Elegans Senses Bacterial Autoinducers." *Applied and Environmental Microbiology* 72 (7): 5135–37. doi:10.1128/AEM.00611-06.

Brenner, S. 1974. "The Genetics of Caenorhabditis Elegans.." *Genetics* 77 (1): 71–94.

Chang, Andy J, Nikolas Chronis, David S Karow, Michael A Marletta, and Cornelia I Bargmann. 2006. "A Distributed Chemosensory Circuit for Oxygen Preference in C. Elegans." *PLoS Biology* 4 (9): e274. doi:10.1371/journal.pbio.0040274.st003.

Chang, Howard C, Jennifer Paek, and Dennis H Kim. 2011. "Natural Polymorphisms in C. Elegans HECW-1 E3 Ligase Affect Pathogen Avoidance Behaviour.." *Nature* 480 (7378): 525–29. doi:10.1038/nature10643.

Chin-A-Woeng, T F, J E Thomas-Oates, B J Lugtenberg, and G V Bloemberg. 2001. "Introduction of the phzH Gene of Pseudomonas Chlororaphis PCL1391 Extends the Range of Biocontrol Ability of Phenazine-1-Carboxylic Acid-Producing Pseudomonas Spp. Strains.." *Molecular Plant-Microbe Interactions : MPMI* 14 (8): 1006–15. doi:10.1094/MPMI.2001.14.8.1006.

Clemente, Jose C, Luke K Ursell, Laura Wegener Parfrey, and Rob Knight. 2012. "The Impact of the Gut Microbiota on Human Health: an Integrative View.." *Cell* 148 (6): 1258–70. doi:10.1016/j.cell.2012.01.035.

Cornelis, Pierre, and Jozef Dingemans. 2013. "Pseudomonas Aeruginosa Adapts Its Iron Uptake Strategies in Function of the Type of Infections.." *Frontiers in Cellular and Infection Microbiology* 3: 75. doi:10.3389/fcimb.2013.00075.

de Bono, Mario, David M Tobin, M Wayne Davis, Leon Avery, and Cornelia I Bargmann. 2002. "Social Feeding in Caenorhabditis Elegans Is Induced by Neurons That Detect Aversive Stimuli.." *Nature* 419 (6910): 899–903. doi:10.1038/nature01169.

Estevez, M, L Attisano, J L Wrana, P S Albert, J Massagué, and D L Riddle. 1993. "The Daf-4 Gene Encodes a Bone Morphogenetic Protein Receptor Controlling C. Elegans Dauer Larva Development.." *Nature* 365 (6447): 644–49. doi:10.1038/365644a0.

Félix, Marie-Anne, and Fabien Duveau. 2012. "Population Dynamics and Habitat Sharing Ofnatural Populations of Caenorhabditis Elegans andC. Briggsae." *BMC Biology* 10 (1). BioMed Central Ltd: 59. doi:10.1186/1741-7007-10-59.

Fierro González, Juan Carlos, Astrid Cornils, Joy Alcedo, Antonio Miranda-Vizuete, and Peter Swoboda. 2011. "The Thioredoxin TRX-1 Modulates the Function of the Insulin-Like Neuropeptide DAF-28 During Dauer Formation in Caenorhabditis Elegans." Edited by Ellen Nollen. *PLoS ONE* 6 (1): e16561. doi:10.1371/journal.pone.0016561.s007.

Flames, Nuria, and Oliver Hobert. 2009. "Gene Regulatory Logic of Dopamine Neuron Differentiation.." *Nature* 458 (7240): 885–89. doi:10.1038/nature07929.

Gallagher, Thomas, Jeongho Kim, Marieke Oldenbroek, Rex Kerr, and Young-jai You. 2013. "ASI Regulates Satiety Quiescence in C. Elegans.." *Journal of Neuroscience* 33 (23): 9716–24. doi:10.1523/JNEUROSCI.4493-12.2013.

Georgi, L L, P S Albert, and D L Riddle. 1990. "Daf-1, a C. Elegans Gene Controlling Dauer Larva Development, Encodes a Novel Receptor Protein Kinase.." *Cell* 61 (4): 635–45.

Greer, Elisabeth R, Carissa L Pérez, Marc R Van Gilst, Brian H Lee, and Kaveh Ashrafi. 2008. "Neural and Molecular Dissection of a C. Elegans Sensory Circuit That Regulates Fat and Feeding." *Cell Metabolism* 8 (2): 118–31. doi:10.1016/j.cmet.2008.06.005.

Gross, Harald, and Joyce E Loper. 2009. "Genomics of Secondary Metabolite Production by Pseudomonas Spp.." *Natural Product Reports* 26 (11): 1408–46. doi:10.1039/b817075b.

Gunther, C V, L L Georgi, and D L Riddle. 2000. "A Caenorhabditis Elegans Type I TGF Beta Receptor Can Function in the Absence of Type II Kinase to Promote Larval Development.." *Development* 127 (15): 3337–47.

Gusarov, Ivan, Laurent Gautier, Olga Smolentseva, Ilya Shamovsky, Svetlana Eremina, Alexander Mironov, and Evgeny Nudler. 2013. "Bacterial Nitric Oxide Extends the Lifespan of C. Elegans.." *Cell* 152 (4): 818–30. doi:10.1016/j.cell.2012.12.043.

Ha, Heon-ick, Michael Hendricks, Yu Shen, Christopher V Gabel, Christopher Fang-Yen, Yuqi Qin, Daniel Colón-Ramos, Kang Shen, Aravinthan D T Samuel, and Yun Zhang. 2010. "Functional Organization of a Neural Network for Aversive Olfactory Learning in

Caenorhabditis Elegans." *Neuron* 68 (6). Elsevier Inc.: 1173–86. doi:10.1016/j.neuron.2010.11.025.

Hart, A C, S Sims, and J M Kaplan. 1995. "Synaptic Code for Sensory Modalities Revealed by C. Elegans GLR-1 Glutamate Receptor.." *Nature* 378 (6552): 82–85. doi:10.1038/378082a0.

Hedgecock, E M, and R L Russell. 1975. "Normal and Mutant Thermotaxis in the Nematode Caenorhabditis Elegans.." *Proceedings of the National Academy of Sciences of the United States of America* 72 (10): 4061–65.

Hilliard, Massimo A, Carmela Bergamasco, Salvatore Arbucci, Ronald H A Plasterk, and Paolo Bazzicalupo. 2004. "Worms Taste Bitter: ASH Neurons, QUI-1, GPA-3 and ODR-3 Mediate Quinine Avoidance in Caenorhabditis Elegans.." *The EMBO Journal* 23 (5): 1101–11. doi:10.1038/sj.emboj.7600107.

Hobert, Oliver. 2002. "PCR Fusion-Based Approach to Create Reporter Gene Constructs for Expression Analysis in Transgenic C. Elegans.." *BioTechniques* 32 (4): 728–30.

Jansen, G, K L Thijssen, P Werner, M van der Horst, E Hazendonk, and R H Plasterk. 1999. "The Complete Family of Genes Encoding G Proteins of Caenorhabditis Elegans.." *Nature Genetics* 21 (4): 414–19. doi:10.1038/7753.

Kim, K, K Sato, M Shibuya, D M Zeiger, R A Butcher, J R Ragains, J Clardy, K Touhara, and P Sengupta. 2009. "Two Chemoreceptors Mediate Developmental Effects of Dauer Pheromone in C. Elegans." *Science* 326 (5955): 994–98. doi:10.1126/science.1176331.

Kim, K, R Kim, and P Sengupta. 2010. "The HMX/NKX Homeodomain Protein MLS-2 Specifies the Identity of the AWC Sensory Neuron Type via Regulation of the Ceh-36 Otx Gene in C. Elegans." *Development* 137 (6): 963–74. doi:10.1242/dev.044719.

Korsager, Signe, Rolf H Taaning, and Troels Skrydstrup. 2013. "Effective Palladium-Catalyzed Hydroxycarbonylation of Aryl Halides with Substoichiometric Carbon Monoxide.." *Journal of the American Chemical Society* 135 (8): 2891–94. doi:10.1021/ja3114032.

Lans, Hannes, Suzanne Rademakers, and Gert Jansen. 2004. "A Network of Stimulatory and Inhibitory Galpha-Subunits Regulates Olfaction in Caenorhabditis Elegans.." *Genetics* 167 (4): 1677–87. doi:10.1534/genetics.103.024786.

Lim, Miranda M, Zuoxin Wang, Daniel E Olazábal, Xianghui Ren, Ernest F Terwilliger, and Larry J Young. 2004. "Enhanced Partner Preference in a Promiscuous Species by Manipulating the Expression of a Single Gene.." *Nature* 429 (6993): 754–57. doi:10.1038/nature02539.

Lyte, Mark. 2013. "Microbial Endocrinology in the Microbiome-Gut-Brain Axis: How Bacterial Production and Utilization of Neurochemicals Influence Behavior." Edited by Virginia

Miller. *PLoS Pathogens* 9 (11): e1003726. doi:10.1371/journal.ppat.1003726.

MacNeil, Lesley T, Emma Watson, H Efsun Arda, Lihua Julie Zhu, and Albertha J M Walhout. 2013. "Diet-Induced Developmental Acceleration Independent of TOR and Insulin in C. Elegans.." *Cell* 153 (1): 240–52. doi:10.1016/j.cell.2013.02.049.

Mavrodi, D V, R F Bonsall, S M Delaney, M J Soule, G Phillips, and L S Thomashow. 2001. "Functional Analysis of Genes for Biosynthesis of Pyocyanin and Phenazine-1-Carboxamide From Pseudomonas Aeruginosa PAO1.." *Journal of Bacteriology* 183 (21): 6454–65. doi:10.1128/JB.183.21.6454-6465.2001.

Mehnaz, Samina, Rahman Shah Zaib Saleem, Basit Yameen, Isabelle Pianet, Gregor Schnakenburg, Halina Pietraszkiewicz, Fred Valeriote, et al. 2013. "Lahorenoic Acids a-C, Ortho-Dialkyl-Substituted Aromatic Acids From the Biocontrol Strain Pseudomonas Aurantiaca PB-St2.." *Journal of Natural Products* 76 (2): 135–41. doi:10.1021/np3005166.

Milward, Kate, Karl Emanuel Busch, Robin Joseph Murphy, Mario de Bono, and Birgitta Olofsson. 2011. "Neuronal and Molecular Substrates for Optimal Foraging in Caenorhabditis Elegans.." *Proceedings of the National Academy of Sciences* 108 (51): 20672–77. doi:10.1073/pnas.1106134109.

Murakami, M, M Koga, and Y Ohshima. 2001. "DAF-7/TGF-Beta Expression Required for the Normal Larval Development in C. Elegans Is Controlled by a Presumed Guanylyl Cyclase DAF-11.." *Mechanisms of Development* 109 (1): 27–35.

Nakata, Kenya, Kouya Gotoh, Keisuke Ono, Kengo Futami, and Isamu Shiina. 2013. "Kinetic Resolution of Racemic 2-Hydroxy-Γ-Butyrolactones by Asymmetric Esterification Using Diphenylacetic Acid with Pivalic Anhydride and a Chiral Acyl-Transfer Catalyst.." *Organic Letters* 15 (6): 1170–73. doi:10.1021/ol303453j.

Niu, D F, L P Xiao, A J Zhang, G R Zhang, Q Y Tan, and J X Lu. 2008. "Electrocatalytic Carboxylation of Aliphatic Halides at Silver Cathode in Acetonitrile." *Tetrahedron.*

Patterson, G I, A Koweek, A Wong, Y Liu, and G Ruvkun. 1997. "The DAF-3 Smad Protein Antagonizes TGF-Beta-Related Receptor Signaling in the Caenorhabditis Elegans Dauer Pathway.." *Genes & Development* 11 (20): 2679–90. doi:10.1101/gad.11.20.2679.

Pocock, Roger, and Oliver Hobert. 2010. "Hypoxia Activates a Latent Circuit for Processing Gustatory Information in C. Elegans.." *Nature Publishing Group* 13 (5): 610–14. doi:10.1038/nn.2537.

Pradel, Elizabeth, Yun Zhang, Nathalie Pujol, Tohey Matsuyama, Cornelia I Bargmann, and Jonathan J Ewbank. 2007. "Detection and Avoidance of a Natural Product From the Pathogenic Bacterium Serratia Marcescens by Caenorhabditis Elegans.." *Proceedings of the National Academy of Sciences of the United States of America* 104 (7): 2295–2300.

doi:10.1073/pnas.0610281104.

Price-Whelan, Alexa, Lars E P Dietrich, and Dianne K Newman. 2006. "Rethinking 'Secondary' Metabolism: Physiological Roles for Phenazine Antibiotics.." *Nature Chemical Biology* 2 (2): 71–78. doi:10.1038/nchembio764.

Pujol, N, E M Link, L X Liu, C L Kurz, G Alloing, M W Tan, K P Ray, R Solari, C D Johnson, and J J Ewbank. 2001. "A Reverse Genetic Analysis of Components of the Toll Signaling Pathway in Caenorhabditis Elegans.." *Current Biology : CB* 11 (11): 809–21.

Raj, Arjun, Patrick van den Bogaard, Scott A Rifkin, Alexander van Oudenaarden, and Sanjay Tyagi. 2008. "Imaging Individual mRNA Molecules Using Multiple Singly Labeled Probes." *Nature Methods* 5 (10): 877–79. doi:10.1038/nmeth.1253.

Reddy, Kirthi C, Erik C Andersen, Leonid Kruglyak, and Dennis H Kim. 2009. "A Polymorphism in Npr-1 Is a Behavioral Determinant of Pathogen Susceptibility in C. Elegans.." *Science* 323 (5912): 382–84. doi:10.1126/science.1166527.

Reddy, Kirthi C, Ryan C Hunter, Nikhil Bhatla, Dianne K Newman, and Dennis H Kim. 2011. "Caenorhabditis Elegans NPR-1-Mediated Behaviors Are Suppressed in the Presence of Mucoid Bacteria.." *Proceedings of the National Academy of Sciences* 108 (31): 12887–92. doi:10.1073/pnas.1108265108.

Reimmann, C, M Beyeler, A Latifi, H Winteler, M Foglino, A Lazdunski, and D Haas. 1997. "The Global Activator GacA of Pseudomonas Aeruginosa PAO Positively Controls the Production of the Autoinducer N-Butyryl-Homoserine Lactone and the Formation of the Virulence Factors Pyocyanin, Cyanide, and Lipase.." *Molecular Microbiology* 24 (2): 309–19.

Ren, P, C S Lim, R Johnsen, P S Albert, D Pilgrim, and D L Riddle. 1996. "Control of C. Elegans Larval Development by Neuronal Expression of a TGF-Beta Homolog.." *Science* 274 (5291): 1389–91.

Rivière, Stéphane, Ludivine Challet, Daniela Fluegge, Marc Spehr, and Ivan Rodriguez. 2009. "Formyl Peptide Receptor-Like Proteins Are a Novel Family of Vomeronasal Chemosensors.." *Nature* 459 (7246): 574–77. doi:10.1038/nature08029.

Sawin, E R, R Ranganathan, and H R Horvitz. 2000. "C. Elegans Locomotory Rate Is Modulated by the Environment Through a Dopaminergic Pathway and by Experience Through a Serotonergic Pathway.." *Neuron* 26 (3): 619–31.

Schackwitz, W S, T Inoue, and J H Thomas. 1996. "Chemosensory Neurons Function in Parallel to Mediate a Pheromone Response in C. Elegans.." *Neuron* 17 (4): 719–28.

Shaw, Wendy M, Shijing Luo, Jessica Landis, Jasmine Ashraf, and Coleen T Murphy. 2007.

"The C. Elegans TGF-B Dauer Pathway Regulates Longevity via Insulin Signaling." *Current Biology* 17 (19): 1635–45. doi:10.1016/j.cub.2007.08.058.

Shtonda, Boris Borisovich, and Leon Avery. 2006. "Dietary Choice Behavior in Caenorhabditis Elegans.." *The Journal of Experimental Biology* 209 (Pt 1): 89–102. doi:10.1242/jeb.01955.

Stensmyr, Marcus C, Hany K M Dweck, Abu Farhan, Irene Ibba, Antonia Strutz, Latha Mukunda, Jeanine Linz, et al. 2012. "A Conserved Dedicated Olfactory Circuit for Detecting Harmful Microbes in Drosophila.." *Cell* 151 (6): 1345–57. doi:10.1016/j.cell.2012.09.046.

Swanson, M M, and D L Riddle. 1981. "Critical Periods in the Development of the Caenorhabditis Elegans Dauer Larva.." *Developmental Biology* 84 (1): 27–40.

Taggi, Andrew E, Jerrold Meinwald, and Frank C Schroeder. 2004. "A New Approach to Natural Products Discovery Exemplified by the Identification of Sulfated Nucleosides in Spider Venom.." *Journal of the American Chemical Society* 126 (33): 10364–69. doi:10.1021/ja047416n.

Tan, M W, S Mahajan-Miklos, and F M Ausubel. 1999. "Killing of Caenorhabditis Elegans by Pseudomonas Aeruginosa Used to Model Mammalian Bacterial Pathogenesis.." *Proceedings of the National Academy of Sciences of the United States of America* 96 (2): 715–20.

Thomas, James H, and Hugh M Robertson. 2008. "The Caenorhabditis Chemoreceptor Gene Families.." *BMC Biology* 6: 42. doi:10.1186/1741-7007-6-42.

Tobin, David, David Madsen, Amanda Kahn-Kirby, Erin Peckol, Gary Moulder, Robert Barstead, Andres Maricq, and Cornelia Bargmann. 2002. "Combinatorial Expression of TRPV Channel Proteins Defines Their Sensory Functions and Subcellular Localization in C. Elegans Neurons.." *Neuron* 35 (2): 307–18.

Watson, Emma, Lesley T MacNeil, Ashlyn D Ritter, L Safak Yilmaz, Adam P Rosebrock, Amy A Caudy, and Albertha J M Walhout. 2014. "Interspecies Systems Biology Uncovers Metabolites Affecting C. Elegans GeneExpression and Life History Traits." *Cell* 156 (4). Elsevier: 759–70. doi:10.1016/j.cell.2014.01.047.

Wei, X, X Huang, L Tang, D Wu, and Y Xu. 2013. "Global Control of GacA in Secondary Metabolism, Primary Metabolism, Secretion Systems, and Motility in the Rhizobacterium Pseudomonas Aeruginosa M18." *Journal of Bacteriology* 195 (15): 3387–3400. doi:10.1128/JB.00214-13.

White, J G, E Southgate, J N Thomson, and S Brenner. 1986. "The Structure of the Nervous System of the Nematode Caenorhabditis Elegans.." *Philosophical Transactions of the Royal Society of London. Series B, Biological Sciences* 314 (1165): 1–340.

Zhang, Xiaodong, and Yun Zhang. 2012. "DBL-1, a TGF-B, Is Essential for Caenorhabditis

Elegans Aversive Olfactory Learning.." *Proceedings of the National Academy of Sciences* 109 (42): 17081–86. doi:10.1073/pnas.1205982109.

Zhang, Yun, Hang Lu, and Cornelia I Bargmann. 2005. "Pathogenic Bacteria Induce Aversive Olfactory Learning in Caenorhabditis Elegans." *Nature* 438 (7065): 179–84. doi:10.1038/nature04216.

Zimmer, Manuel, Jesse M Gray, Navin Pokala, Andy J Chang, David S Karow, Michael A Marletta, Martin L Hudson, David B Morton, Nikos Chronis, and Cornelia I Bargmann. 2009. "Neurons Detect Increases and Decreases in Oxygen Levels Using Distinct Guanylate Cyclases.." *Neuron* 61 (6): 865–79. doi:10.1016/j.neuron.2009.02.013.

Zugasti, Olivier, and Jonathan J Ewbank. 2009. "Neuroimmune Regulation of Antimicrobial Peptide Expression by a Noncanonical TGF-B Signaling Pathway in Caenorhabditis Elegans Epidermis." *Nature Immunology* 10 (3): 249–56. doi:10.1038/ni.1700.

Zwaal, R R, J E Mendel, P W Sternberg, and R H Plasterk. 1997. "Two Neuronal G Proteins Are Involved in Chemosensation of the Caenorhabditis Elegans Dauer-Inducing Pheromone.." *Genetics* 145 (3): 715–27.

Supplemental Information

Figure S1, Related to Figure 1

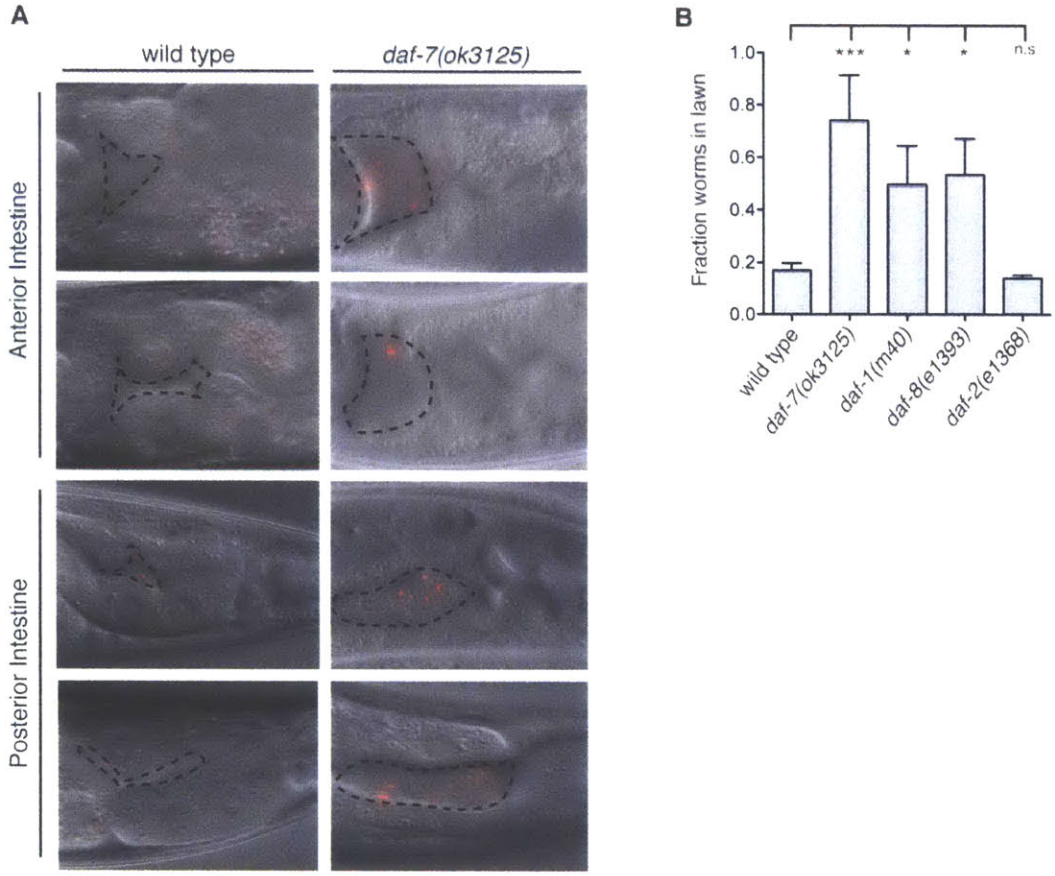

Figure S1. Pathogen avoidance behavior reduces the dose of ingested bacteria and is genetically distinct from dauer diapause entry, related to Figure 1

(A) Merged DIC and red fluorescence images of animals exposed to lawns of *P. aeruginosa* containing red fluorescent beads after 15 h. Dashed lines indicate the intestinal lumen that appears distended due to the increased ingestion of pathogenic bacteria. (B) Lawn occupancy of animals on *P. aeruginosa* after 15 h. Animals defective for components of DAF-7/TGF-β signaling show avoidance defects but mutants in the insulin receptor DAF-2 show no *P. aeruginosa* avoidance defect. *** $P < 0.001$, * $P < 0.05$ as determined by one-way ANOVA followed by Dunnett's Multiple Comparison Test. n.s. = not significant. Error bars indicate standard deviation. We note that all animals being tested for avoidance and susceptibility phenotypes were raised at the permissive temperature such that they bypass the dauer diapause state.

Figure S2, Related to Figure 2

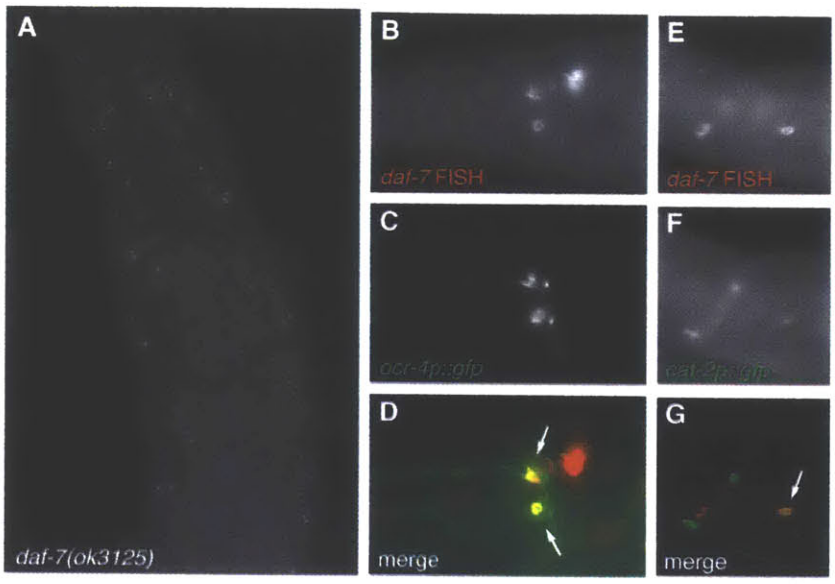

Figure S2. The *daf-7* smFISH neuronal expression pattern is specific and includes the OLQ and ADE mechanosensory neurons, related to Figure 2

(A) *daf-7* single molecule FISH in *daf-7(ok3125)* animals carrying a 664 bp deletion in the *daf-7* gene. Non-specific fluorescence is restricted to muscle tissue. (B-D) *daf-7* is expressed in the OLQ neurons (white arrows). *daf-7* smFISH (B), *ocr-4::gfp* in OLQ neurons (Tobin et al. 2002)(C), and merge (D). (E-F) *daf-7* is expressed in the ADE neurons (white arrow). *daf-7* smFISH (E), *cat-2::gfp* in ADE neurons (and other neurons) (Flames and Hobert 2009) (F), and merge (G).

Figure S3, Related to Figure 3

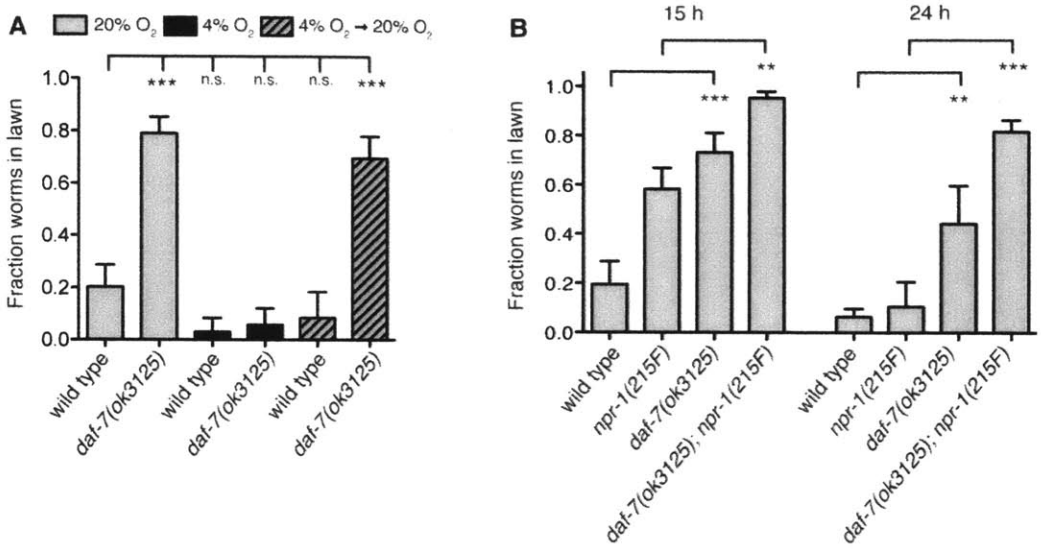

Figure S3. DAF-7 promotes *P. aeruginosa* avoidance through altering aerotaxis behavior and acts in parallel to NPR-1, related to Figure 3

(A-B) Lawn occupancy of animals on *P. aeruginosa*. All measurements taken after 15 h unless otherwise noted. *** $P < 0.001$, ** $P < 0.01$ as determined by one-way ANOVA followed by Tukey's Multiple Comparison Test. n.s. = not significant. Error bars indicate standard deviation. (A) Grey bars indicate animals at normoxia (20% O_2) and black bars indicate animals incubated in a hypoxic chamber (~4% O_2). After the same animals from the hypoxic chamber were allowed to equilibrate at normoxia for 2.5 h (hatched bars), the *daf-7* mutants reentered the lawn of *P. aeruginosa* while the wild-type animals did not, further implicating oxygen preference as the driving force underlying the *daf-7* pathogen avoidance defect. (B) Wild isolates of *C. elegans* carry the *npr-1(215F)* allele and display oxygen preference similar to *daf-7* mutants (A. J. Chang et al. 2006). The *daf-7(ok3125); npr-1(215F)* double mutant was markedly deficient in avoidance of *P. aeruginosa* relative to *npr-1(215F)* animals. This was especially evident at 24 h, at which point *npr-1(215F)* animals had exited the *P. aeruginosa* lawn while *daf-7(ok3125); npr-1(215F)* animals remained almost entirely inside the lawn. These data support the model in which *npr-1* and *daf-7* act in parallel to modulate oxygen-related behaviors (A. J. Chang et al. 2006; de Bono et al. 2002).

Figure S4, Related to Figure 4

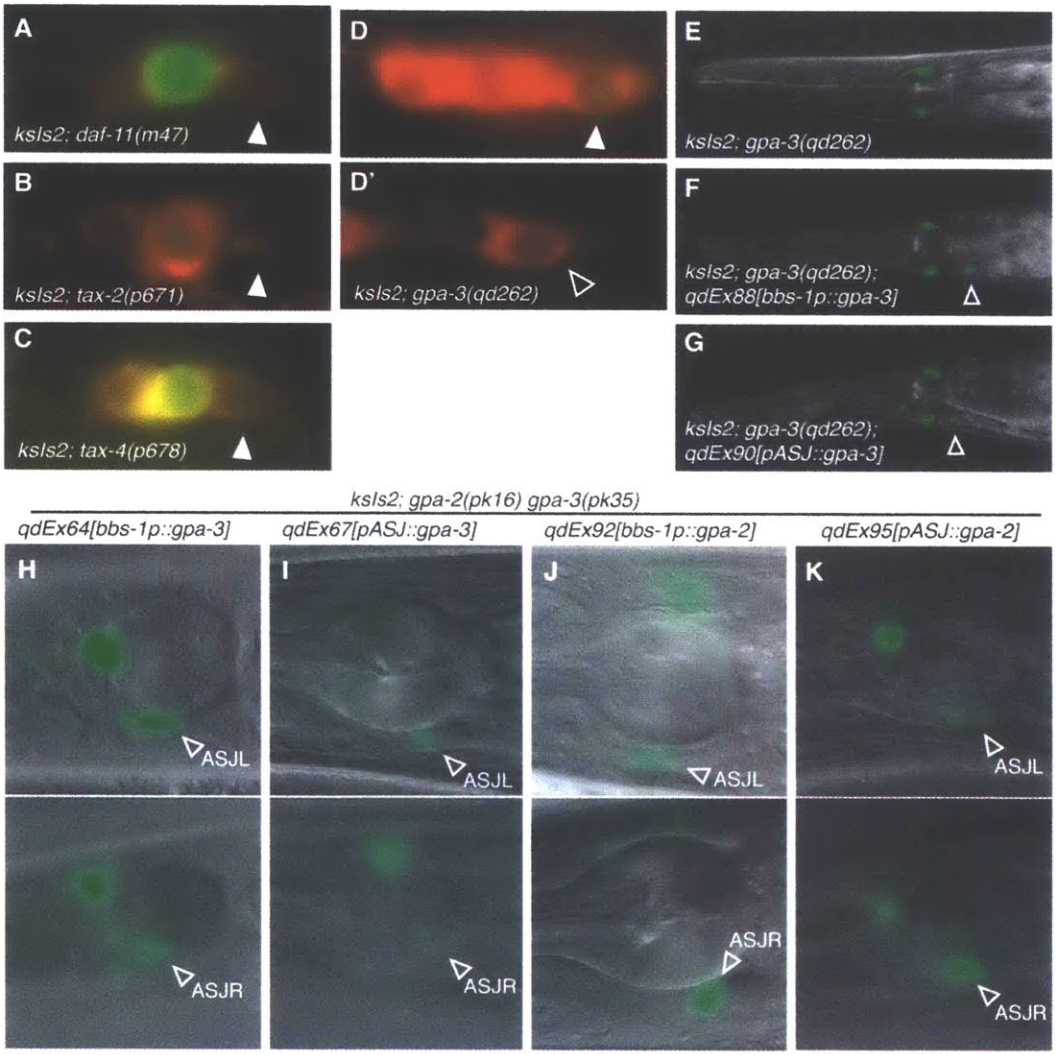

Figure S4. GPA-3 and GPA-2 are necessary for *daf-7* expression in ASJ, whereas DAF-11 and TAX-2/TAX-4 are necessary for *daf-7* expression in both ASI and ASJ, related to Figure 4

(A-D) Co-localization of *daf-7p::gfp* expression and DiI staining (red) in animals on *P. aeruginosa* after 16 h. In the dorsal view dye-filled neurons are, from left to right, ASK, ADL, and ASI. Filled triangles indicate ASI neurons. In the *daf-11, tax-2,* and *tax-4* mutant backgrounds no GFP fluorescence was observed in the ASI or ASJ neurons, but faint GFP fluorescence was observed in two additional amphid neurons that we identified as the ADL neuron pair. (D') In the ventral view the empty triangle indicates the ASJ neuron, which fails to express GFP on *P. aeruginosa* in the *gpa-3(qd262)* background. (E-K) *daf-7p::gfp* expression on *P. aeruginosa* in various genetic backgrounds at 10X magnification (E-G) and 40X magnification (H-K). In (H-K) the ASJL and ASJR neurons from the same animal are indicated with empty triangles.

Figure S5, Related to Figure 5

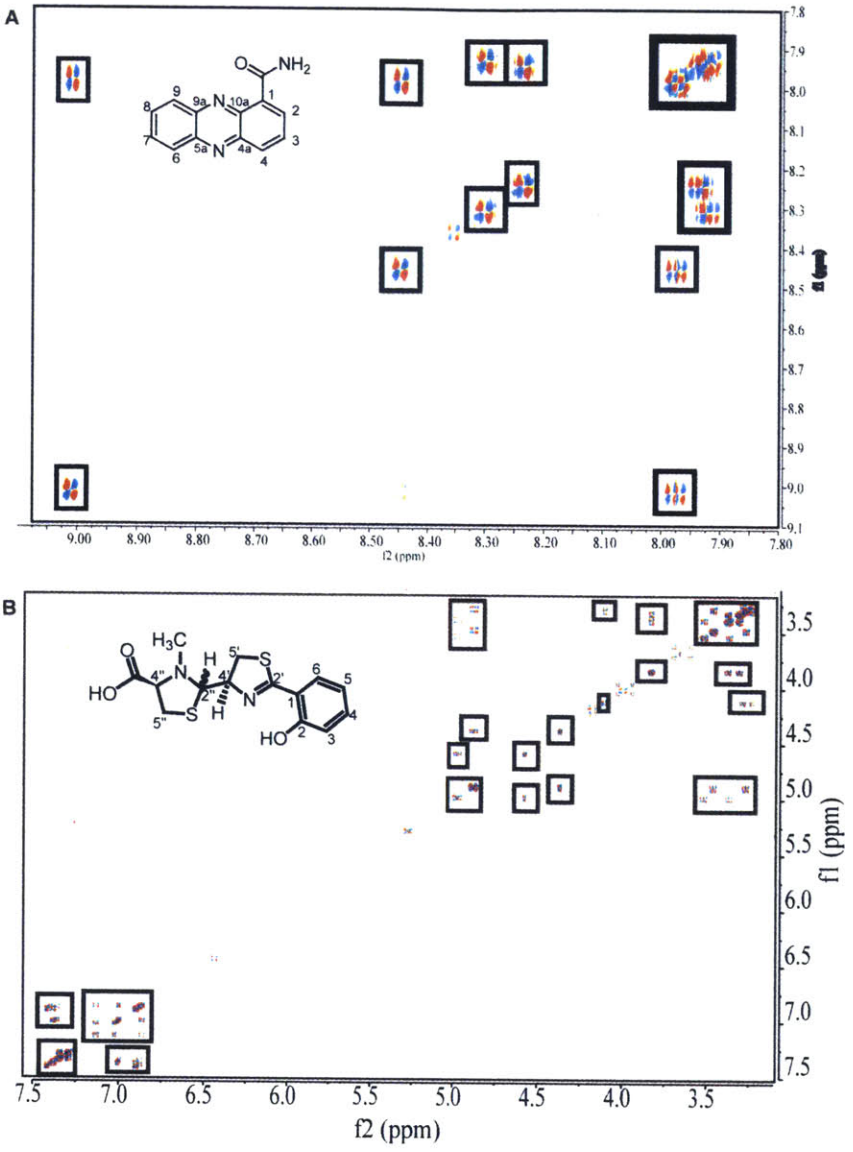

Figure S5. DQF-COSY spectrum of CombiFlash fraction of *P. aeruginosa* metabolome extract reveals presence of phenazine-1-carboxamide and pyochelin, related to Figure 5; see also Tables S1 and S2.

(A) Section of DQF-COSY spectrum (600 MHz, $CDCl_3$) with boxed cross-peaks indicative of major component phenazine-1-carboxamide. See Table S1. (B) Section of DQF-COSY spectrum (600 MHz, $CDCl_3$) with boxed crosspeaks indicative of major component pyochelin. See Table S2.

Figure S6, Related to Figure 6

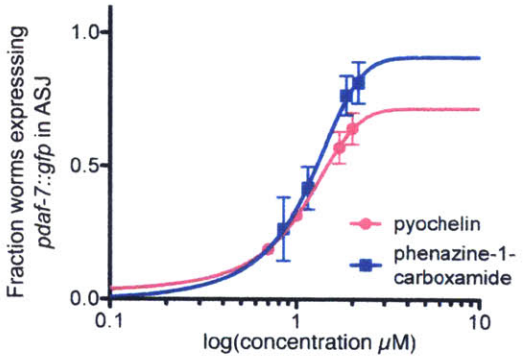

Figure S6. Dose-dependence of the *daf-7* transcriptional response to pyochelin and phenazine-1-carboxamide, related to Figure 6. Fraction animals expressing *daf-7::gfp* in the ASJ neurons after exposure to *E. coli* supplemented with either PCN or pyochelin. Data represent the average of three independent experiments and error bars indicate standard error. The data have been fit using a three-parameter dose-response curve and plotted on a semi-log scale. EC_{50} values for pyochelin and PCN are 11.7 μM and 13.4 μM, respectively, and maximum response values for pyochelin and PCN are 0.7 and 0.9, respectively.

Table S1. NMR spectroscopic data of Phenazine-1-Carboxamide, related to Figure S5. ^{1}H (600 MHz), ^{13}C (151 MHz), and important HMBC NMR spectroscopic data for PCN in $CDCl_3$. Chemical shifts were referenced to ($C\underline{H}Cl_3$) = 7.26 ppm and ($\underline{C}DCl_3$) = 77.16 ppm. Multiplicities are indicated in parentheses.

Carbon No.	δ (ppm)	Proton No.	δ (ppm)	J (Hz)	HMBC correlations
-		NH_2	10.80 (bs)		-
Carbonyl	170.01	-	-		-
1	128.41	-	-		-
2	134.38	2	8.45 (d)	$J_{2,3}$ = 8.8	C-4, C-10a
3	129.88	3	7.98 (dd)		C-4, C-1
4	135.99	4	9.01 (d)	$J_{3,4}$ = 8.8	C-3, C-2, C-4a
4a	140.67	-	-		-
5a	141.43	-	-		-
6	129.60	6	8.30 (m)		C-5a, C-7
7	131.05	7	7.93 (m)		C-6, C-5a
8	129.02	8	7.94 (m)		C-9, C-9a
9	128.02	9	8.24 (d)	$J_{8,9}$ = 8.8	C-7, C-9a
9a	143.09	-	-		
10a	140.80	-	-		

Table S2. NMR spectroscopic data of Pyochelin, related to Figure S5. ^{1}H (600 MHz), ^{13}C (151 MHz), and important HMBC NMR spectroscopic data for pyochelin in $CDCl_3$. Chemical shifts were referenced to ($C\underline{H}Cl_3$) = 7.26 ppm and ($\underline{C}DCl_3$) = 77.16 ppm. Multiplicities are indicated in parentheses.

Carbon No.	δ (ppm)	Proton No.	δ (ppm)	J (Hz)	HMBC correlations
1	115.97	-	-		-
2	159.14	-	-		-
3	117.17	3	7.01 (m)		C-1, C-5, C-2
4	130.65	4	7.38 (m)		C-6
5	120.44	5	6.90 (m)		C-1, C-3, C-4, C-6
6	133.50	6	7.42 (d)	$J_{5,6}$ = 8.5	C-2
2'	173.75	-	-		-
4'	80.02	4'	4.89 (m)		C-5', C-2', C-2"
5'	33.19	5a', 5b'	3.28, 3.47 (dd)		C-2', C-4', C-2"
2"	77.74	2"	4.38 (d)	$J_{2",4'}$ = 8.7	C-4', C-5'
4"	73.51	4"	3.84 (t)		C-5", C-2", COOH
5"	33.24	5a", 5b"	3.39, 3.32 (dd)		C-4", C-2", COOH
Methyl	43.62	Methyl	2.71 (s)		C-2", C-4"
Carboxylic acid	172.53	-	-		-

Table S3. Complete list of *C. elegans* strains used in this study, related to Experimental Procedures.

STRAIN	GENOTYPE
N2	wild type
ZD715	*daf-7(ok3125)* 5x Backcrossed
CB1372	*daf-7(e1372)*
DR40	*daf-1(m40)*
CB1393	*daf-8(e1393)*
DR1572	*daf-2(e1368)*
DA650	*npr-1(215F)*
NL348	*gpa-2(pk16) gpa-3(pk35)*
ZD907	*daf-7(ok3125); daf-3(e1376)*
ZD889	*daf-7(ok3125); dgk-1(nu62)*
ZD890	*goa-1(n1134); daf-7(ok3125)*
ZD910	*tdc-1(n3420); daf-7(ok3125)*
ZD911	*daf-7(ok3125); tbh-1(n3722)*
ZD634	*gcy-35(ok769); daf-7(ok3125)*
KQ143	*daf-7(e1372); daf-12 (m20)*
ZD919	*daf-7(ok3125); npr-1(215F)*
ZD695	*daf-7(ok3125); qdEx34[trx-1p::daf-7 + ges-1p::gfp]*
ZD696	*daf-7(ok3125); qdEx35[trx-1p::daf-7 + ges-1p::gfp]*
ZD729	*daf-7(ok3125); qdEx37[daf-7p::daf-7 + ges-1p::gfp]*
ZD730	*daf-7(ok3125); qdEx38[daf-7p::daf-7 + ges-1p::gfp]*
ZD735	*daf-7(ok3125); qdEx43[str-3p::daf-7 + ges-1p:gfp]*
ZD736	*daf-7(ok3125); qdEx44[str-3p::daf-7 + ges-1p:gfp]*
ZD732	*daf-7(ok3125); qdEx40[trx-1p::daf-7 + ges-1p::gfp]*
ZD733	*daf-7(ok3125); qdEx41[trx-1p::daf-7 + ges-1p::gfp]*
KQ251	*daf-1(m40); ftEX69[pegl-3::daf-1::GFP; odr-1::dsRED]*
KQ252	*daf-1(m40); ftEX70[pbbs-1::daf-1::GFP; odr-1::dsRED]*
KQ265	*daf-1(m40); ftEX83[posm-6::daf-1::GFP; odr-1::dsRED]*
KQ280	*daf-1(m40); ftEX98[pdaf-1::daf-1::GFP; odr-1::dsRED]*
KQ380	*daf-1(m40); ftEX205[ptdc-1::daf-1-gfp; odr-1::dsRED]*
ZD762	*mgIs40[daf-28p::nls-GFP]; jxEx100[trx-1::ICE + ofm-1::gfp]*
ZD763	*mgIs40[daf-28p::nls-GFP]; jxEx102[trx-1::ICE + ofm-1::gfp]*
ZD818	*mgIs40; daf-3(e1376); jxEx100*
ZD819	*mgIs40; daf-3(e1376); jxEx102*
ZD820	*mgIs40; daf-3(ok3610); jxEx100*
ZD821	*mgIs40; daf-3(ok3610); jxEx102*

FK181	*ksIs2[daf-7p::GFP + rol6(su1006)]*
ZD682	*ksIs2; daf-11(m47)*
ZD714	*ksIs2; tax-4(p678)*
ZD726	*tax-2(p671) ksIs2*
ZD884	*ksIs2; gpa-3(qd262)*
ZD887	*ksIs2; gpa-2(pk16) gpa-3(pk35)*
ZD1083	*ksIs2; gpa-2(pk16)*
ZD1047	*ksIs2; gpa-3(pk35)*
ZD971	*ksIs2; gpa-2(pk16) gpa-3(pk35); qdEx64[bbs-1p::gpa-3 + ofm-1::gfp]*
ZD974	*ksIs2; gpa-2(pk16) gpa-3(pk35); qdEx67[trx-1p::gpa-3 + ofm-1::gfp]*
ZD1059	*ksIs2; gpa-3(qd262); qdEx88[bbs-1p::gpa-3 + ofm-1::gfp]*
ZD1061	*ksIs2; gpa-3(qd262); qdEx90[trx-1p::gpa-3 + ofm-1::gfp]*
ZD1111	*ksIs2; gpa-2(pk16) gpa-3(pk35); qdEx92[bbs-1p::gpa-2 + ofm-1::gfp]*
ZD1114	*ksIs2; gpa-2(pk16) gpa-3(pk35); qdEx95[trx-1p::gpa-2 + ofm-1::gfp]*
ZD1115	*ksIs2; gpa-2(pk16) gpa-3(pk35); qdEx96[ceh-36p::gpa-2 + ofm-1::gfp]*
OE3010	*lin-15B(n765); ofEx4[pBLH98: lin-15(+) + trx-1::GFP]*
CX5478	*lin-15B(n765); kyEx581[ocr-4::GFP + lin-15(+)]*
OH7547	*otIs199[cat-2::GFP + rgef-1::dsRed + rol-6(su1006)]*
ZD1184	*qdEx103[trx-1p::GCaMP5 + ofm-1::gfp]*

Table S4. Complete list of oligos used in this study, related to Experimental Procedures.

Oligos used for *daf-7* smFISH Probe	**Oligos used for *gpa-2* smFISH Probe**
5'-ttcatttctgggtccattgg-3'	5'-cgttgactttccacattctc-3'
5'-atacatctccaggtagactg-3'	5'-agcaatctcatctgcttgag-3'
5'-tcgtccttctccagtaagtc-3'	5'-atctgtgtactgttttgacg-3'
5'-catttcaacgcccatatcct-3'	5'-ttggcctgcgtcaaaagttc-3'
5'-gatctttggcggtgtagaat-3'	5'-aactatgtttgtgtatacca-3'
5'-gacgggttctctccataact-3'	5'-tgctttgactaaatgatcca-3'
5'-gtcaaacttggcaacaagct-3'	5'-aaattcaatccggcagctgg-3'
5'-gcttctttccaaatcatttg-3'	5'-atcatgttctctcatcggat-3'
5'-tgagtgtggcctgaagaata-3'	5'-aatgtagagggtcagcatgt-3'
5'-gcaggaatctcaattgatac-3'	5'-gttggaagtttttatgttgc-3'
5'-ttgaagcatccctgaatcct-3'	5'-tttctccacatgatctgcag-3'
5'-cgtaaacttgaacttgaaca-3'	5'-ttcaattcttttctctcggc-3'
5'-attgatccatcctcgttctt-3'	5'-aagtattccgtgttatcacc-3'
5'-tccagaagtgaccatctctc-3'	5'-atattcttggcaggttttca-3'
5'-cggatccctttgtagcgaaa-3'	5'-tcgcatttgggtgataatct-3'
5'-ggaagttgaatgctgatacg-3'	5'-gtccgcaaaagaagggtgtc-3'
5'-ccaacttttgacagtatcaa-3'	5'-tgaatattctccttcttgat-3'
5'-cttggatcggagaaattgtg-3'	5'-tcgatattccggaaacgcct-3'
5'-agcattgccttgacgaagat-3'	5'-tttcagcgtaattttgctct-3'
5'-atgaagggcaacgttgcgcc-3'	5'-ttcgtcttgataaatgcgac-3'
5'-aacgtcagcagtggtctgtt-3'	5'-gttattggaaagcgcctcga-3'
5'-agagctgaagacgcatgttg-3'	5'-gcacgtagaatgtcttcttc-3'
5'-cgggacccctttggacgagt-3'	5'-tgtgtctgttgcgcatgttt-3'
5'-tttggcatgagaacggcgtt-3'	5'-ccaaaatcttttgcacttga-3'
5'-tgtgcttcggcattgcaaac-3'	5'-agagtccagatttgtgtagg-3'
Oligos used for *daf-7* rescue constructs	
5'-ATGGAAGCTTCGGCAACTAA-3'	*daf-7p* forward
5'-GAGTGAAGATGCCATGAACATGGCTGAACTTCAAGCGGGCTGAACC-3'	*daf-7p* reverse + *daf-7* homology
5'-ATATTTTGTTGGCCCATCGT-3'	*str-3p* forward
5'-GAGTGAAGATGCCATGAACATGTTCCTTTTGAAATTGAGGC-3'	*str-3p* reverse + *daf-7* homology
5'-ATGGATACCTGATCATTC-3'	*trx-1p* forward
5'-GAGTGAAGATGCCATGAACATAAGTGAGAAGATGAAGAG-3'	*trx-1p* reverse + *daf-7* homology
5'-ATGTTCATGGCATCTTCACTC-3'	*daf-7* cDNA forward
5'-TAGGGATGTTGAAGAGTAATTGGACTTATGAGCAACCGCATTTCTT-3'	*daf-7* cDNA reverse + unc-54 homology
5'-GTCCAATTACTCTTCAACATCCCTA-3'	*unc-54* 3'UTR forward

5'-CAGTTATGTTTGGTATATTGGGAATG-3'	*unc-54* 3'UTR reverse
Oligos used for *gpa-3* and *gpa-2* rescue constructs	
5'-TTGCAAAGAAGCACATCAAAA-3'	*bbs-1p* forward
5'-GCAGATTGGCATAATCCCATTTTTTGTTAATTTTGGAGCAC-3'	*bbs-1p* reverse + *gpa-3* homology
5'-TCACTTTGGCACAGACCCATTTTTTGTTAATTTTGGAGCAC-3'	*bbs-1p* reverse + *gpa-2* homology
5'-TGAGTTGGGCACTTCGTAGA-3'	*trx-1p* forward
5'-GCAGATTGGCATAATCCCATGATCAATTGCTCAAAGTCAC-3'	*trx-1p* reverse + *gpa-3* homology
5'-TCACTTTGGCACAGACCCATGATCAATTGCTCAAAGTCAC-3'	*trx-1p* reverse + *gpa-2* homology
5'-acgtggttttcacatttgtgca-3'	*ceh-36p* forward
5'-TCACTTTGGCACAGACCCATtgtgcatgcgggggcagg-3'	*ceh-36p* reverse + *gpa-2* homology
5'-ATGGGATTATGCCAATCTGC-3'	*gpa-3* cDNA forward
5'-TAGGGATGTTGAAGAGTAATTGGACTCAGTACAAACCGCATCCTT-3'	*gpa-3* cDNA reverse + *unc-54* homology
5'-ATGGGTCTGTGCCAAAGTGA-3'	*gpa-2* cDNA forward
5'-TAGGGATGTTGAAGAGTAATTGGACTTAATAGAGTCCAGATTTGTGTAGGT-3'	*gpa-2* cDNA reverse + *unc-54* homology
5'-GTCCAATTACTCTTCAACATCCCTA-3'	*unc-54* 3'UTR forward
5'-ATTTGCGCGGGAATTCAA-3'	*unc-54* 3'UTR reverse
Oligos used for GCaMP5 construct	
5'-TGAGTTGGGCACTTCGTAGA-3'	*trx-1p* forward
5'-GATGATGATGATGATGAGAACCCATGATCAATTGCTCAAAGTCAC-3'	*trx-1p* reverse + GCaMP homology
5'-ATGGGTTCTCATCATCATCATCATC-3'	GCaMP5 Forward
5'-TAGGGATGTTGAAGAGTAATTGGACTCACTTCGCTGTCATCATTTGTAC-3'	GCaMP5 Reverse + *unc-54* homology
5'-GTCCAATTACTCTTCAACATCCCTA-3'	*unc-54* 3'UTR forward
5'-CAGTTATGTTTGGTATATTGGGAATG-3'	*unc-54* 3'UTR reverse

Chapter Three

Inhibition of Lithium-Sensitive Phosphatase BPNT-1 Causes Selective Neuronal Dysfunction in *C. elegans*

Joshua D. Meisel and Dennis H. Kim

This paper is currently *in review* for publication.

Summary

Lithium has been a mainstay for the treatment of bipolar disorder, yet the molecular mechanisms underlying its action remain enigmatic. Bisphosphate 3'-nucleotidase (BPNT-1) is a lithium-sensitive phosphatase that catalyzes the breakdown of cytosolic 3'phosphoadenosine 5'-phosphate (PAP), a byproduct of sulfation reactions utilizing the universal sulfate group donor 3'phosphoadenosine 5'-phosphosulfate (PAPS) (Figure 1A) (Murguía, Bellés, and Serrano 1995; Spiegelberg et al. 1999; López-Coronado et al. 1999). Loss of BPNT-1 leads to the toxic accumulation of PAP in yeast and non-neuronal cell types in mice (Hudson et al. 2013; Spiegelberg et al. 2005). Intriguingly, BPNT-1 is expressed throughout the mammalian brain (Hudson et al. 2013), and it has been hypothesized that inhibition of BPNT-1 could contribute to the effects of lithium on behavior (Spiegelberg et al. 2005). Here, we show that loss of BPNT-1 in *Caenorhabditis elegans* results in the selective dysfunction two neurons, the bilaterally symmetric pair of ASJ chemosensory neurons. As a result, BPNT-1 mutants are defective in behaviors dependent on the ASJ neurons, such as dauer exit and pathogen avoidance. Acute treatment with lithium also causes dysfunction of the ASJ neurons, and we show that this effect is reversible, and mediated specifically through inhibition of BPNT-1. Finally, we show that the selective effect of lithium on the nervous system is due in part to the limited expression of the cytosolic sulfotransferase SSU-1 in the ASJ neuron pair. Our data suggest that lithium, through inhibition of BPNT-1 in the nervous system, can cause selective toxicity to specific neurons, resulting in corresponding effects on behavior of *C. elegans.*

Graphical Abstract

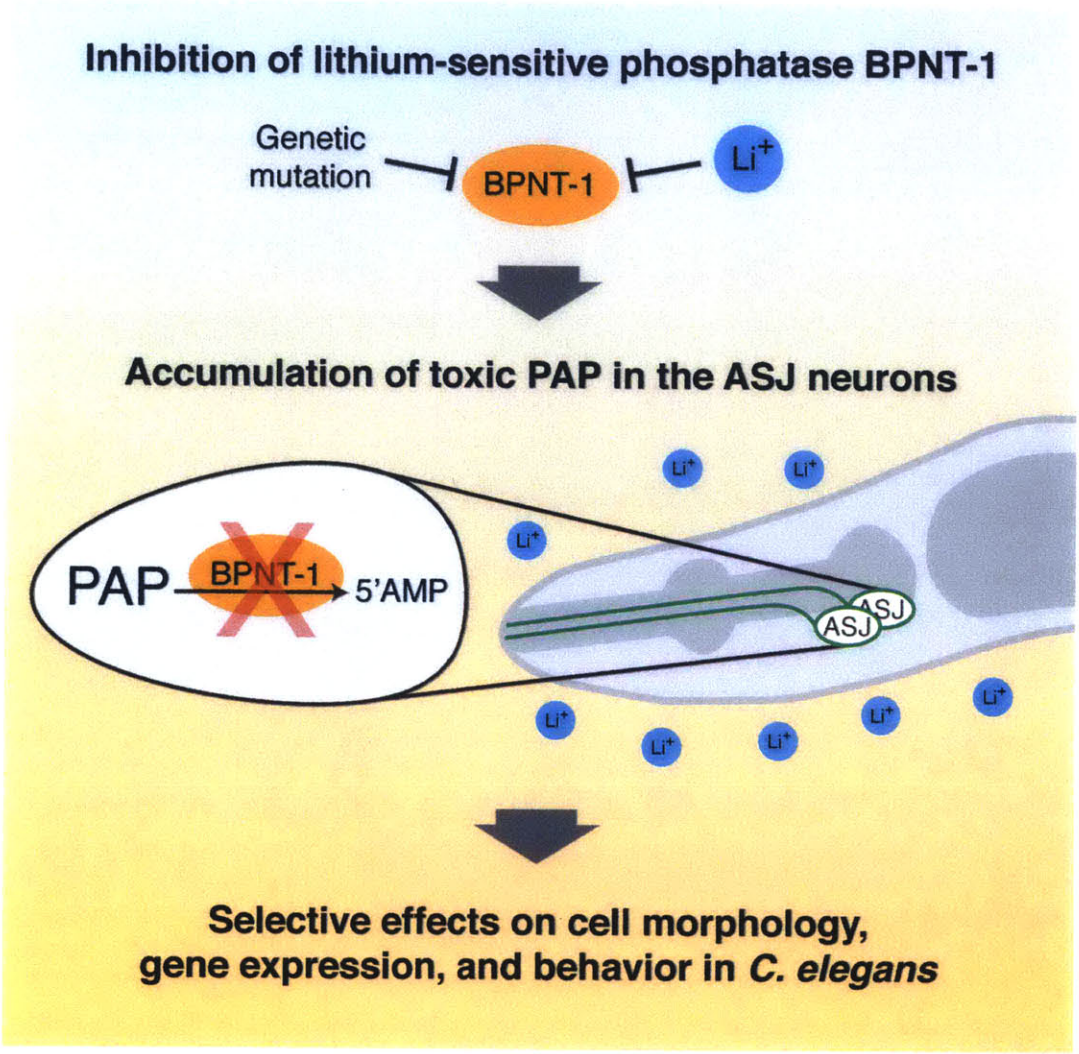

Results and Discussion

We have previously shown that the *daf-7* gene, encoding a TGF-β ligand that regulates diverse behaviors in *C. elegans* (Ren et al. 1996; Schackwitz, Inoue, and Thomas 1996), is transcriptionally activated in the ASJ chemosensory neuron pair upon exposure to the pathogenic bacteria *Pseudomonas aeruginosa* (Meisel et al. 2014). We conducted a forward genetic screen for animals defective in this transcriptional response, and identified one such mutant, *qd257*, which carries a D119N missense mutation in *bpnt-1* (Figures 1B-C). This aspartic acid residue is conserved from yeast to humans, and is required for the catalytic activity of the superfamily of lithium-sensitive phosphatases (Pollack et al. 1993; Albert et al. 2000). Confirming the identity of *qd257* as an allele of *bpnt-1*, we used CRISPR/Cas9-mediated genome editing to generate a loss-of-function *bpnt-1* allele, *qd303*, in which a deletion/insertion leads to a frameshift at amino acid 20 followed by a premature stop codon. Animals carrying *bpnt-1(qd303),* or the W294X nonsense mutation *bpnt-1(gk469190),* also fail to express *daf-7* in the ASJ neurons when exposed to *P. aeruginosa* (Figures 1B-C). Notably, the constitutive expression of *daf-7* in the ASI neuron pair is unaffected by loss of *bpnt-1* (Figure 1B). These data suggest that BPNT-1 is required for the expression of *daf-7* specifically in the ASJ neurons.

BPNT-1 is conserved in all eukaryotes, and belongs to a family of lithium-sensitive phosphatases that includes inositol monophosphatase and inositol polyphosphate-1-phosphatase (Figure S1). Loss of BPNT-1 in mice leads to the toxic accumulation of PAP and death by liver failure at 45 days (Hudson et al. 2013), and so we were surprised that *bpnt-1* mutants were viable and appeared healthy. We used fluorescent *in situ* hybridization to analyze the *bpnt-1* expression pattern and observed

Figure 1

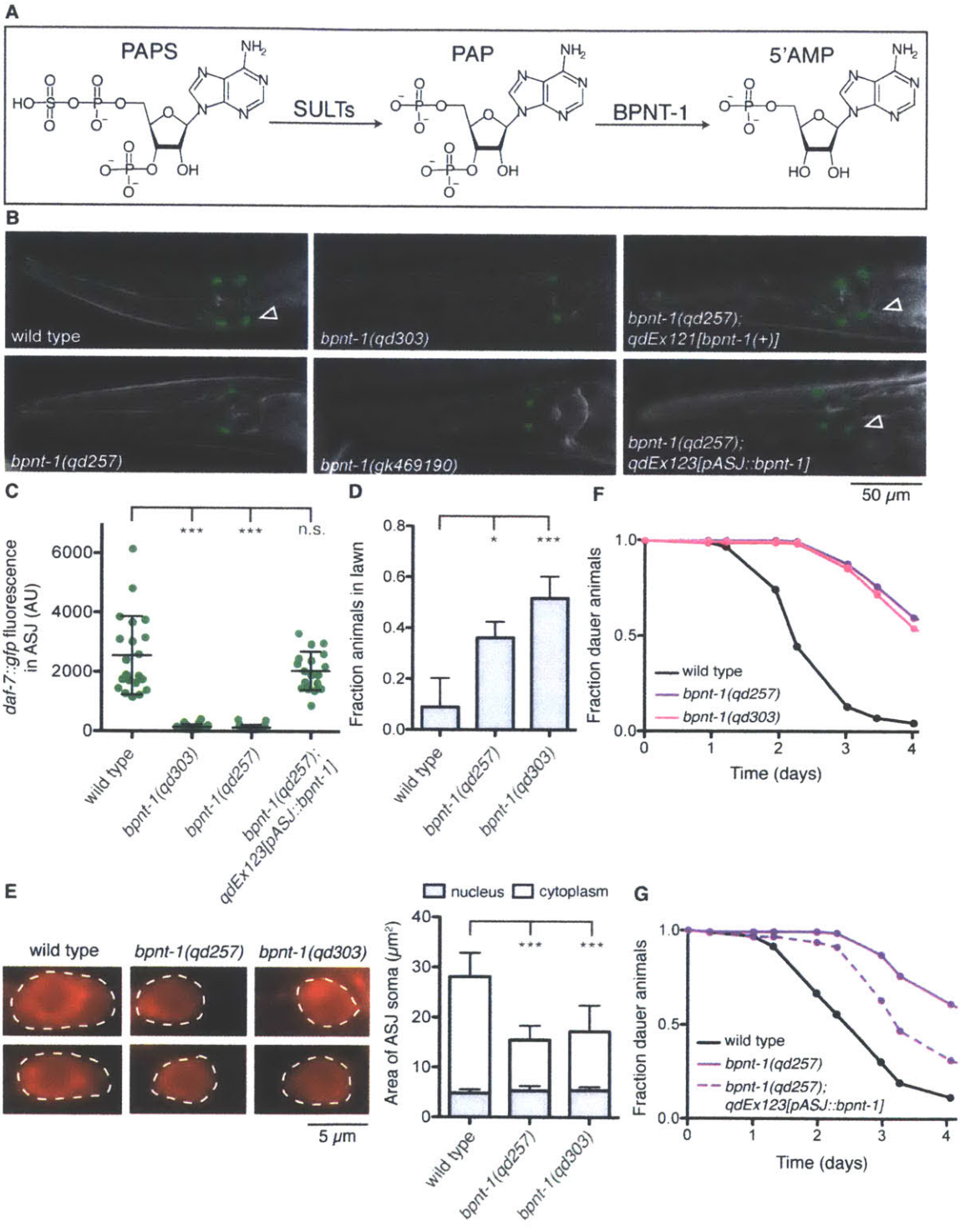
A
PAPS
PAP
5'AMP
SULTs
BPNT-1
B
wild type
bpnt-1(qd303)
bpnt-1(qd257); qdEx121[bpnt-1(+)]
bpnt-1(qd257)
bpnt-1(gk469190)
bpnt-1(qd257); qdEx123[pASJ::bpnt-1]
50 μm
C
daf-7::gfp fluorescence in ASJ (AU)
***
***
n.s.
wild type
bpnt-1(qd303)
bpnt-1(qd257)
bpnt-1(qd257); qdEx123[pASJ::bpnt-1]
D
Fraction animals in lawn
*
***
wild type
bpnt-1(qd257)
bpnt-1(qd303)
F
Fraction dauer animals
wild type
bpnt-1(qd257)
bpnt-1(qd303)
Time (days)
E
wild type
bpnt-1(qd257)
bpnt-1(qd303)
5 μm
nucleus
cytoplasm
Area of ASJ soma (μm²)
***
***
wild type
bpnt-1(qd257)
bpnt-1(qd303)
G
Fraction dauer animals
wild type
bpnt-1(qd257)
bpnt-1(qd257); qdEx123[pASJ::bpnt-1]
Time (days)

Figure 1. Bisphosphate 3'-nucleotidase (BPNT-1) is required for the function of the ASJ neurons. (A) BPNT-1 catalyzes the breakdown of cytosolic 3'phosphoadenosine 5'-phosphate (PAP), a byproduct of sulfation reactions utilizing the universal sulfur donor 3'phosphoadenosine 5'-phosphosulfate (PAPS). **(B)** *daf-7* expression pattern in animals exposed to *P. aeruginosa* for 16 h. Empty triangles indicate the ASJ neurons (posterior) when visible. The ASI neuron pair (anterior) is unaffected by loss of BPNT-1. All genotypes contain *ksIs2[daf-7p::gfp]*. **(C)** Maximum fluorescence of *daf-7p::gfp* in the ASJ neurons after 16 h exposure to *P. aeruginosa*. All genotypes contain *ksIs2[daf-7p::gfp]*. **(D)** Lawn occupancy of animals on *P. aeruginosa* after 20 h. All genotypes contain *npr-1(215F)*. **(E)** Fluorescence microscopy of the ASJ cell body (dashed line) visualized with a red-fluorescent lipophilic dye (left). Area of the ASJ cell body divided into nuclear and cytoplasmic compartments (right). **(F-G)** Fraction of animals that have exited the dauer developmental diapause state. All genotypes contain *daf-2(e1368)*. For all panels: *** $P < 0.001$, * $P < 0.05$ as determined by one-way ANOVA followed by Dunnett's Multiple Comparison Test. n.s. = not significant. Error bars indicate standard deviation. See also Figures S1 and S2.

broad mRNA expression throughout the animal (Figure S2), confirming previous high-throughput expression analysis (Dupuy et al. 2007). *bpnt-1* mRNA was almost entirely absent in the *bpnt-1(qd303)* mutant, demonstrating that the *bpnt-1* expression pattern was specific (Figure S2). Transgenic expression of genomic *bpnt-1* DNA, or *bpnt-1* cDNA under a promoter that drives expression exclusively in the ASJ neurons, each rescued the *daf-7* expression defect in the ASJ neurons (Figures 1B-C). Consistent with this observation and our previous results that established a role for *daf-7* induction in promoting pathogen avoidance (Meisel et al. 2014), *bpnt-1* mutant animals are defective in the protective behavioral avoidance of *P. aeruginosa* (Figure 1D). We therefore conclude that despite its widespread expression, BPNT-1 is not essential in *C. elegans,* and is acting cell-autonomously to promote the function of the ASJ neurons.

We determined that the gross morphology of the ASJ neurons was still intact in the *bpnt-1* mutant background through labeling with a lipophilic dye. However, we also observed a reduction in the cytoplasmic volume of the ASJ neurons (Figure 1E). This led us to ask if the expression of other genes in the ASJ neurons and additional ASJ-dependent behaviors might be affected in the *bpnt-1* mutant. Indeed, expression of the insulin-like peptide *daf-28* (Li, Kennedy, and Ruvkun 2003), the G protein alpha subunit *gpa-9* (Jansen et al. 1999), and the thioredoxin *trx-1* (Miranda-Vizuete et al. 2006) were all decreased in the *bpnt-1* mutant (Figures 2A-C). Expression of *gpa-9* in tail neurons and expression of *daf-28* in the ASI neurons was unaffected by loss of *bpnt-1* (data not shown), further suggestive of ASJ-specific effects of the loss of BPNT-1 function. In addition, exit from the dauer reproductive diapause state, a behavior which requires the ASJ neurons (Cornils et al. 2011; Bargmann and Horvitz 1991), was severely impaired in

Figure 2

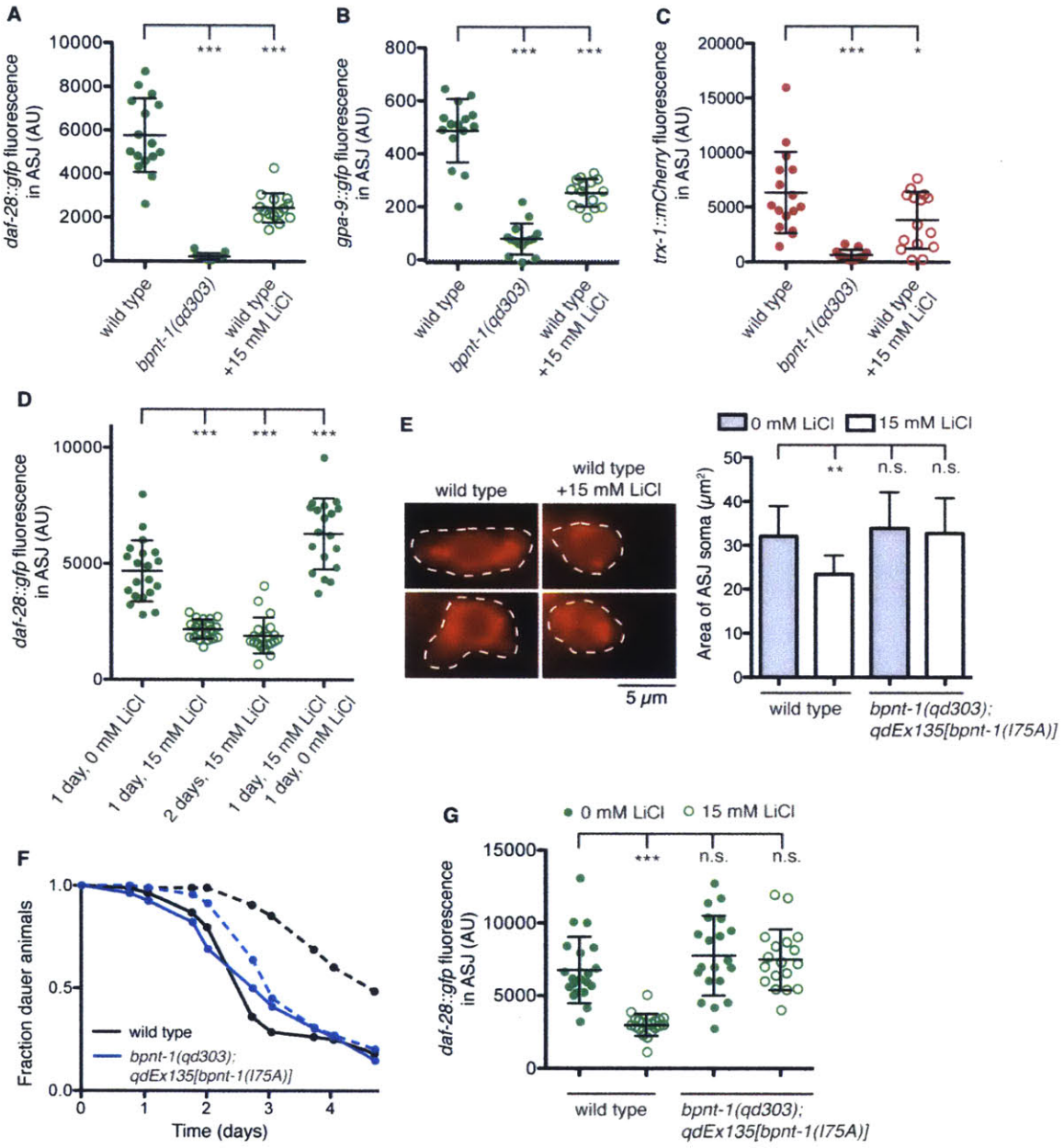
A
daf-28::gfp fluorescence in ASJ (AU)
wild type
bpnt-1(qd303)
wild type +15 mM LiCl
B
gpa-9::gfp fluorescence in ASJ (AU)
C
trx-1::mCherry fluorescence in ASJ (AU)
D
daf-28::gfp fluorescence in ASJ (AU)
1 day, 0 mM LiCl
1 day, 15 mM LiCl
2 days, 15 mM LiCl
1 day, 15 mM LiCl 1 day, 0 mM LiCl
E
wild type
wild type +15 mM LiCl
5 μm
0 mM LiCl
15 mM LiCl
Area of ASJ soma (μm²)
n.s.
wild type
bpnt-1(qd303); qdEx135[bpnt-1(I75A)]
F
Fraction dauer animals
Time (days)
wild type
bpnt-1(qd303); qdEx135[bpnt-1(I75A)]
G
0 mM LiCl
15 mM LiCl
daf-28::gfp fluorescence in ASJ (AU)
wild type
bpnt-1(qd303); qdEx135[bpnt-1(I75A)]

Figure 2. Lithium induces dysfunction of the ASJ neurons through inhibition of BPNT-1. (A, D, G) Maximum fluorescence of *daf-28::gfp* in the ASJ neurons. All genotypes contain *mgIs40[daf-28p::nls-GFP]*. **(B)** Maximum fluorescence of *gpa-9::gfp* in the ASJ neurons. All genotypes contain *pkIs586[gpa-9p::GFP]*. **(C)** Maximum fluorescence of *trx-1::mCherry* in the ASJ neurons. All genotypes contain *qdEx133[trx-1p::mCherry]*. **(E)** Fluorescence microscopy of the ASJ cell body (dashed line) visualized with a red-fluorescent lipophilic dye (left). Area of the ASJ cell body (right). All genotypes contain *mgIs40[daf-28p::nls-GFP]*. **(F)** Fraction of animals that have exited the dauer developmental diapause state. All genotypes contain *daf-2(e1368)*. Dashed lines indicate addition of 15 mM LiCl. For all panels: Open circles indicate addition of 15 mM LiCl. *** $P < 0.001$, ** $P < 0.01$, * $P < 0.05$ as determined by one-way ANOVA followed by Dunnett's Multiple Comparison Test. n.s. = not significant. Error bars indicate standard deviation. See also Figure S3.

animals lacking BPNT-1 (Figure 1F). The dauer exit defect was partially rescued by expressing *bpnt-1* from an ASJ-specific promoter, demonstrating that BPNT-1 activity in the ASJ neurons is required for the dauer exit behavior (Figure 1G). From these observations we conclude that ASJ transcription and ASJ-dependent behaviors are defective in BPNT-1 mutants.

Given that BPNT-1 enzymatic activity is potently inhibited by lithium *in vitro* (Spiegelberg et al. 1999; López-Coronado et al. 1999; Murguía, Bellés, and Serrano 1995), we asked whether the effects of lithium on *C. elegans* would mimic the loss of BPNT-1. Indeed, acute exposure to 15 mM LiCl significantly decreased the expression of all ASJ-specific genes, including *daf-28, gpa-9,* and *trx-1* (Figures 2A-C). Similar to the effects of loss of BPNT-1, expression of these genes in other neurons was not affected by lithium treatment (data not shown). The inhibitory effects of lithium treatment were reversible – following 24 hours recovery, *daf-28::gfp* expression in the ASJ neurons had increased to levels slightly above untreated animals (Figure 2D). Acute lithium exposure also reduced the cytoplasmic volume of the ASJ neurons (Figure 2E). Additionally, dauer exit behavior was inhibited by lithium treatment to levels similar to *bpnt-1* mutant animals (Figure 2F). These results indicate that the ASJ neurons are selectively and reversibly inhibited by lithium.

Lithium can inhibit the activity of phosphatases other than BPNT-1, such as inositol phosphatases, and we wondered if the effects of lithium were mediated by inhibition of BPNT-1. A mutation in the BPNT-1 yeast homolog MET22/HAL2 (V70A) has been characterized that does not affect its catalytic activity but confers 10-fold resistance to inhibition by lithium (Albert et al. 2000). This hydrophobic residue is

conserved not only in all BPNT-1 homologs, but in the homologous inositol phosphatases as well. In fact, introduction of the corresponding mutation into human inositol monophosphatase (I68A) or a bacterial inositol monophosphatase (L81A) renders these proteins lithium insensitive (Albert et al. 2000; Nigou, Dover, and Besra 2002), suggesting that the homologous change would be effective on the much more closely related *C. elegans* BPNT-1. Introduction of this BPNT-1 variant (I75A in *C. elegans*) into the *bpnt-1(qd303)* mutant fully rescued the ASJ expression defect of *daf-28* and in addition rendered the ASJ neuron resistant to the transcriptional and morphological effects of lithium treatment (Figures 2E and 2G). Animals expressing BPNT-1(I75A) were also resistant to the effects of lithium treatment on dauer exit, strongly suggestive that the effects of lithium on *C. elegans* dauer exit behavior are due to the inhibition of BPNT-1 (Figure 2F). Additionally, mutations in lithium-sensitive inositol monophosphatase TTX-7 or Golgi-resident PAP phosphatase GPAP-1 did not mimic the addition of lithium (Figure S3A). These data suggest that the inhibitory effects of lithium on the ASJ neurons are mediated through inhibition of the lithium-sensitive phosphatase BPNT-1.

To identify the molecular mechanism by which loss of BPNT-1 leads to dysfunction of the ASJ neuron, we undertook cross-species rescue experiments with homologs of restricted substrate specificity. In addition to catalyzing the breakdown of PAP into 5'-AMP, BPNT-1 has been shown to have *in vitro* inositol polyphosphate-1-phosphatase (IPP) activity (López-Coronado et al. 1999; Spiegelberg et al. 1999). Intriguingly, although IPP was present in the common ancestor of all animals, as evidenced by its presence in cnidarians and sponges, IPP was lost in the nematode

lineage (Figure S1). We therefore sought to determine if BPNT-1 might be functioning as an IPP in *C. elegans* neurons. Expression of *bpnt-1* cDNA from *C. elegans* or *D. melanogaster* driven by the endogenous *C. elegans bpnt-1* promoter rescued the *daf-7* expression defect in the ASJ neurons (Figures 3A-B). However introduction of *D. melanogaster* or *H. sapiens* IPP cDNA was unable to rescue the *daf-7* expression defect in *bpnt-1* mutants, suggesting that the ASJ defect of *bpnt-1* mutant animals is not due a loss of IPP activity (Figures 3A-B). Instead, introduction of the *S. cerevisiae* BPNT-1 homolog MET22/HAL2, which has been shown to have PAP phosphatase activity but weak IPP activity (Spiegelberg et al. 1999; Murguía, Bellés, and Serrano 1995), fully rescued the *bpnt-1(qd303) daf-7* expression phenotype (Figures 3A-B). These data support our hypothesis that loss of BPNT-1 causes ASJ neuronal dysfunction through the accumulation of PAP.

How could loss of BPNT-1, which is widely expressed in *C. elegans*, selectively increase PAP levels and inhibit the two ASJ neurons? PAP is generated in the cytosol as a byproduct of sulfation reactions in which cytosolic sulfotransferases transfer a sulfate group from PAPS onto endogenous and xenobiotic targets such as hormones and catecholamines (Strott 2002). This is in contrast to Golgi-derived PAP which is generated by sulfotransferases that act on proteins and carbohydrates and is degraded by a Golgi-resident PAP 3'-phosphatase that is homologous to BPNT-1 (Frederick et al. 2008). Surprisingly, *C. elegans* has only one cytosolic sulfotransferase in its genome, SSU-1, and SSU-1 is exclusively expressed in the ASJ neurons (Hattori et al. 2006; Carroll et al. 2006). We therefore asked if loss of SSU-1 could suppress the ASJ defect in BPNT-1 mutants. Indeed, loss of SSU-1 could partially suppress the *daf-28* and *daf-7* expression

Figure 3

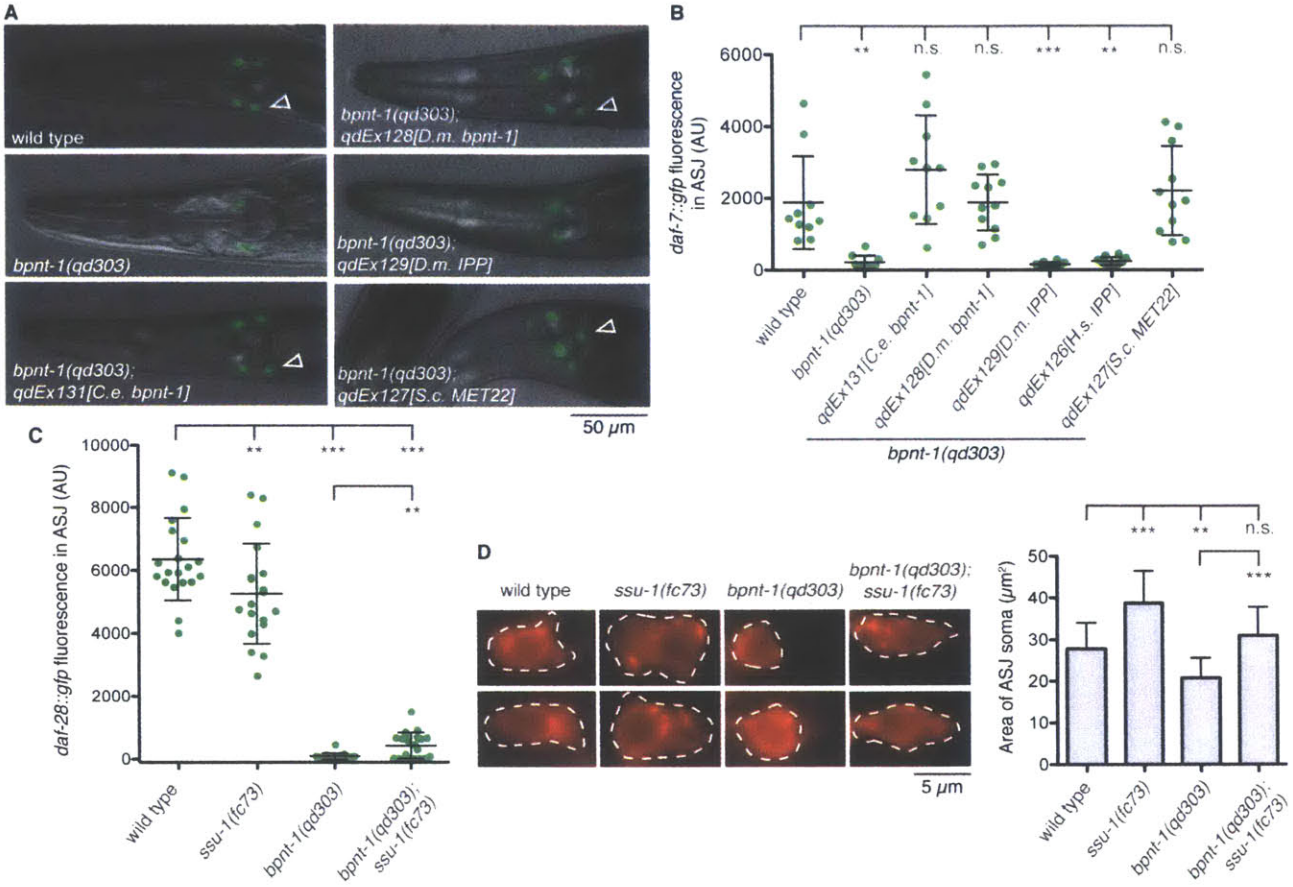
A
wild type
bpnt-1(qd303);
qdEx128[D.m. bpnt-1]
bpnt-1(qd303)
bpnt-1(qd303);
qdEx129[D.m. IPP]
bpnt-1(qd303);
qdEx131[C.e. bpnt-1]
bpnt-1(qd303);
qdEx127[S.c. MET22]
50 μm
B
daf-7::gfp fluorescence in ASJ (AU)
6000
4000
2000
0
**
n.s.
n.s.
***
**
n.s.
wild type
bpnt-1(qd303)
qdEx131[C.e. bpnt-1]
qdEx128[D.m. bpnt-1]
qdEx129[D.m. IPP]
qdEx126[H.s. IPP]
qdEx127[S.c. MET22]
bpnt-1(qd303)
C
daf-28::gfp fluorescence in ASJ (AU)
10000
8000
6000
4000
2000
0
**
***
***
**
wild type
ssu-1(fc73)
bpnt-1(qd303)
bpnt-1(qd303);
ssu-1(fc73)
D
wild type
ssu-1(fc73)
bpnt-1(qd303)
bpnt-1(qd303);
ssu-1(fc73)
5 μm
Area of ASJ soma (μm²)
50
40
30
20
10
0
***
**
n.s.
***
wild type
ssu-1(fc73)
bpnt-1(qd303)
bpnt-1(qd303);
ssu-1(fc73)

Figure 3. Loss of BPNT-1 inhibits the ASJ neurons through accumulation of cytosolic PAP. (A) *daf-7* expression pattern in animals exposed to *P. aeruginosa* for 16 h. Empty triangles indicate the ASJ neurons (posterior) when visible. All genotypes contain *ksIs2[daf-7p::gfp].* **(B)** Maximum fluorescence of *daf-7p::gfp* in the ASJ neurons after 16 h exposure to *P. aeruginosa.* All genotypes contain *ksIs2[daf-7p::gfp].* **(C)** Maximum fluorescence of *daf-28::gfp* in the ASJ neurons. All genotypes contain *mgIs40[daf-28p::nls-GFP].* **(D)** Fluorescence microscopy of the ASJ cell body (dashed line) visualized with a red-fluorescent lipophilic dye (left). Area of the ASJ cell body (right). All genotypes contain *mgIs40[daf-28p::nls-GFP].* For all panels: *** $P < 0.001$, ** $P < 0.01$, * $P < 0.05$ as determined by one-way ANOVA followed by Dunnett's Multiple Comparison Test. n.s. = not significant. Error bars indicate standard deviation. See also Figure S3.

defects of BPNT-1 mutants, even though *ssu-1* mutants themselves were slightly defective in these assays (Figures 3C and S3B). Loss of SSU-1 could also partially suppress the reduction of cytoplasmic volume of the ASJ cell body we observe in BPNT-1 mutant animals (Figure 3D). These data suggest that the specific expression of the cytosolic sulfotransferase SSU-1 in the ASJ neuron pair may contribute to the selective neuronal dysfunction caused by loss of BPNT-1.

The incomplete suppression of *bpnt-1* phenotypes by mutation in *ssu-1* could be due to residual cytosolic PAP produced by additional unidentified cytosolic sulfotransferases. Alternatively, Golgi-derived PAP may be enter the cytosol via PAPS/PAP antiporters in the Golgi membrane (Dejima et al. 2010; Ozeran, Westley, and Schwartz 1996). Golgi-derived PAP is normally degraded by a Golgi-resident PAP 3'-phosphatase homologous to BPNT-1 (GPAP-1 in *C. elegans*), and like *bpnt-1* we find that animals carrying a loss-of-function mutation in *gpap-1* are viable and appear healthy. However we constructed a balanced strain carrying mutations in both *bpnt-1* and *gpap-1* and found the double mutants to be inviable, displaying early larval lethality. This observation suggests that BPNT-1 and GPAP-1 act redundantly throughout the organism to degrade Golgi-produced PAP, which may explain the broad expression pattern of *bpnt-1*. However in the ASJ neuron pair, where there exists a unique source of cytosolic PAP due to expression of *ssu-1*, and perhaps an increased source of Golgi-derived PAP due to the secretory nature of the ASJ neurons, BPNT-1 is required for cellular function.

Inositol monophosphatase and inositol polyphosphate-1-phosphatase belong to a family of evolutionarily conserved phosphatases that are inhibited by lithium at therapeutic concentrations (York and Majerus 1990; Diehl et al. 1990), which has led to

the "inositol depletion" hypothesis for explaining lithium's effects on the mammalian brain (Berridge, Downes, and Hanley 1982). BPNT-1 has also been proposed to be a potential therapeutic target of lithium (Spiegelberg et al. 2005). Here we provide evidence that inhibition of BPNT-1 can cause cell-selective dysfunction resulting in neuron-specific effects on behavior in *C. elegans*. The ASJ neurons of *C. elegans* are acutely sensitive to both the loss of BPNT-1 and the addition of lithium, perhaps due to their expression of the cytosolic sulfotransferase SSU-1 that generates cytosolic PAP (Figure 4). Accumulation of PAP can interfere with numerous cellular processes including sulfotransferase activity, RNA processing, nucleotide phosphorylation, and PARP activity (Ramaswamy and Jakoby 1987; Dichtl, Stevens, and Tollervey 1997; Schneider et al. 1998; Ozeran, Westley, and Schwartz 1996; Toledano et al. 2012). Our data suggest that the differential expression of cytosolic sulfotransferases may result in neuron-selective effects of lithium through inhibition of BPNT-1 and buildup of cytosolic PAP. Intriguingly, cytosolic sulfotransferases are expressed selectively in the mammalian brain, particularly in neurons that synthesize catecholamine neurotransmitters (Salman, Kadlubar, and Falany 2009; Sidharthan, Minchin, and Butcher 2013), and we hypothesize that these populations of neurons may display enhanced susceptibility to inhibition of BPNT-1. We anticipate that our data in *C. elegans* on the neuron-selective effects of lithium, which acts through inhibition of the evolutionarily conserved phosphatase BPNT-1, may have implications for understanding the remarkable, and yet mechanistically poorly understood, effects of lithium therapy and toxicity in humans.

Figure 4

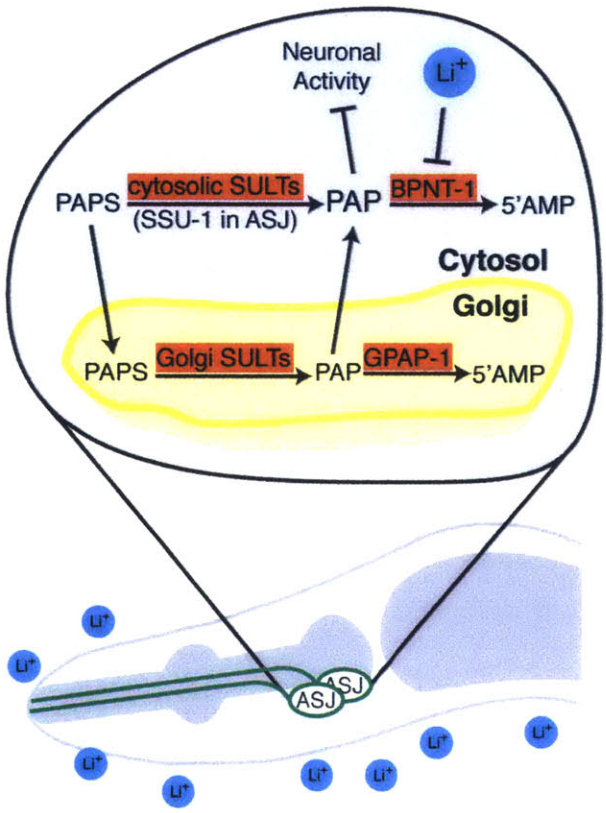

Figure 4. Lithium selectively inhibits the ASJ neurons of *C. elegans* through inhibition of BPNT-1. We hypothesize that inhibition of the cytosolic PAP phosphatase BPNT-1 by lithium or genetic mutation leads to a buildup of toxic PAP, due to ASJ-specific expression of the cytosolic sulfotransferase SSU-1. PAP, in turn, causes alterations in cell morphology, transcription, and behavioral outputs of the ASJ neurons. BPNT-1 can also degrade PAP transported into the cytosol from the Golgi, which may explain the synthetic lethality between BPNT-1 and the Golgi-resident PAP phosphatase GPAP-1.

Author Contributions

J.D.M. performed experiments. J.D.M. and D.H.K analyzed the data, interpreted results, and wrote the paper.

Acknowledgements

We thank W. Gilbert, H. R. Horvitz, the *C. elegans* Million Mutation Project and Knockout Consortium, and the *Caenorhabditis* Genetics Center (which is supported by the NIH, Office of Research Infrastructure Programs) for providing strains and reagents. We thank R. Saunders, F. Meisel, and the Kim and Horvitz lab members for helpful discussions. This study was supported by the NIH (GM084477 to D.H.K.).

Experimental Procedures

C. elegans Strains

C. elegans was maintained on *E. coli* OP50 as previously described (Brenner 1974). BPNT-1 was formerly known as *C. elegans* TAG-231/ZK430.2. GPAP-1 was formerly known as *C. elegans* Y6B3B.5. The *bpnt-1(qd257)* allele (D119N) was isolated from an EMS mutagenesis screen and cloned through SNP mapping followed by whole-genome sequencing. The *bpnt-1(qd303)* allele (insertion/deletion) was generated using CRISPR-based targeting (Friedland et al. 2013). The *bpnt-1(gk577587)* (G287R) and *bpnt-1(gk469190)* (W294X) alleles were isolated from the *C. elegans* Million Mutation Project and also conferred *daf-7* expression defects in the ASJ neurons. For assays in which a synchronized population of animals was required, strains were egg-prepped in bleach and arrested overnight in M9 buffer at the L1 larval stage. For a complete list of strains used in this study see below.

ASJ Gene Expression and Morphology

To measure the expression of *daf-7* in the ASJ neurons on *P. aeruginosa* PA14, an overnight culture of PA14 was grown in 3 mL LB at 37°C, and the following morning 7 µL of culture was seeded onto 3.5 cm SKA plates as previously described (Tan, Mahajan-Miklos, and Ausubel 1999). PA14 plates were grown overnight at 37°C and then grown for an additional two days at room temperature. Animals at the L4 larval stage were then picked onto the center of the bacterial lawn, incubated at 25°C, and scored for GFP expression 16 h later. For quantifying the area of the ASJ cell body, animals were incubated in the lipophilic dye DiI (Molecular Probes) at 10 µg/ml in M9

buffer for 3 hours. Animals were then destained for 1 hour on a lawn of *E. coli* prior to imaging. To measure the expression of *daf-28, gpa-9,* and *trx-1* in the ASJ neurons, L4 larval animals were transferred to *E. coli* plates with or without 15 mM LiCl and incubated overnight at 20°C. Images were acquired with an Axioimager Z1 microscope using animals anaesthetized in 50 mM sodium azide. To quantify fluorescence animals were imaged at 40x magnification and the maximum intensity value within the ASJ neuron was determined using FIJI software. Statistical analysis was performed using GraphPad Prism Software.

P. aeruginosa Avoidance and Dauer Exit Assays

Plates for *P. aeruginosa* avoidance assays were prepared as above. 30 animals at the L4 larval stage were transferred to the center of PA14 lawns, incubated at 25°C, and scored for avoidance 15-20 h later. For dauer exit assays, all strains carried a mutation in the dauer constitutive gene *daf-2*. Gravid adults were egg-laid at 25°C on plates with *E. coli* and the experiment began two days later when all animals had entered the dauer developmental stage. Dauer animals were moved onto NGM plates seeded with *E. coli* with or without 15 mM LiCl. Animals continued to be incubated at 25°C and scored over the next week for dauer exit.

Single Molecule Fluorescent *In Situ* Hybridization

smFISH was performed as previously described (Raj et al. 2008). Briefly, *C. elegans* were fixed in 4% formaldehyde for 45 min at room temperature. After washing with PBS, larvae were resuspended in 70% EtOH and incubated overnight at 4°C. The following

day fixed larvae were transferred into hybridization solution with the smFISH probe and incubated overnight at 30°C. The *bpnt-1* probe was constructed by pooling 32 unique 20 nucleotide DNA oligos that tile the *bpnt-1* coding region and coupling them to Cy5 dye. For a complete list of oligos see below. Images were acquired with a Nikon Eclipse Ti Inverted Microscope outfitted with a Princeton Instruments PIXIS 1024 camera. Data were analyzed using FIJI software; images presented in Figure S2 are maximum intensity z-projections of 30 stacked exposures.

Generation of Transgenic Animals

To generate the genomic *bpnt-1* rescue construct, a 3.8 kb PCR fragment containing 1.4 kb of upstream promoter was amplified from genomic DNA and cloned into the pGEM-T Easy vector. To generate the *bpnt-1(I75A)* lithium-insensitive rescue construct the above plasmid was edited using a QuikChange II XL Site-Directed Mutagenesis Kit from Agilent Technologies. To generate the ASJ-specific *bpnt-1* and *mCherry* expression constructs, the *trx-1* promoter (Fierro González et al. 2011) (1.1 kb) was amplified by PCR from genomic DNA. *bpnt-1* cDNA was amplified by PCR from a cDNA library generated with an Ambion RETROscript Kit. The *unc-54* 3-prime UTR was amplified by PCR from Fire Vector pPD95.75. The *mCherry::unc-54 3'UTR* fragment was amplified from plasmid pCFJ104. DNA constructs (promoter::gene::*unc-54* 3'UTR) were synthesized using PCR fusion as previously described (Hobert 2002) and cloned into the pGEM-T Easy vector. To generate the cross-species *bpnt-1* rescue constructs, *D. melanogaster* BPNT-1/CG7789 cDNA (clone LD34542) and IPP cDNA (clone RE60387) were amplified from plasmids from the Drosophila Genomic Resource Center.

H. sapiens IPP cDNA (clone 3845956) was amplified from a plasmid from GE Healthcare Dharmacon. *S. cerevisiae* MET22/HAL2 DNA was amplified from genomic yeast DNA. *C. elegans bpnt-1* cDNA was amplified as above. These cDNAs were then cloned into the above genomic *bpnt-1* rescue construct using Gibson Assembly. All constructs were injected into animals at a concentration of 50 ng/µL along with a plasmid carrying the co-injection marker *ofm-1p::gfp* (50 ng/µL). At least three independent transgenic lines were analyzed for each construct. For a complete list of primers used in this study see below.

Phylogenetic Analysis

NCBI protein BLAST was used to collect homologs of all lithium-sensitive phosphatases in the following species: yeast (*Saccharomyces cerevisiae)*, sponge (*Amphimedon queenslandica)*, sea anemone (*Nematostella vectensis), Caenorhabditis elegans,* fly (*Drosophila melanogaster*), zebrafish (*Danio rerio)*, and human (*Homo sapiens)*. A protein alignment of conserved residues was generated using ClustalX, and a maximum-likelihood tree with 100 bootstrapped data sets was generated using PhyML (Guindon et al. 2010). Graphical trees were generated using FigTree.

Complete list of *C. elegans* strains used in this study

STRAIN	GENOTYPE	FIGURE
FK181	*ksIs2[daf-7p::GFP + rol6(su1006)] I*	1b-c, 3a-b, S3b
ZD886	*ksIs2; bpnt-1(qd257)*	1b-c, S3b
ZD1147	*ksIs2; bpnt-1(gk469190) 7xBackcrossed*	1b
ZD1146	*ksIs2; bpnt-1(gk577587) 6xBackcrossed*	Text
ZD1181	*ksIs2; bpnt-1(qd303)*	1b-c, 3a-b, S3b
ZD1150	*ksIs2; bpnt-1(qd257); qdEx121[bpnt-1(+) + ofm-1::gfp]*	1b
ZD1159	*ksIs2; bpnt-1(qd257); qdEx123[trx-1p::bpnt-1 cDNA + ofm-1::gfp]*	1b-c
DA650	*npr-1(215F) X*	1d
ZD1441	*bpnt-1(qd257); npr-1(215F)*	1d
ZD1442	*bpnt-1(qd303); npr-1(215F)*	1d
N2	wild type Bristol strain	1e, S2
ZD1169	*bpnt-1(qd257) II*	1e
ZD1224	*bpnt-1(qd303) II*	1e, S2
DR1572	*daf-2(e1368) III*	1f-g, 2f
ZD1396	*bpnt-1(qd257); daf-2(e1368)*	1f-g
ZD1425	*bpnt-1(qd303); daf-2(e1368)*	1f
ZD1519	*bpnt-1(qd257); daf-2(e1368); qdEx123[trx-1p::bpnt-1 cDNA + ofm-1::gfp]*	1g
GR1455	*mgIs40[daf-28p::nls-GFP] IV*	2a, 2d-e, 2g, 3c-d, S3a
ZD1572	*bpnt-1(qd303); mgIs40*	2a, 3c-d, S3a
NL1606	*dpy-20(e1282); pkIs586[gpa-9::GFP; dpy-20]*	2b
ZD1500	*bpnt-1(qd303); pkIs586[gpa-9::GFP; dpy-20]*	2b
ZD1446	*qdEx133[trx-1p::mCherry::unc-54 3'UTR + ofm-1::gfp]*	2c
ZD1578	*bpnt-1(qd303); qdEx133[trx-1p::mCherry::unc-54 3'UTR + ofm-1::gfp]*	2c
ZD1601	*bpnt-1(qd303); mgIs40; qdEx135[bpnt-1(I75A) + ofm-1::gfp]*	2e, 2g
ZD1755	*bpnt-1(qd303); daf-2(e1368); qdEx135[bpnt-1(I75A) + ofm-1::gfp]*	2f
ZD1528	*ksIs2; bpnt-1(qd303); qdEx127[bpnt-1p::S.c. MET22 cDNA::bpnt-1 3'UTR + ofm-1::gfp]*	3a-b
ZD1529	*ksIs2; bpnt-1(qd303); qdEx128[bpnt-1p::D.m. bpnt-1 cDNA::bpnt-1 3'UTR + ofm-1::gfp]*	3a-b
ZD1530	*ksIs2; bpnt-1(qd303); qdEx129[bpnt-1p::D.m. IPP cDNA::bpnt-1 3'UTR + ofm-1::gfp]*	3a-b
ZD1533	*ksIs2; bpnt-1(qd303); qdEx131[bpnt-1p::C.e. bpnt-1 cDNA::bpnt-1 3'UTR + ofm-1::gfp]*	3a-b
ZD1527	*ksIs2; bpnt-1(qd303); qdEx126[bpnt-1p::H.s. IPP cDNA::bpnt-1 3'UTR + ofm-1::gfp]*	3b
ZD1687	*mgIs40; ssu-1(fc73)*	3c-d
ZD1648	*bpnt-1(qd303); mgIs40; ssu-1(fc73)*	3c-d
ZD1701	*gpap-1(ok2805); mgIs40*	S3a
ZD1705	*ttx-7(nj50); mgIs40*	S3a

ZD1539	*ksIs2; ssu-1(fc73)*	S3b
ZD1540	*ksIs2; bpnt-1(qd303); ssu-1(fc73)*	S3b
ZD1622	*gpap-1(ok2805) ksIs2; bpnt-1(qd303)/mIn1[mIs14 dpy-10(e128)]*	Text

Complete list of DNA oligos used in this study

All sequences are listed in the 5' to 3' direction.

Primers used to generate *bpnt-1* rescue constructs	
acaaggccgaggagtctttg	*bpnt-1* genomic rescue forward
ggactcgacgaggaggaatc	*bpnt-1* genomic rescue reverse
tttttacctcttcgccggcaatattaatattcttg aaatgcttctgcagaga	*bpnt-1* QuickChange I75A forward
tctctgcagaagcatttcaagaatattaatattgc cggcgaagaggtaaaaa	*bpnt-1* QuickChange I75A reverse
Primers used to generate ASJ-specific *bpnt-1* and mCherry constructs	
TGAGTTGGGCACTTCGTAGA	*trx-1* promoter forward
TGAGAAAACTCGCTTTGTTGAACATGATCAATTGC TCAAAGTCAC	*trx-1* promoter reverse + *bpnt-1* tag
CTTCTTCACCCTTTGAGACCATGATCAATTGCTCA AAGTCAC	*trx-1* promoter reverse + *mCherry* tag
ATGTTCAACAAAGCGAGTTTTCTCA	*bpnt-1* cDNA forward
TAGGGATGTTGAAGAGTAATTGGACTCACTTTTTC GATGAAATCTCCGG	*bpnt-1* cDNA reverse + *unc-54* 3'UTR tag
ATGGTCTCAAAGGGTGAAGAAG	*mCherry* forward
GTCCAATTACTCTTCAACATCCCTA	*unc-54* 3'UTR forward
CAGTTATGTTTGGTATATTGGGAATG	*unc-54* 3'UTR reverse
Primers used to generate cross-species *bpnt-1* rescue constructs	
tctgaagcattccaaatttaatttttttcc	Gibson backbone forward
ttcaactggtgccgaaatcattc	Gibson backbone reverse
tcggcaccagttgaaATGTTCAACAAAGCGAGTTT TCTCA	*Ce_BPNT1* cDNA Forward + Gibson tag
ttggaatgcttcagaTCACTTTTTCGATGAAATCT CCGG	*Ce_BPNT1* cDNA Reverse + Gibson tag
tcggcaccagttgaaATGGCTGCAACTGCTCCG	*Dm_BPNT1* cDNA Forward + Gibson tag
ttggaatgcttcagaTCACTTGGCTCCCACTGC	*Dm_BPNT1* cDNA Reverse + Gibson tag
tcggcaccagttgaaATGGCATTGGAAAGAGAATT ATTGGTTG	*Sc_Met22* cDNA Forward + Gibson tag
ttggaatgcttcagaTTAGGCGTTTCTTGACTGAA TGAC	*Sc_Met22* cDNA Reverse + Gibson tag
tcggcaccagttgaaATGAGCGGCGTGGAGGAG	*Dm_IPP* cDNA Forward + Gibson tag
ttggaatgcttcagaTCATTGCTCGGCCAATTTGG	*Dm_IPP* cDNA Reverse + Gibson tag

tcggcaccagttgaaatgtcagatatcctccggga gc	*Hs_IPP* cDNA Forward + Gibson tag
ttggaatgcttcagactaggtatgcgtctctgcag g	*Hs_IPP* cDNA Reverse + Gibson tag
Oligos used to generate *bpnt-1* smFISH probe	
gtctcgtgagaaaactcgct	
cctctgaaactcggacagac	
atttttaataagacccccgg	
tgattttgagatctccgccg	
gatccgtgctccgatttatc	
cttccgtttgtggatcgtag	
gaactatgcagtattgagcc	
cactgaatcccatttcgatt	
atcaggcgttccatttggag	
tcctggatattcttgagctc	
cacccagactacaacatcat	
ttctgatgttccatccaacg	
tattcttaactgccaacgcg	
tgctccaacaatgccatatt	
gcgattccaatcaacacagt	
gatgaataattccagccacc	
cttccaagcttctcatgata	
caaccttgaatcgcccaaac	
ccggaacaactccatgaact	
tgagatggcttcgagttgtc	
agggcgttggagacagattc	
cgccaaatttcgagttttca	
caccgacttttttcaacgcta	
aaagacatacgctgcacacc	
catttcttacaaccagcact	
agtcaacacggcttcaactg	
aatgtccgtaagagttcctc	
tcatatcgaatatcacggcc	
tactcctcccgtattattaa	
cttatgcttgacccatgaag	
ttcttgtggaatcgtatcga	
cgatgaaatctccggcaaca	

References

Albert, A, L Yenush, M R Gil-Mascarell, P L Rodriguez, S Patel, M Martínez-Ripoll, T L Blundell, and R Serrano. 2000. "X-Ray Structure of Yeast Hal2p, a Major Target of Lithium and Sodium Toxicity, and Identification of Framework Interactions Determining Cation Sensitivity.." *Journal of Molecular Biology* 295 (4): 927–38. doi:10.1006/jmbi.1999.3408.

Bargmann, C I, and H R Horvitz. 1991. "Control of Larval Development by Chemosensory Neurons in Caenorhabditis Elegans.." *Science* 251 (4998): 1243–46.

Berridge, M J, C P Downes, and M R Hanley. 1982. "Lithium Amplifies Agonist-Dependent Phosphatidylinositol Responses in Brain and Salivary Glands.." *The Biochemical Journal* 206 (3): 587–95.

Brenner, S. 1974. "The Genetics of Caenorhabditis Elegans.." *Genetics* 77 (1): 71–94.

Carroll, Bryan T, George R Dubyak, Margaret M Sedensky, and Phil G Morgan. 2006. "Sulfated Signal From ASJ Sensory Neurons Modulates Stomatin-Dependent Coordination in Caenorhabditis Elegans.." *The Journal of Biological Chemistry* 281 (47): 35989–96. doi:10.1074/jbc.M606086200.

Cornils, A, M Gloeck, Z Chen, Y Zhang, and J Alcedo. 2011. "Specific Insulin-Like Peptides Encode Sensory Information to Regulate Distinct Developmental Processes." *Development* 138 (6): 1183–93. doi:10.1242/dev.060905.

Dejima, Katsufumi, Daisuke Murata, Souhei Mizuguchi, Kazuko H Nomura, Tomomi Izumikawa, Hiroshi Kitagawa, Keiko Gengyo-Ando, et al. 2010. "Two Golgi-Resident 3'-Phosphoadenosine 5'-Phosphosulfate Transporters Play Distinct Roles in Heparan Sulfate Modifications and Embryonic and Larval Development in Caenorhabditis Elegans.." *Journal of Biological Chemistry* 285 (32): 24717–28. doi:10.1074/jbc.M109.088229.

Dichtl, B, A Stevens, and D Tollervey. 1997. "Lithium Toxicity in Yeast Is Due to the Inhibition of RNA Processing Enzymes.." *The EMBO Journal* 16 (23): 7184–95. doi:10.1093/emboj/16.23.7184.

Diehl, R E, P Whiting, J Potter, N Gee, C I Ragan, D Linemeyer, R Schoepfer, C Bennett, and R A Dixon. 1990. "Cloning and Expression of Bovine Brain Inositol Monophosphatase.." *The Journal of Biological Chemistry* 265 (11): 5946–49.

Dupuy, Denis, Nicolas Bertin, César A Hidalgo, Kavitha Venkatesan, Domena Tu, David Lee, Jennifer Rosenberg, et al. 2007. "Genome-Scale Analysis of in Vivo Spatiotemporal Promoter Activity in Caenorhabditis Elegans.." *Nature Biotechnology* 25 (6): 663–68. doi:10.1038/nbt1305.

Fierro González, Juan Carlos, Astrid Cornils, Joy Alcedo, Antonio Miranda-Vizuete, and Peter Swoboda. 2011. "The Thioredoxin TRX-1 Modulates the Function of the

Insulin-Like Neuropeptide DAF-28 During Dauer Formation in Caenorhabditis Elegans." Edited by Ellen Nollen. *PLoS ONE* 6 (1): e16561. doi:10.1371/journal.pone.0016561.s007.

Frederick, Joshua P, A Tsahai Tafari, Sheue-Mei Wu, Louis C Megosh, Shean-Tai Chiou, Ryan P Irving, and John D York. 2008. "A Role for a Lithium-Inhibited Golgi Nucleotidase in Skeletal Development and Sulfation.." *Proceedings of the National Academy of Sciences* 105 (33): 11605–12. doi:10.1073/pnas.0801182105.

Friedland, Ari E, Yonatan B Tzur, Kevin M Esvelt, Monica P Colaiácovo, George M Church, and John A Calarco. 2013. "Heritable Genome Editing in C. Elegans via a CRISPR-Cas9 System.." *Nature Methods* 10 (8): 741–43. doi:10.1038/nmeth.2532.

Guindon, Stéphane, Jean-François Dufayard, Vincent Lefort, Maria Anisimova, Wim Hordijk, and Olivier Gascuel. 2010. "New Algorithms and Methods to Estimate Maximum-Likelihood Phylogenies: Assessing the Performance of PhyML 3.0.." *Systematic Biology* 59 (3): 307–21. doi:10.1093/sysbio/syq010.

Hattori, Kenji, Masayuki Inoue, Takao Inoue, Hiroyuki Arai, and Hiro-omi Tamura. 2006. "A Novel Sulfotransferase Abundantly Expressed in the Dauer Larvae of Caenorhabditis Elegans.." *Journal of Biochemistry* 139 (3): 355–62. doi:10.1093/jb/mvj041.

Hobert, Oliver. 2002. "PCR Fusion-Based Approach to Create Reporter Gene Constructs for Expression Analysis in Transgenic C. Elegans.." *BioTechniques* 32 (4): 728–30.

Hudson, Benjamin H, Joshua P Frederick, Li Yin Drake, Louis C Megosh, Ryan P Irving, and John D York. 2013. "Role for Cytoplasmic Nucleotide Hydrolysis in Hepatic Function and Protein Synthesis.." *Proceedings of the National Academy of Sciences* 110 (13): 5040–45. doi:10.1073/pnas.1205001110.

Jansen, G, K L Thijssen, P Werner, M van der Horst, E Hazendonk, and R H Plasterk. 1999. "The Complete Family of Genes Encoding G Proteins of Caenorhabditis Elegans.." *Nature Genetics* 21 (4): 414–19. doi:10.1038/7753.

Li, Weiqing, Scott G Kennedy, and Gary Ruvkun. 2003. "Daf-28 Encodes a C. Elegans Insulin Superfamily Member That Is Regulated by Environmental Cues and Acts in the DAF-2 Signaling Pathway.." *Genes & Development* 17 (7): 844–58. doi:10.1101/gad.1066503.

López-Coronado, J M, J M Bellés, F Lesage, R Serrano, and P L Rodriguez. 1999. "A Novel Mammalian Lithium-Sensitive Enzyme with a Dual Enzymatic Activity, 3'-Phosphoadenosine 5'-Phosphate Phosphatase and Inositol-Polyphosphate 1-Phosphatase.." *The Journal of Biological Chemistry* 274 (23): 16034–39.

Meisel, Joshua D, Oishika Panda, Parag Mahanti, Frank C Schroeder, and Dennis H Kim. 2014. "Chemosensation of Bacterial Secondary Metabolites Modulates Neuroendocrine Signaling and Behavior of C. Elegans.." *Cell* 159 (2): 267–80.

doi:10.1016/j.cell.2014.09.011.

Miranda-Vizuete, Antonio, Juan Carlos Fierro González, Gabriele Gahmon, Jan Burghoorn, Plácido Navas, and Peter Swoboda. 2006. "Lifespan Decrease in a Caenorhabditis Elegans Mutant Lacking TRX-1, a Thioredoxin Expressed in ASJ Sensory Neurons.." *FEBS Letters* 580 (2): 484–90. doi:10.1016/j.febslet.2005.12.046.

Murguía, J R, J M Bellés, and R Serrano. 1995. "A Salt-Sensitive 3'(2"),5-"Bisphosphate Nucleotidase Involved in Sulfate Activation.." *Science* 267 (5195): 232–34.

Nigou, Jérôme, Lynn G Dover, and Gurdyal S Besra. 2002. "Purification and Biochemical Characterization of Mycobacterium Tuberculosis SuhB, an Inositol Monophosphatase Involved in Inositol Biosynthesis.." *Biochemistry* 41 (13): 4392–98.

Ozeran, J D, J Westley, and N B Schwartz. 1996. "Kinetics of PAPS Translocase: Evidence for an Antiport Mechanism.." *Biochemistry* 35 (12): 3685–94. doi:10.1021/bi951302u.

Pollack, S J, M R Knowles, J R Atack, H B Broughton, C I Ragan, S Osborne, and G McAllister. 1993. "Probing the Role of Metal Ions in the Mechanism of Inositol Monophosphatase by Site-Directed Mutagenesis.." *European Journal of Biochemistry / FEBS* 217 (1): 281–87.

Raj, Arjun, Patrick van den Bogaard, Scott A Rifkin, Alexander van Oudenaarden, and Sanjay Tyagi. 2008. "Imaging Individual mRNA Molecules Using Multiple Singly Labeled Probes." *Nature Methods* 5 (10): 877–79. doi:10.1038/nmeth.1253.

Ramaswamy, S G, and W B Jakoby. 1987. "(2')3",5-"Bisphosphate Nucleotidase.." *The Journal of Biological Chemistry* 262 (21): 10044–47.

Ren, P, C S Lim, R Johnsen, P S Albert, D Pilgrim, and D L Riddle. 1996. "Control of C. Elegans Larval Development by Neuronal Expression of a TGF-Beta Homolog.." *Science* 274 (5291): 1389–91.

Salman, Emily D, Susan A Kadlubar, and Charles N Falany. 2009. "Expression and Localization of Cytosolic Sulfotransferase (SULT) 1A1 and SULT1A3 in Normal Human Brain.." *Drug Metabolism and Disposition: the Biological Fate of Chemicals* 37 (4): 706–9. doi:10.1124/dmd.108.025767.

Schackwitz, W S, T Inoue, and J H Thomas. 1996. "Chemosensory Neurons Function in Parallel to Mediate a Pheromone Response in C. Elegans.." *Neuron* 17 (4): 719–28.

Schneider, B, Y W Xu, J Janin, M Véron, and D Deville-Bonne. 1998. "3'-Phosphorylated Nucleotides Are Tight Binding Inhibitors of Nucleoside Diphosphate Kinase Activity.." *The Journal of Biological Chemistry* 273 (44): 28773–78.

Sidharthan, Neelima P, Rodney F Minchin, and Neville J Butcher. 2013. "Cytosolic

Sulfotransferase 1A3 Is Induced by Dopamine and Protects Neuronal Cells From Dopamine Toxicity: Role of D1 Receptor-N-Methyl-D-Aspartate Receptor Coupling.." *Journal of Biological Chemistry* 288 (48): 34364–74. doi:10.1074/jbc.M113.493239.

Spiegelberg, B D, J P Xiong, J J Smith, R F Gu, and J D York. 1999. "Cloning and Characterization of a Mammalian Lithium-Sensitive Bisphosphate 3'-Nucleotidase Inhibited by Inositol 1,4-Bisphosphate.." *The Journal of Biological Chemistry* 274 (19): 13619–28.

Spiegelberg, Bryan D, June Dela Cruz, Tzuo-Hann Law, and John D York. 2005. "Alteration of Lithium Pharmacology Through Manipulation of Phosphoadenosine Phosphate Metabolism.." *The Journal of Biological Chemistry* 280 (7): 5400–5405. doi:10.1074/jbc.M407890200.

Strott, Charles A. 2002. "Sulfonation and Molecular Action.." *Endocrine Reviews* 23 (5): 703–32. doi:10.1210/er.2001-0040.

Tan, M W, S Mahajan-Miklos, and F M Ausubel. 1999. "Killing of Caenorhabditis Elegans by Pseudomonas Aeruginosa Used to Model Mammalian Bacterial Pathogenesis.." *Proceedings of the National Academy of Sciences of the United States of America* 96 (2): 715–20.

Toledano, Elie, Vasily Ogryzko, Antoine Danchin, Daniel Ladant, and Undine Mechold. 2012. "3'-5' Phosphoadenosine Phosphate Is an Inhibitor of PARP-1 and a Potential Mediator of the Lithium-Dependent Inhibition of PARP-1 in Vivo.." *The Biochemical Journal* 443 (2): 485–90. doi:10.1042/BJ20111057.

York, J D, and P W Majerus. 1990. "Isolation and Heterologous Expression of a cDNA Encoding Bovine Inositol Polyphosphate 1-Phosphatase.." *Proceedings of the National Academy of Sciences of the United States of America* 87 (24): 9548–52.

Supplemental Information

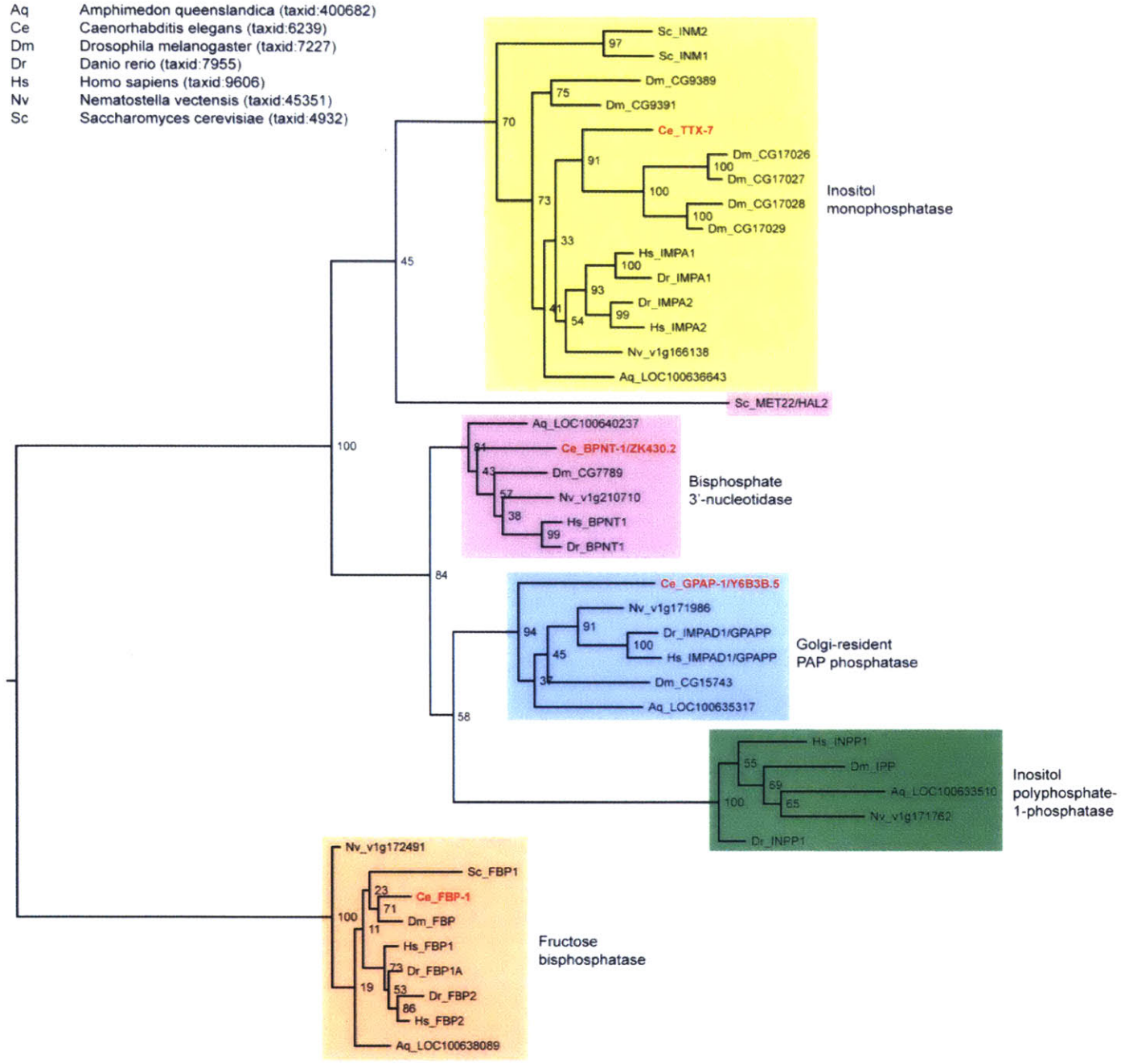

Figure S1. Phylogenetic analysis of the conserved family of lithium-sensitive phosphatases, related to Figure 1. Maximum-likelihood phylogenetic analysis of conserved regions of the inositol monophosphatase, bisphosphate 3'-nucleotidase (BPNT-1), Golgi-resident PAP phosphatase, inositol polyphosphate-1-phosphatase, and fructose bisphosphatase proteins. Colored boxes denote functional homologs. Nodes are labeled with bootstrap values (out of 100 replicates). Branch lengths are proportional to number of amino acid changes. *C. elegans* genes are indicated in red.

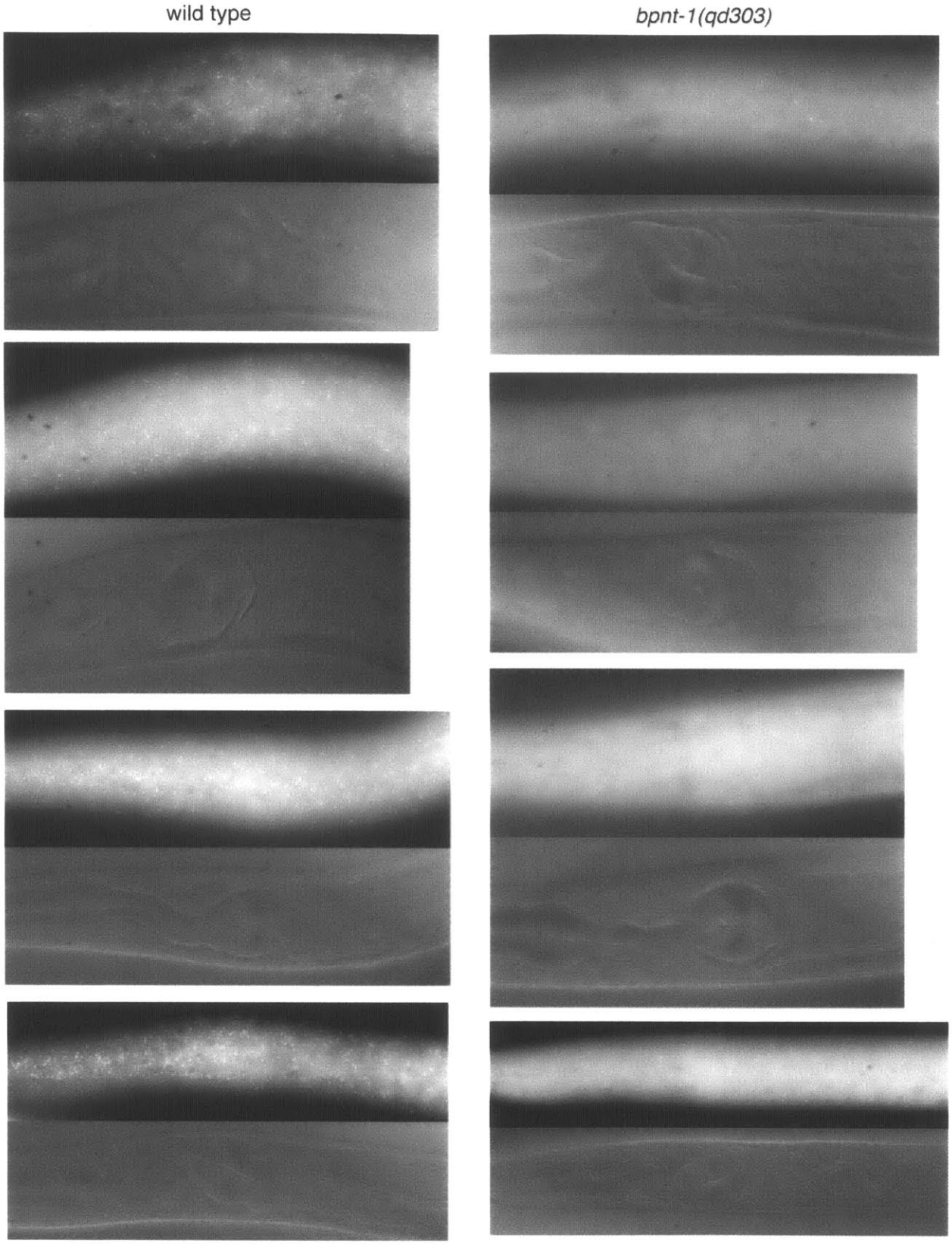
wild type
bpnt-1(qd303)

Figure S2. The *bpnt-1* expression pattern is broad and not limited to the ASJ neurons, related to Figure 1. Single molecule fluorescent *in situ* hybridization of *bpnt-1* mRNA in wild type and *bpnt-1(qd303)* mutant animals. Images presented are maximum intensity z-projections of 30 stacked exposures of *bpnt-1* mRNA (above) and trans-illumination (below). Animals presented are representative samples from a mixed-stage population. All images were taken at 100x magnification.

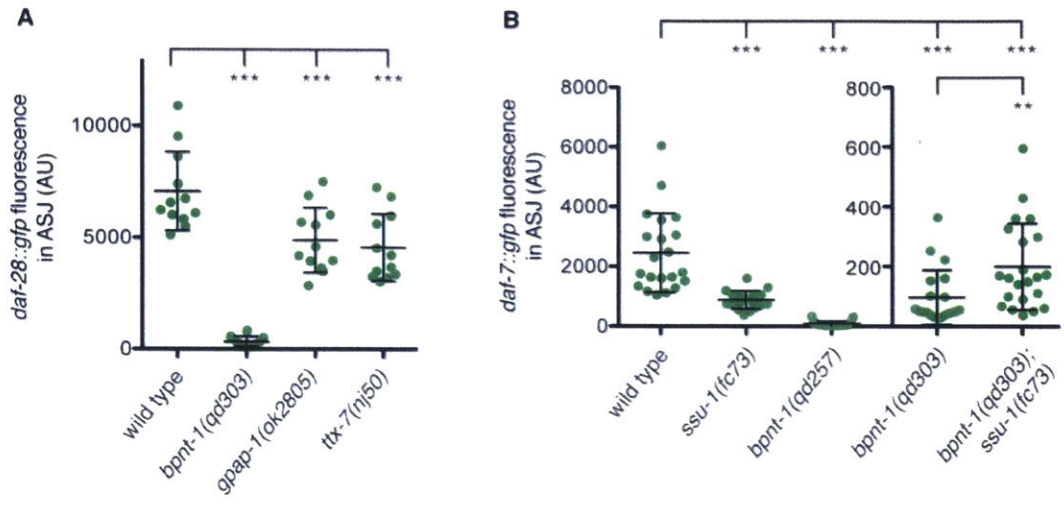

Figure S3. BPNT-1, but not GPAP-1 or TTX-7, is required for ASJ function partially due to expression of cytosolic sulfotransferase SSU-1, related to Figures 2 and 3. (A) Maximum fluorescence of *daf-28::gfp* in the ASJ neurons. All genotypes contain *mgIs40[daf-28p::nls-GFP]*. **(B)** Maximum fluorescence of *daf-7p::gfp* in the ASJ neurons after 16 h exposure to *P. aeruginosa*. All genotypes contain *ksIs2[daf-7p::gfp]*. *** $P < 0.001$, ** $P < 0.01$ as determined by one-way ANOVA followed by Dunnett's Multiple Comparison Test. Error bars indicate standard deviation.

Chapter Four

Future Directions

Joshua D. Meisel

Identification of genes coupling microbial detection to neuronal transcription

C. elegans has the remarkable ability to modulate its innate behavioral attraction to bacteria when confronted with a pathogenic threat. However the molecular and genetic mechanisms that couple sensory detection of a pathogenic bacterium to a change in behavior remain enigmatic. Prior to this thesis work, a forward genetic approach to this question would have been challenging. For example, a screen for animals defective in the behavioral avoidance of *P. aeruginosa*, a population-based assay in which 5-10% of wild type animals will remain inside the bacterial lawn, would require a F3 clonal screen. In Chapter Two, we identify a highly penetrant transcriptional response in a chemosensory neuron to pathogen exposure. Specifically, the neuromodulator DAF-7/TGF-β, normally expressed exclusively in the ASI neurons, is activated in the chemosensory ASJ neurons after five minutes on *P. aeruginosa*. This induction can easily be followed using a GFP reporter for *daf-7* transcription and a fluorescent microscope, facilitating a forward genetic approach to identify genes required for the neuronal response to pathogen exposure.

We conducted a screen for mutants defective in the induction of *daf-7* in the ASJ neurons on *P. aeruginosa*. Class 1 mutants failed to induce *daf-7* in the ASJ neurons, but also lacked wild type expression of *daf-7* in the ASI neurons (Figure 1). We believe such genes to act upstream of *daf-7* in all tissues, or to be required for development of the nervous system as a whole, and not act specifically in the signaling response to *P. aeruginosa*. For all Class 1 mutants, ASJ-specific rescue experiments will be important for distinguishing between cell-autonomous and cell-nonautonomous effects. In Chapter Two the guanylate cyclase DAF-11 and the cyclic

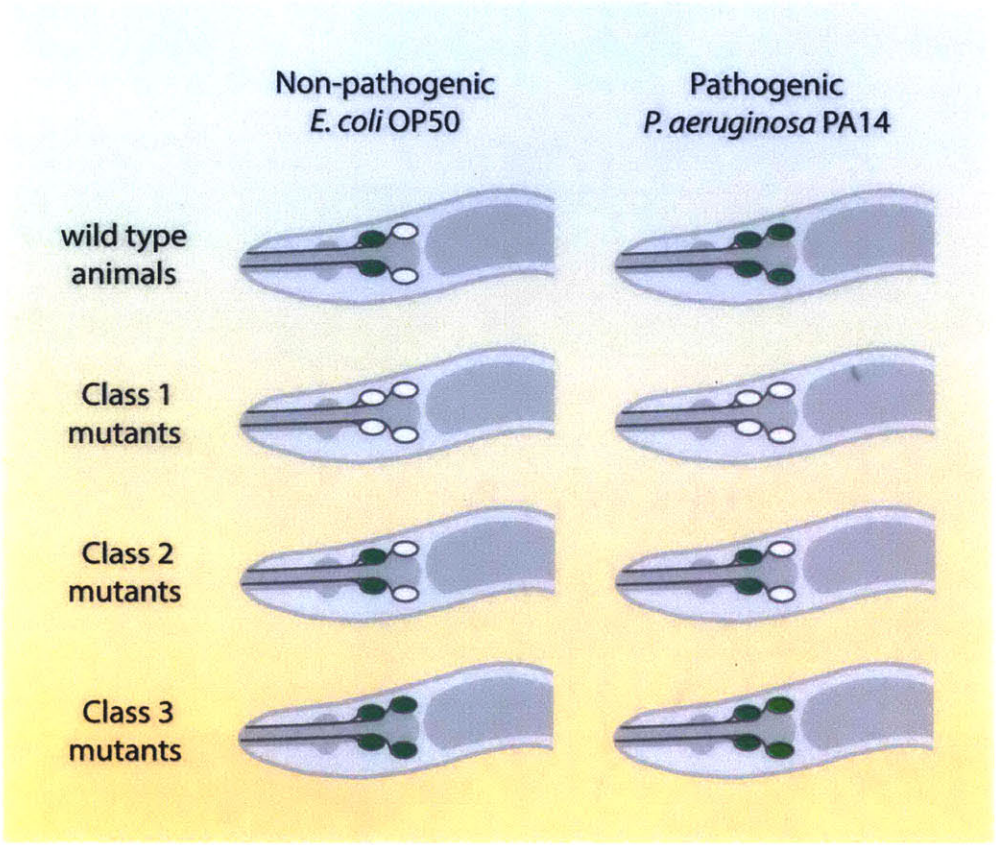

Figure 1. Classification of mutants defective in the induction of *daf-7* in the ASJ neurons. On *E. coli,* wild type animals express *daf-7* exclusively in the ASI pair of sensory neurons, but following exposure to *P. aeruginosa, daf-7* is additionally expressed in the ASJ pair of chemosensory neurons. Class 1 mutants fail to induce *daf-7* expression in ASJ neurons, but are also defective in expression of *daf-7* in the ASI neurons. Class 2 mutants are specifically defective in the induction of *daf-7* in the ASJ neurons following exposure to *P. aeruginosa.* Class 3 mutants constitutively express *daf-7* in the ASJ neurons on *E. coli*, but are still able to induce expression on *P. aeruginosa* to higher levels.

nucleotide-gated channel encoded by TAX-2/TAX-4 are presented as Class 1 mutants. It is possible that transcription factors responsible for activating *daf-7* will be common between ASI and ASJ neurons, and characterization of additional Class 1 mutants may identify such DNA binding proteins.

Class 2 mutants failed to induce *daf-7* in the ASJ neurons on *P. aeruginosa* but displayed wild type expression of *daf-7* in the ASI neurons. The G protein alpha subunits GPA-2 and GPA-3 presented in Chapter Two are such mutants, and we believe they act cell-autonomously in the ASJ neurons to transduce the *P. aeruginosa* signal into a transcriptional response. A Class 2 mutant could also in principal disrupt the ASJ neuron more globally, and so we confirmed that in *gpa-2* and *gpa-3* mutants the ASJ neurons were still intact and expressed other ASJ-specific genes at wild type levels (e.g. *trx-1, daf-28)*. One Class 2 mutant that did not pass this secondary screen was BPNT-1, discussed in Chapter Three, loss of which globally disrupted the ASJ neuron through accumulation of toxic PAP. Identification of additional Class 2 mutants will provide insights into the signaling mechanisms coupling neuronal activation to *daf-7* transcription in the ASJ neurons, or shed light on the unique biology of the ASJ neurons.

An additional class of mutants was identified that displayed constitutive expression of *daf-7* in the ASJ neurons. These Class 3 mutants expressed *daf-7* in the ASJ neurons when propagated on benign *E. coli*, but could still induce *daf-7* to a greater extent when exposed to *P. aeruginosa* (Figure 2). We therefore hypothesize that Class 3 mutants act in parallel to the pathway that responds to *P. aeruginosa*, and function to inhibit *daf-7* transcription during favorable conditions. Perhaps when a transcriptional program is poised to be rapidly activated by an environmental cue, regulatory networks that prevent inappropriate transcription are critical for

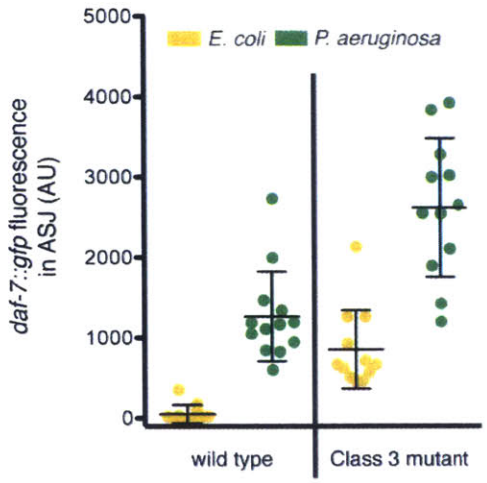

Figure 2. Class 3 mutants inhibit inappropriate expression of *daf-7* in the ASJ neurons.

Maximum fluorescence of *daf-7p::gfp* in the ASJ neurons after 16 h following transfer to *E. coli* OP50 (yellow) or *P. aeruginosa* PA14 (green). All genotypes contain *ksIs2[daf-7p::gfp]*.

a robust response. Identification of Class 3 mutants will allow for cell-specific rescue experiments and epistasis analysis with Class 1 and Class 2 mutants. These data will establish the neuronal and genetic pathways controlling *daf-7* transcription and lend insights into how rapid transcriptional programs are regulated in neurons.

A conserved role for BPNT-1 in mammals?

In Chapter Three we demonstrate that inhibition of the conserved phosphatase BPNT-1 by lithium leads to selective neuronal dysfunction. The cell-specificity of this inhibition by lithium is due in part to selective expression of the cytosolic sulfotransferase SSU-1 in the ASJ neuron pair. Intriguingly, BPNT-1 is expressed in the mammalian brain, and cytosolic sulfotransferases are selectively expressed in mammalian neurons that synthesize catecholamine neurotransmitters (Hudson et al. 2013; Salman, Kadlubar, and Falany 2009; Sidharthan, Minchin, and Butcher 2013). Future studies could ask whether lithium may be exerting its inhibitory effects on the mammalian brain through inhibition of BPNT-1. A recent study by Mertens *et al.* analyzed neurons *in vitro* generated from induced pluripotent stem-cells from patients with bipolar disorder (Mertens et al. 2015). These neurons were hyperexcitable in culture, and this phenotype was reversibly inhibited by lithium, but only in neurons generated from patients who also responded to lithium treatment. Would knockdown or knockout of BPNT-1 in these neurons mimic lithium treatment? Would expression of the lithium-insensitive BPNT-1 mutant (discussed in Chapter Three) blunt the effects of lithium? Analysis of transgenic mice in which BPNT-1 is eliminated or mutated selectively in the brain would also lend insights into how lithium may be acting to affect mammalian behavior.

References

Hudson, Benjamin H, Joshua P Frederick, Li Yin Drake, Louis C Megosh, Ryan P Irving, and John D York. 2013. "Role for Cytoplasmic Nucleotide Hydrolysis in Hepatic Function and Protein Synthesis.." *Proceedings of the National Academy of Sciences* 110 (13): 5040–45. doi:10.1073/pnas.1205001110.

Mertens, Jerome, Qiu-Wen Wang, Yongsung Kim, Diana X Yu, Son Pham, Bo Yang, Yi Zheng, et al. 2015. "Differential Responses to Lithium in Hyperexcitable Neurons From Patients with Bipolar Disorder.." *Nature* 527 (7576): 95–99. doi:10.1038/nature15526.

Salman, Emily D, Susan A Kadlubar, and Charles N Falany. 2009. "Expression and Localization of Cytosolic Sulfotransferase (SULT) 1A1 and SULT1A3 in Normal Human Brain.." *Drug Metabolism and Disposition: the Biological Fate of Chemicals* 37 (4): 706–9. doi:10.1124/dmd.108.025767.

Sidharthan, Neelima P, Rodney F Minchin, and Neville J Butcher. 2013. "Cytosolic Sulfotransferase 1A3 Is Induced by Dopamine and Protects Neuronal Cells From Dopamine Toxicity: Role of D1 Receptor-N-Methyl-D-Aspartate Receptor Coupling.." *Journal of Biological Chemistry* 288 (48): 34364–74. doi:10.1074/jbc.M113.493239.